Robot System Characterization: Error Modeling, Identification, Analysis, and Minimization

by

Ravinder Srinivas Voruganti

Dissertation submitted to the Faculty of the
Virginia Polytechnic Institute and State University
in partial fulfillment of the requirements for the degree of

Doctor of Philosophy

in

Mechanical Engineering

APPROVED:

Charles F. Reinholtz, Chairman

Sanjay G. Dhande | Harry H. Robertshaw | Robert L. West

John S. Bay | Robert J. Salerno

December 1995

Blacksburg, Virginia

Key words: Robot, Calibration, Optimization, Sensitivity, Accuracy

Robot System Characterization: Error Modeling, Identification, Analysis, and Minimization

by

Ravinder Srinivas Voruganti

Charles F. Reinholtz, Chairman

Mechanical Engineering

(ABSTRACT)

This dissertation describes the development and application of a characterization methodology that improves the performance of robotic systems. To achieve accurate positioning, robot geometry must be precisely defined, both in new system design and in upgrading existing robots. This can be accomplished by developing rigorous calibration methods to model, identify, analyze, and minimize errors in robot geometric parameters. Throughout this work, the geometric parameters that describe the kinematics of a given robot are treated as unknowns. The robot characterization process involves finding the optimal values of these parameters to best fit a set of measured or simulated positions of the robot end-effector.

In this dissertation, well-established robot kinematic link transformation techniques are first used to model the robotic manipulator system. Next, engineering knowledge of the robot system, its work environment and detailed component specifications are used to identify possible sources of error. This results in a list of error parameters and their range. A system sensitivity analysis is performed on these parameters to determine which have the greatest effect on system accuracy. To characterize an existing robot, experimental calibration data is gathered using a suitable measurement technique. Using this data, optimization of the previously isolated critical parameters is performed. The newly determined values of these

parameters are implemented into the control system and performance is compared before and after the characterization process.

To design a new robot system, the isolated critical parameters are again found through optimization. In this case, however, the measured data is gathered by a simulation, with the error parameter values randomly generated each time. The performance of the system is analyzed after this exhaustive simulation. In both of the cases described, the characterization process is iterative.

The characterization process has been successfully applied to the design of a positioning system for a mobile, underwater nuclear-reactor-vessel-inspection robot. Also, the performance of an existing PUMA 562 industrial robot has been improved using this characterization procedure.

The advantages of this methodology over previous ones are that it can be applied to both new and existing robot systems and it is specifically aimed at meeting performance goals. A cost-performance tradeoff is accomplished by optimizing only for the critical parameters required to meet the specified performance objectives.

Dedicated to the memory of my dear sister

Voruganti Dakshayini

Acknowledgments

I would like to express sincere thanks to my graduate advisor, Dr. Charles F. Reinholtz, and to Dr. Sanjay G. Dhande for their guidance, encouragement and support throughout my graduate studies. It is hard to find two more selfless and caring men. They are the true embodiment of "friend, philosopher, and guide". My goal is to become more like them.

I gratefully acknowledge the advice given by the members of my doctoral committee, Dr. Harry Robertshaw, Dr. Robert West, Dr. John Bay, and Dr. Robert Salerno. I wish to thank Dr. Paul Tidwell for kindly agreeing to serve on my examining committee.

Special thanks are extended to Dr. Robert West and David Coe for the acoustic digitizer. I thank the machine shop; the electronics shop - especially Ben Poe; the department office - especially Lynne Ellis, Eloise McCoy, Willie Hylton, and Mike Harness; and the Multimedia Lab - especially Gordon Miller.

This work would not have been possible without the financial and technical support of B&W Nuclear Technologies. Specifically, I would like to thank Bill Glass. Acknowledgments are due Virginia's Center for Innovative Technology (Wayne Hawkins), and the National Science Foundation for their financial support.

I feel indebted to the many people who have sincerely helped me in accomplishing this work. I have received significant assistance and advice from Barry Fallon, Joe Calkins and Jay Gayle. I also thank the senior design team that worked on the base positioning system design for URSULA. I acknowledge the help given to me by my colleagues in the Robotics and Mechanisms Group at Virginia Tech - especially Jimmy Asher, Steve Canfield, Angela Carr, John Collier, Tony Ganino, Anil Garg, Amber Jenkins, John Stulce, and Ryan Vallance.

I wish to thank Jeri Reinholtz for her wonderful patience and understanding when we spent long hours at the Reinholtz residence.

I am indebted to my father and mother for their encouragement, love, and support. They made it easier for me to achieve my dreams.

Finally, I extend my heartfelt gratitude to my wife, Tripura. She was always there to pick me up during tough times. Her support, patience, and encouragement are deeply appreciated.

Table of Contents

List of Figures

List of Tables

1. Introduction

The development and application of a new robot system characterization methodology is presented in this dissertation. The purpose of this calibration process is to improve the end-effector positioning accuracy in robot systems.

In this chapter, the motivation for this work is discussed followed by definitions and brief descriptions of robot systems, pose (position and orientation) errors, and sources of pose errors. Finally, a short presentation of the robot calibration methodology is included.

1.1 Motivation and Overview

The work presented in this dissertation evolved from and was motivated by recent nuclear service and inspection robot development efforts. It became apparent that robot

calibration issues are significant for accurate performance. Some of the calibration needs that were identified from this experience are also presented in this section.

1.1.1 Robot Development Experience

The United States produces nearly 100,000 MW of electric power using nuclear reactors. This is about 20 percent of the total domestic electric power consumption. Pressurized water reactors (PWRs) account for about two-thirds of the commercial nuclear-based power generation units. Each PWR has between two to four steam generators which are inspected and repaired every 15-18 months while the reactor is being refueled. Steam generators, in conjunction with pressurized water reactors, produce steam which powers turbines and generates electric power.

Steam generators are shell-and-tube heat exchangers consisting of between 5,000 and 15,000 tubes arranged vertically and supported at their ends by a thick tubesheet (Figure 1.1). Water is heated in the nuclear reactor and circulated through the primary inlet tubes and primary outlet of the steam generator before returning to the reactor. As the primary water flows through the tubes, heat is transferred across the tube wall to the secondary water which is converted to steam. The steam generator tubes form a boundary between the high pressure, primary water from the reactor and the secondary water and steam, which is under relatively lower pressure. To maintain the pressure boundary, power utilities spend about three weeks servicing steam generators out of the total six to eight week refueling outage. Minimization of inspection and repair time and also the amount

of radiation exposure to workers is important. Outage time cost is estimated as the cost of electricity lost due to reactor shut-down. This cost to the power utility can be as much as two million dollars for each day the unit is out of service.

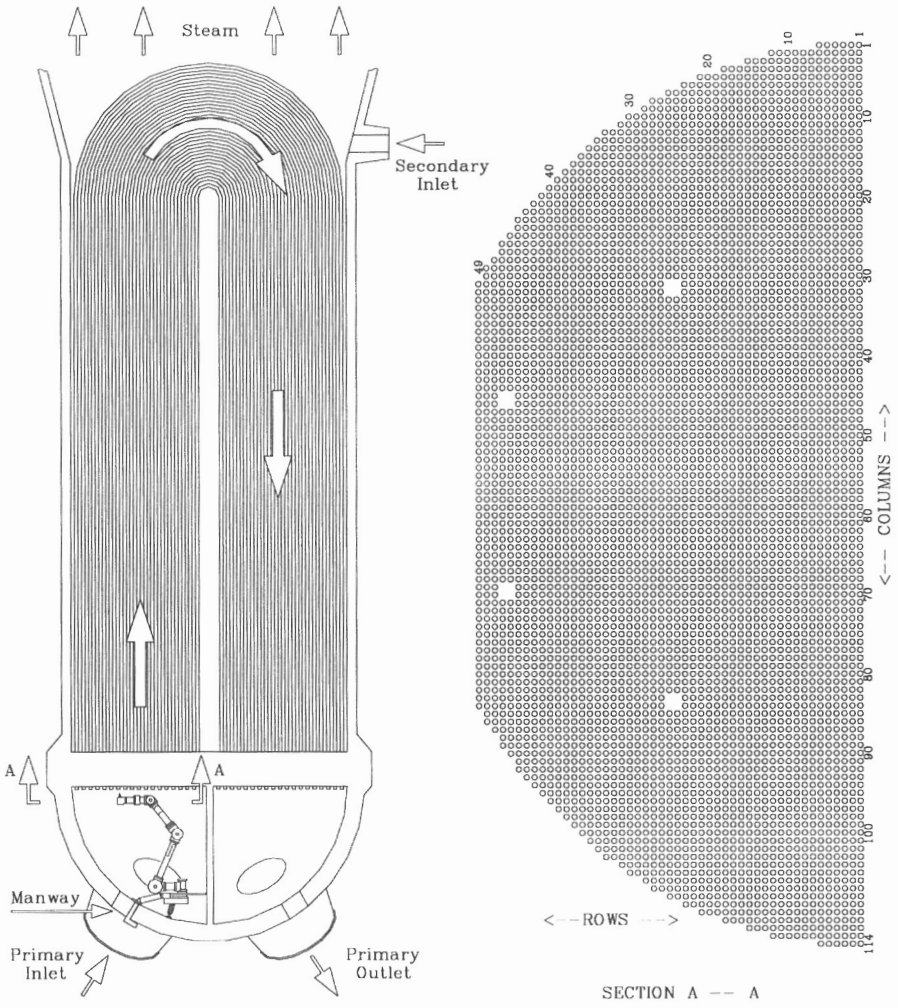

Figure 1.1: Steam Generator

Steam generator tube-ends are accessed for servicing by installing a portable robot through a 0.4 m (16 in.) diameter manway into a hemispherical bowl beneath the tubesheet as shown in Figure 1.1 (Tidwell et al., 1991 and 1994). One such manipulator,

developed by B&W Nuclear Technologies (BWNT), is called Cobra. Cobra's task is to position a variety of tools at particular open tube-ends for inspection and repair activities. Since Cobra must be installed through a small manway to access over 3.23 sq m (5000 sq in.) of tubesheet, it is classified as a limited access workspace (LAWs) robot (Shooter et al., 1992). Although it weighs only 50 kg (110 lb), Cobra can lift 68.2 kg (150 lb) at full extension of 1.94 m (77 in.). The accuracy requirements are quite high considering its strength-to-weight ratio and remote mounting. An absolute positional accuracy of ± 0.5 mm (± 0.02 in.) in the horizontal tubesheet plane is required to calibrate the manipulator base position. An accuracy of ± 1.25 mm (± 0.05 in.) is required for tool positioning. Figure 1.2 shows a photograph of Cobra inside a steam generator.

Cobra is controlled by solving the inverse kinematic equations to determine the joint angles needed to position a tool at a desired tube. The joint proportional integral and derivative (PID) controller compares these reference angle inputs with feedback angles from joint synchro sensors to produce an error signal. The tool is positioned by moving the joints through angles such that the error signals to the controller become smaller and finally disappear. The position of the tool with respect to a particular tube in the tubesheet is found by knowing the steam generator and the robot geometry and measuring joint angles.

Since the robot and the environment are not perfect, there is an error in the tool position. This is due to the propagation of errors from various sources such as link lengths, link

offsets, link twists, initial joint angles, robot base position and orientation, tool geometry and pose (position and orientation), workpiece geometry and pose, compliance in joints and links, compliance in robot base, and relative joint angles. Since the error signal to the controller has ceased, a manual correction may have to be applied to the tool position to guide it under a tube. Manual correction is accomplished by an operator viewing the tool and tubesheet through a robot-mounted CCD camera.

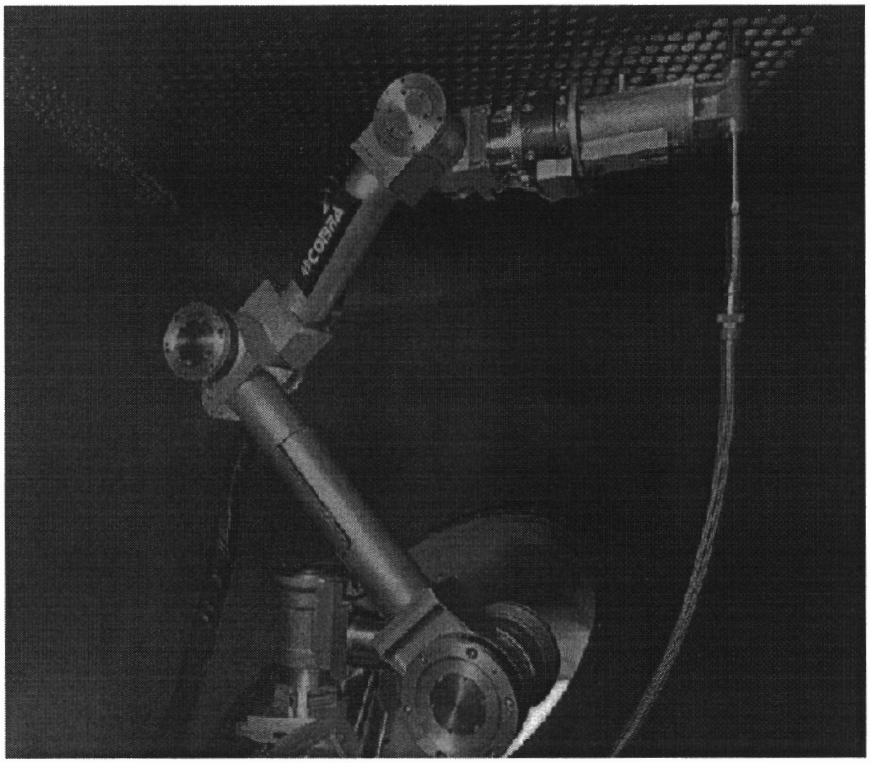

Figure 1.2: Cobra Inside Steam Generator

Currently, error accumulation is minimized by precisely measuring intrinsic robot and tool parameters off-line, calibrating robot base pose parameters with a calibration process after Cobra is installed in the steam generator (Shooter and Reinholtz, 1992), and on-line

compensation for deflections in the robot and in the base mounting (Calkins, 1994). Of the three robot base orientation parameters, two are known beforehand since the robot base is initially mounted level with the tubesheet. The remaining four unknown base pose parameters consist of three position and one orientation parameters. To calibrate these parameters, the robot is tele-operated to three or more specific tubes and the tool-tip is docked on the ends of these tubes. With the known robot and tubesheet geometry, the base parameters are computed and used by the controller throughout the outage.

This method of separately measuring the intrinsic parameters and calibrating the base pose parameters is time-consuming and may not reflect the robot geometry exactly. This is because it may not be possible to physically measure the kinematic link lengths, link twists and joint offsets. Also, these quantities will change as the manipulator joints become worn or as a result of deformation due to impact or overload. A general calibration procedure that identifies intrinsic as well as base pose parameters at the same time without having to disassemble and physically measure each link is attractive.

In addition to steam generator maintenance, nuclear reactor vessel welds must also be inspected periodically to ensure the pressure boundary integrity (Fallon et al., 1994b). Full vessel weld inspection (approximately sixteen kilometers of ultrasonic scanning) is required prior to initial service and every tenth year thereafter. Intermediate piping nozzle inspection is also required forty months into each ten year period. A typical power station reactor vessel is about nine meters high and has an inside diameter of about 4.5 m. Full

weld inspections are performed on the interior of the vessel after the closure head and the fuel rods are removed. The vessel remains full of borated water, which provides shielding against the residual radioactivity emanating from the vessel walls. The vessel geometry and underwater radiation environment are very demanding for robotic inspection systems. Reactor vessel inspections were performed by BWNT, a nuclear service company, for many years using a robot called ARIS (Automated Reactor vessel Inspection System). ARIS is a large, long-reach cylindrical manipulator, weighing over 13,182 kg (29,000 lb), requiring approximately 3 days for on-site assembly.

In 1992, the Robotics and Mechanisms group at Virginia Tech participated in a conceptual design effort with BWNT to develop the next generation of reactor vessel inspection systems. The objectives of the new reactor scanning system were to reduce the time required for all on-site reactor vessel examination activities, reduce employee radiation exposure, reduce the site impact created by scanning system maintenance, and reduce costs that result from off-site storage, maintenance, testing, training, and transportation. The concept that was born from the extensive conceptual design process is a mobile manipulator called URSULA (Ultrasonic Reactor Scanner Un-Like ARIS). URSULA consists of a six degree-of-freedom manipulator attached to a moveable base, as illustrated in Figure 1.3. The manipulator arm can reach over 2.3 m (90 in.) from the base, and the total system weight is less than 455 kg (1000 lb). Lee et al. (1993) have developed the inverse kinematics for URSULA. Suction cups hold the manipulator base to the vessel wall while the arm generates precise scanning paths on the curved vessel

surface. After completing a scanning area, the manipulator is repositioned manually using a long pole. Since URSULA is a mobile robot, it needs a base positioning scheme (BPS) that can find the position and orientation of the base after each move. The design, calibration and simulation of a BPS for URSULA using the methodology described in this dissertation is presented in detail in Chapter 6.

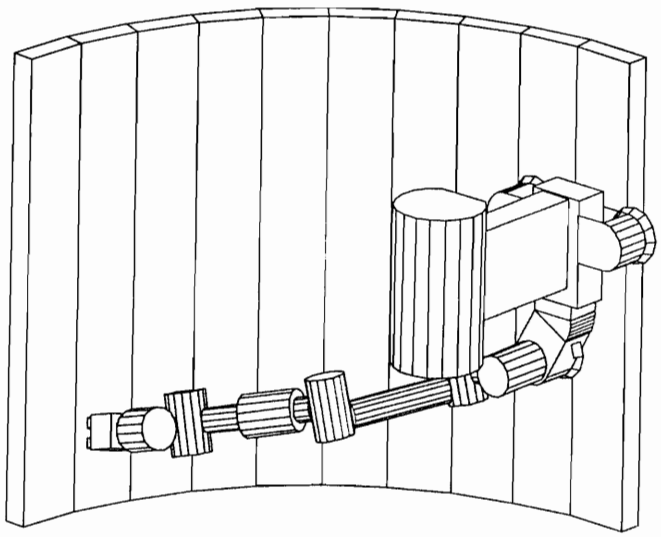

Figure 1.3: Model of URSULA

Currently, the intrinsic parameters of URSULA are precisely measured off-line. This method suffers from the same flaws as described earlier. The parameters being physically measured by this technique are not a direct measure of the kinematic parameters needed.

1.1.2 Calibration Philosophy

The experiences with Cobra and URSULA led to the philosophy that pose error and calibration of kinematic parameters (extrinsic and intrinsic) should be investigated in a unified way with respect to modeling, identification, analysis, and minimization. This methodology should be aimed at impacting the design of new robot systems as well as improving performance of existing systems. An example of new system design is the URSULA BPS design, which is described in Chapter 6. Calibration of URSULA's or Cobra's manipulator intrinsic parameters would be considered as existing system calibration. Another important consideration in the development of this calibration process is specific performance accuracy requirements for the robot system. This is critical because previous calibration techniques do not ensure specific accuracy. Further, a better understanding of the design is gained through error sensitivity analysis, which is an integral part of the proposed methodology. This understanding is useful in providing insight into future robot system design efforts or component upgrades in existing systems. These issues led to the development of the robust calibration methodology presented in this dissertation.

It should be noted that these calibration issues are also common to machine tools, plotters, and other positioning devices. Therefore, this general calibration philosophy can be applied to any computer-controlled mechanical positioning machine.

1.2 Robot Systems

Automation and robotics are closely related technologies. In an industrial context, automation can be defined as a technology that uses mechanical, electronic, and computer-based systems in the operation and control of production. Examples of industrial automation include transfer lines, mechanized assembly machines, numerically controlled machine tools, and robots. There are two broad classes of industrial automation: fixed (or hard) automation, and programmable (or soft) automation. Hard automation is used when the volume of production is high and therefore it is appropriate to design specialized equipment to perform predetermined functions in a manufacturing process very efficiently and at high production rates. An example of hard automation is in the automobile industry where machining operations are performed on engine components in highly integrated transfer lines with many workstations. Programmable or soft automation is used when the volume of production is relatively low and there are a variety of products to be made. In this case, the production equipment is designed to be adaptable to variations in product configuration. This adaptability is made possible by the use of a controller with a program of instructions specifically prepared for the given product. The products are made in batches.

Robotics is a subset of soft automation. An industrial robot is a general-purpose, computer-controlled manipulator which possesses certain anthropomorphic, or humanlike, characteristics. The manipulator typically consists of several rigid links

connected in series by revolute or prismatic joints to form an open chain. The robot can be programmed to move its arm through a sequence of motions in order to perform certain tasks. A complete robot system consists of a robot base, manipulator arm, end-effector tool, a computer/controller, all the necessary cables, feedback devices, and control elements. The term robot originated from a Czechoslovakian play in the early 1920s by Karel Capek, called *Rossum's Universal Robots.* The Czech word "robota" means forced worker, and when translated into English, the word became robot.

Most common industrial robots are permanently installed in a location and are part of a workcell that has been developed for the automation task. More frequently, however, robots are finding application in servicing tasks in hazardous environments such as nuclear plants, toxic chemical sites, and also in deep-sea and space exploration. In such applications, the robot must be able to adapt to the existing environment. New classes of robots have emerged due to these new applications. To better classify these new robot applications, researchers have defined two new classes of robots, namely, portable robots, and mobile robots. Another class comprises robots with parallel manipulators as opposed to serial manipulators.

A portable robot is one that is transported to the field of operation and then installed once. The robot performs all of its functions while installed in this fixed location. The robot base pose needs to be calibrated every time the robot is installed. A good example of a portable robot is Cobra which was described in Section 1.1.1.

A mobile robot performs with its base being moved from one location to another. Every time the robot moves, its base pose needs to be calculated and a suitable base positioning system (BPS) is required. One example is URSULA, where the base is planted at one location and the base pose is found. Then the arm scans the reactor welds and URSULA is moved to a new location and the process is repeated. Another example of a mobile robot is a crawling vehicle that can be used in various applications like environmental site remediation (Stulce, 1995). This type of mobile robot may also function while it is moving.

Parallel manipulators consist of links connected to form one or more closed loops. Salerno (1993) proposes a special parallel manipulator for radioactive waste removal applications. The advantage of parallel manipulators is that the primary members are predominantly two-force members with pure tension or compression. They have a high stiffness-to-weight ratio which enables a light manipulator to carry heavy payloads. They are especially useful when a long reach is desired and serial manipulators are not practical because of bending and torsional loads developed over a long reach.

The robot calibration methodology presented in this dissertation can be applied to any of the classes of robots discussed in this section.

1.3 Pose Errors

Pose is defined as the position and orientation of an object in three-dimensional space. To completely define the pose of an object, six parameters are required. Three parameters are associated with position and three are associated with orientation of the object. If these six parameters are known, then the pose of the object is known.

The pose of a robot end-effector depends on the robot geometry. If there are any errors in the geometric parameters, they can propagate and result in errors in the pose of the end-effector.

1.4 Sources of Pose Errors

Several sources contribute to robot end-effector pose errors. There are three broad classes of pose error sources. These are kinematic or geometric errors, static compliance errors, and dynamic errors. Kinematic errors are errors in the link lengths, link offsets, link twists, initial joint angles, and object geometries. Static compliance errors include link bending and torsional deflections, joint compliance, robot base deflections, etc. Dynamic errors result from dynamic forces and the resulting deflections, and from control system errors. Control system errors consist of overshoot, settling time, and steady-state errors during joint actuation. Backlash in joints is another source of error which does not fall into any of the three previously described classes.

This dissertation addresses the issues of kinematic error sources only. Compliance errors, dynamic errors, and backlash are the subject of future work. Except in special cases like Cobra, deflections are generally not a significant source of errors because, for most industrial manipulators, the payload is only a small fraction of the manipulator link weight. The study of dynamic errors and backlash is beyond the scope of this work.

1.5 Characterization Methodology

The term "characterization" as used in the title of this dissertation is defined as the process of determining the as-built or actual robot system kinematic parameter values. This is required in order to improve the positioning accuracy of robots by minimizing pose errors. The term characterization is a better description for this methodology than calibration. Calibration usually refers to compensation by means of a functional relationship, for example, a look-up table or graph. In the methodology presented in this dissertation, the as-built kinematic parameters are updated in the robot controller. Therefore this process is different than traditional calibration.

The set of geometric parameter values that best fits the measured or simulated robot end-effector position data is identified by using this characterization methodology.

The characterization methodology is summarized as follows. The first step in the process is robot system modeling. The specific problem at hand is studied carefully and the robot is kinematically modeled using well-established link transformation techniques. This

modeling involves the representation of various link parameters like lengths, offsets, and twists and also joint parameters like initial and relative joint angles. This may also involve modeling the workspace, workpiece and tool geometry, robot base pose, and tool pose.

The next step in the process is to use the knowledge gathered about the robot system and its operating environment to identify sources of pose error in the system. This is accomplished by listing all the parameters that are in the system mathematical model. Then, each parameter is studied and, based on the knowledge of the robot component machine tolerances, component specifications (like encoders, joint motors, etc.), tool geometry, workpiece geometry, robot base location tolerances, and other information that is pertinent to the specific problem, the parameters are assigned a range or tolerance of error.

A sensitivity analysis is performed on the error parameters using the previously identified range of error. This helps in identifying and ranking critical parameters based on contribution to pose error. The sensitivity analysis is always modeled to check the effect of errors individually on the bottom-line performance objective. This is a powerful technique because it gives a good insight into the robot system design and performance. The effect of each parameter on the pose error of the robot characterization goal can be visualized directly. This also helps in future design efforts.

If an existing robot system is to be characterized, the next step is experimental data gathering. The robot should be set up in its working environment or an equivalent mockup and the required measurement equipment also should be set up. The measurement equipment should have an accuracy better than the desired robot-performance accuracy. A collected set of pose data is then used to solve the critical parameters previously identified. These parameter values are then incorporated into the controller. The accuracy of the robot should be significantly improved after this procedure.

In the case of new robot system design, this methodology is applied using simulation. In this case the experimental data is gathered using computer simulations. Using this data the values for the critical parameters are determined and then another simulation is performed with these new parameters to check the design performance. Based on the results of the simulation, the design is modified to improve performance or a decision is made to characterize certain parameters.

This characterization methodology is discussed in more depth in Chapters 3 and 4.

1.6 Research Contributions

It is believed that this dissertation represents a significant contribution to the area of robot characterization. Some of the most significant contributions are enumerated below.

1. This research is comprehensive from the development of the robot system characterization methodology through the application of this process.
2. It has been shown that this general robot system characterization methodology is applicable to both an existing industrial robot and to the design of a base positioning system for a mobile robot. Results of these applications are obtained and they are shown to meet the predefined performance goals.
3. This is a performance-goal-oriented approach to robot characterization. The required robot accuracy is specified before the methodology is applied and iteration is performed until the goals are met or until no further improvement is obtained.
4. In the design of new systems this process can be used to gain a cost-performance advantage. If the desired performance is obtained in the simulation, then some manufacturing tolerances can be relaxed or lower resolution components may be sufficient to achieve desired performance.

1.7 Overview of Dissertation Contents

The remaining contents of this dissertation will lay a foundation for general robot system characterization and performance enhancement. Chapter 2 contains a literature review in the areas of robot design and calibration, error modeling, sensitivity analysis and optimization techniques, mathematics, software, and hardware. Chapter 3 contains the description of the first part of the robot system characterization methodology. This includes robot system modeling, identification of error sources, and sensitivity analysis. In Chapter 4, various techniques of experimental data measurement are described followed by optimization techniques and implementation of error parameter values into

the control system. A section is also included that describes the simulation strategy for new robot design. The application of this characterization to a Unimation PUMA 562 industrial robot is described in Chapter 5 along with a presentation of results. Chapter 6 includes the application of this characterization process to the design of a base positioning system for an underwater, mobile, nuclear-reactor-vessel-inspection robot (URSULA). Results are presented at the end of the chapter. Finally, conclusions, recommendations, and suggestions for future work are included in Chapter 7.

2. Literature Review

The literature that is relevant to the work described in this dissertation has been divided into the following five areas: (1) robot system design and calibration; (2) error modeling and analysis; (3) sensitivity analysis and optimization techniques; (4) mathematics and statistics; and (5) hardware. When necessary, a review of the available software has been included in the appropriate section.

2.1 Robot System Design and Calibration

The texts by Craig (1989) and McKerrow (1991) are excellent sources for fundamentals on robot principles, manipulator link representations, forward kinematics, inverse kinematics, etc. Industrial robotics concepts have been described well in Groover et al. (1986).

The problem of improving robot accuracy has been the focus of much attention since the early 1980's. Many industrial robots have repeatability which is several times better than their absolute positioning accuracy. Therefore, there is scope for considerable improvement. Improved positioning accuracy becomes especially critical if the robot is programmed off-line, rather than through a sequence of pretaught positions. In off-line programming, motion of the robot is always described in an absolute sense, and referenced to some global coordinate system.

Hayati (1983) and Hayati and Mirmirani (1985) presented a method for estimating serial-link robot parameter errors. They use a linear kinematic model and add a separate error transform for each link. For non-parallel consecutive joints they use the Denavit-Hartenberg (DH) notation (Denavit and Hartenberg, 1955) and propose a new model for parallel consecutive joint axes for both revolute and prismatic joints because of the singularity associated with the standard link-length definition. They presented results from a computer simulation of the calibration of a PUMA 560 and the Stanford Arm but have not applied it to actual robots. Hayati et al. (1988) build on their previous work and also present a technique to solve the inverse kinematics of the updated robot. Whitney et al. (1984) present the calibration problem and model both geometric and non-geometric errors. The non-geometric errors are gear transmission error, compliance, and backlash. They use a fixed-angle representation to model the links. This includes six parameters per link whereas the DH notation describes a link with only four parameters. Although the geometric model they used is general, the non-geometric errors are modeled for a

specific robot by making direct measurements. They report a sixteen-fold improvement in accuracy. Mooring (1983) studied the effects of joint axis misalignment on robot positioning accuracy. He did not include any of the other link parameters in his study. Mooring and Tang (1984) present a method for robot calibration that is based on using an angle-axis model for link representation. This results in six calibration parameters per link. To model the errors in the links they concatenate six error transformation matrices per link to each of the six links, resulting in an excessive computational burden. They solve the equations by formulating the Jacobian (the problem is linearized by using the first-order terms in a Taylor's series approximation for sine and cosine). No minimization is performed to find the best set of parameters. Stone et al. (1986) have developed an S-Model to describe the robot link kinematics. Each link is represented by 6 parameters. After the link parameter values are estimated, they are mapped into the equivalent DH parameters. Experimental results show the average positioning error was reduced by a factor of 5 to 10. Stone and Sanderson (1988) continued their work with the S-Model and performed a statistical evaluation of the technique. They compare the statistical performance of the S-Model with a conventional model based on mechanical design specifications. Their methodology utilizes Monte-Carlo simulation techniques for the generation of end-effector positioning and orienting errors. Veitschegger and Wu (1986 and 1987) propose adding a fifth parameter to the DH convention to eliminate the consecutive parallel axes singularity. They also include second-order terms in the Taylor's series for sine and cosine in the error matrix model. They compare a first-order

model with the second-order model. The addition of a separate error matrix to the nominal link transformation matrix again makes the problem computationally complex. Chen and Chao (1987) use Euler-angle convention to model the links in the robot. The equations are solved by linearizing them similar to Mooring and Tang (1984). Everett et al. (1987) discuss various error modeling schemes by comparing them using three concepts, which they call completeness, equivalence, and proportionality. They do not recommend any particular model. They also discuss possible higher-pair joints and ways of modeling them. Shamma and Whitney (1987) present a method for inverse robot calibration. Inverse calibration involves finding the best joint angles required to position the robot end-effector at a desired location. The link and joint parameters representing the geometry of the robot are not found. The method consists of finding approximation functions by which corrections are made to the encoder readings. It does not provide insight into the robot link and joint errors. The method has not been tested on an actual robot. Broderick and Cipra (1988) describe a shape matrix concept of calibration. The shape matrix for each link is calculated using geometry. Each joint is individually and successively moved beginning with the last joint and ending with the first. Knowing the two positions of the end-effector for the isolated joint motion, a shape matrix can be determined. Thus the geometry of each link is calculated without any information of the link known beforehand. They have performed a computer simulation of this method. Hollerbach and Bennet (1988) use a laser-interferometry motion tracking system that is automatic so that there is minimal operator interaction required for the measurements of

the robot end-effector position. Menq et al. (1988 and 1989), and Borm and Menq (1991) have studied error parameter space and defined an observability measure. When this measure is increased, the effect of unmodeled and measurement errors are reduced. Therefore, this measure can be used to determine optimal measurement configurations for robot calibration.

The significant references found in the area of robot calibration prior to 1989 have been described so far. There have also been three review papers during this period. Roth et al. (1987) have given an overview of work done in robot calibration. They present basic issues in calibration such as modeling, measurement, identification, and correction. They have classified robot calibration into three levels. Level 1 calibration is defined as "joint level" calibration. The goal is to find the joint zero offsets. A level 2 calibration is defined as the entire robot kinematic model calibration. Level 3 calibration is defined as "non-kinematic" calibration. Here, they include effects like joint compliance, friction, clearance, and link compliance. For each level, the authors describe the four steps involved in the calibration procedure, i.e., modeling, measurement, identification, and correction. They do not present any new research findings. They only discuss work done by other researchers. Ziegert and Datseris (1988) present basic considerations for robot calibration. They examine the effect of kinematic model choice on robot calibration. Section 3.1.1. of this dissertation presents these issues with detailed discussions as applicable to this work. They have also done an extensive review of literature available in the robot calibration area prior to 1988. Hollerbach (1989) presents a survey of

kinematic calibration. This survey is divided into five categories - parametric estimation of endpoint location, nonparametric estimation of endpoint location, robot repeatability, robot registration, and advanced instrumentation for endpoint tracking. There is a comprehensive review of literature until 1989.

After 1989, there was continued work in robot calibration but there have been no new survey papers. Zhuang et al. (1991 and 1992b) have presented observability issues of robot kinematic parameter errors by studying the relationship between end-effector and link Cartesian errors. Based on the error kinematic model and the measurement configuration, they have defined an observability measure. This measure is useful in finding optimal measurement configurations to identify error parameter values. Zhuang et al. (1992) present a kinematic model for robots that is complete and parametrically continuous (CPC). They use six parameters to represent a link. They present the mapping between DH model and the CPC model and present the application to robot calibration. Zhuang and Roth (1991) use the CPC model and a particular sequence of robot pose measurements to present a method for finding the actual kinematic parameters of a robot from the forward kinematic model. Zhuang et al. (1993) build upon their previous work and update the CPC model to bring it closer to the DH model. They call this model the modified CPC model (MCPC). They believe this is a much simpler error model than the CPC model. This model still has six parameters for each link. Berg (1991) performed calibration on three Kuka industrial robots. End-effector position measurements were taken using four theodolites. The theoretical model used for

calibration was not described. Ishii (1991) presents a review of robot calibration. He discusses the need for calibration, geometric and non-geometric errors, kinematic modeling schemes, and measurement techniques. Khalil et al. (1991) have used a modified DH model to represent the kinematics of a robot. They also calculate the number of optimum measurement points by finding the condition number of the Jacobian matrix. Powell's method is used to perform the optimization to solve for the values of the error parameters. The results presented in this work are based on a simulation of the robot calibration process. Renders et al. (1991) have cited various sources and estimate that the positioning error of the end-effector due to non-geometric effects like gear backlash, joint and link compliance, gear transmission errors, and temperature effects is about 10% of the total error. Therefore they address geometric error sources only. They use a modified DH model to represent the robot link kinematics. They have used precision linear axes as a measuring device which has three linear, mutually perpendicular axes. They have modeled the measurement errors of the device by introducing a link between the tool and the measuring device. Another unique aspect of their work is that they use a statistical approach based on a maximum likelihood estimator for errors due to noise and uncertainties like backlash. They have also determined the joint offsets using a separate procedure. They show the position error dropping to 0.5 mm after the calibration. Huang and Masory (1991) present a method for taking robot end-effector position measurements. They use a measurement device that is physically connected to the manipulator end-effector and forms a closed-loop mechanism with the

robot. The measurement device is an articulated mechanical linkage instrumented with position sensors. They have performed simulation studies and show this approach to be feasible, but they do not address the accuracy or calibration of the articulated linkage (measurement device) itself. Toyama and Hatae (1992) have calibrated a SCARA robot based on condition number and error map. The condition number is used to evaluate the measurement configurations. They show results that reduced the position error from 2.2 mm to 0.25 mm. Yang and Sadler (1992) have addressed the problem of joint and link compliance. They present a finite element model to represent the joints and links of revolute jointed robots. They call this element the joint-beam element. Their case studies reveal that joint compliance can contribute significant dynamically induced positioning errors. This modeling technique can be used to include link and joint compliance to the overall robot calibration.

Bay (1993) describes a technique for autonomous robot calibration. A Kalman filter is the basis of the method described. It is used as a linear recursive estimator for automatically finding the next measurement configuration or position. This direction is computed such that the estimates of the kinematic parameters converge faster. This technique has been simulated for a planar two-link robot. The estimator is optimal only for linear parameters. A formulation has been presented to apply this technique to general robots having six revolute joints. The advantage of this method is that a robot could calibrate itself from an initial condition without any operator input. This method is more complete than the technique presented by Borm and Menq (1991), since the

measurement configurations are determined off-line by Borm and Menq before the actual measurements are taken. The noise of the measuring device is not considered in this work. If Bay's technique is successfully applied to a robot with six revolute joints, it may be very useful for autonomous calibration. Goswami et al. (1993) perform calibration on a six degree-of-freedom robot by measuring a single linear position parameter (with a Linear Variable Differential Transformer). They use a data collection scheme that in effect mimics a Stewart's platform for each configuration of the robot. This can be a very time consuming process. Prenninger et al. (1993) present a real time 6 DOF pose measurement system for robot end-effectors. It is composed of a laser tracking system (LTS) that employs one laser beam. This is one of the few systems that can measure both position and orientation. Since it can measure pose in real time, it is an attractive system to use for autonomous robot calibration. This LTS system could be employed in conjunction with the algorithm of Bay (1993). Zak et al. (1991) employ a weighted least squares approach to robot kinematic parameter estimation. Weighting factors for the different measurement configurations are determined from the statistics on the data. They give a greater weight to measurements where the standard deviation of the noise in the data is lower. Zak et al. (1993) have developed a simulation of the calibration process and its evaluation. This is a system that can be used before the actual calibration is performed to evaluate its effectiveness.

2.1.1 *Conclusions from the Robot Calibration Literature Survey*

From the preceding survey, it is clear that no one has attempted to perform a sensitivity analysis of the various error parameters involved on the pose error of the robot. Another aspect that becomes apparent is that none of the previous robot characterization methods have been used in the design of a new robot system. These are two major aspects of the work presented in this dissertation. The literature review is used in this dissertation to provide answers regarding the different robot kinematic models and which models to use. These questions are discussed in detail in section 3.1.1.

2.1.2 *Machine Tool Calibration*

There has been ongoing research in the area of accuracy of machine tools since the mid 80's. Machine tools can also be modeled as robots. They primarily consist of prismatic joints. Some of the papers in the area are by Ferreira and Liu (1986a, 1986b, 1993), Kim and Kim (1991), Kiridena and Ferreira (1994a, 1994b, 1994c), Lin and Ehmann (1993), Wang and Ehmann (1994a, 1994b), Lo et al. (1994), and Mou and Liu (1994). The characterization methodology described in this dissertation can also be applied to machine tool accuracy improvement.

2.2 Error Modeling and Analysis

In this section, a review of literature in error modeling and analysis is presented. This literature is not limited to the area of robot calibration. Some of the literature in error

modeling for robot calibration has already been reviewed in the previous section. The purpose of the literature review presented here is to show the wide scope and importance of error modeling and analysis in engineering.

Chiu et al. (1993) present an analysis method for plane cams. They make use of the principle of offset curve to a plane curve. The offset curves are used in modeling the tool path to manufacture a certain cam profile. The pitch curve of the cam is also an offset curve of the cam profile curve and tool path. The authors perform a sensitivity analysis of the errors which occur during manufacture and assembly of cams. This is useful in the computer aided design and computer aided manufacture of plane cam mechanisms. Menq and Borm (1988) have characterized the position error of robot manipulators. They have studied the statistical properties of the position errors and have characterized them over the workspace. They formulated a linear relationship between the end-effector errors and the link parameter errors via direct geometric projection. There are six parameters describing each link-joint pair. The mathematical model is used to determine the end-effector position error envelopes via the standard linear transformation of random vectors while assuming the individual geometric errors to be independent and normally distributed. These envelopes are shown to be elliptic and are contours of equal probability of position error random vectors. To evaluate the total probability within an error ellipsoid, a variable with Chi-Squared distribution is introduced. The result provides a statistical measure of the position error of the end-effector at the given robot configuration. To characterize the error field over the workspace, five error measure

indices are proposed to show the quantitative distribution of the position error ellipsoid. This work is useful in the design and application of manipulators. Green and Philpott (1994) present an error modeling procedure for reverse-engineered free-form surfaces. This Integrated Reverse Engineering System (IRES) was developed as a research vehicle for process capability analysis, process control, and error tracking during replication. The authors have successfully demonstrated the ability to produce reverse engineered parts directly from an "unknown" surface, and to measure and evaluate associated dimensional errors. They have analyzed the form errors involved in the process by running experiments. The repeatability of the process is good and this process is iterative. A surface is error compensated during each iteration. Convergence to a final form of improved accuracy is therefore achieved. This research also has helped identify the numerous error-creating mechanisms present. Future error compensation algorithms can be improved based on this knowledge. Yang (1992) developed a technique to perform the transmission error analysis of a parallel symmetric geared linkage mechanism. Unsymmetric force transmission between two sides of a parallel symmetric mechanism can occur due to dimensional errors in the mechanism and the clearances in the kinematic pairs. This reduces the efficiency of the machine and also reduces the power-transmission capacity. The author presents the error analysis of a punch press which is a parallel symmetric geared slider-crank mechanism. Yang and Menq (1993) presented a study of the form accuracy of parts having end-milled sculptured surfaces. Their proposed method involves using discrete measurement data from coordinate measuring

machines. This method involves three steps: optimal match, decomposition, and compensation. The optimal match is used to find the best fit between the measurement data and the design form to determine sampled form errors. Decomposition involves characterizing the sampled form errors into the deterministic and the random components, which are associated with the waviness and the roughness of the form errors, respectively. Finally, compensation for the waviness is applied to improve the form accuracy of the end-milled sculptured surface. This process involves at least one sample part to be milled so that measurements can be taken. Yao and Mohd Yusoff (1992) have presented a CAD-based error mapping and layout facility for precision robotic operations. The purpose of this system is to predict the distribution of the end-effector errors over the working volume of the robot. This error distribution is displayed in terms of an error map, such that the spot(s) with the minimum error, consistent with the nature of an operation, can be chosen to carry out the operation or the layout of the robotic cell can be altered. This system is useful in evaluation of robot operations and it reduces trial and error layout and operation tests. The drawback of this system is that it does not include a robot calibration module. This system, in conjunction with a robot calibration system, would be useful for industrial robot operations. Bhatti and Rao (1988) have developed a technique for reliability analysis of robot manipulators. A probabilistic approach to robot kinematics is presented and the concept of manipulator reliability is introduced to obtain a better evaluation of the performance of manipulators. Techniques to compute this reliability are presented. The relationship of manipulator reliability to the geometric

parameters such as tolerances and arm configuration are discussed. Accuracy and repeatability of manipulators are explained in terms of reliability. Dhande and Chakraborty (1973 and 1975) used a stochastic approach for the error analysis and synthesis of linkages and cam-follower systems. Dhande and Chakraborty (1978) build upon their previous work and use a stochastic approach for mechanical error analysis of spatial linkages. Stochastic models of spherical, prismatic, and revolute joints are developed considering random clearances. Following this, stochastic models of RSSR and RRSS linkages are then developed. Mallik and Dhande (1987) again use a stochastic approach to perform the analysis and synthesis of mechanical error in path-generating linkages. The work by Dhande and Chakraborty (1973, 1975, and 1978), and Mallik and Dhande (1987) shows that stochastic modeling of mechanical allowances enables a designer to allocate tolerances and clearances on different design parameters. Moon et al. (1992) have established a statistical model to estimate the effects of robot geometric and nongeometric errors on the quality of operation for various operating speeds. Also, a stochastic optimization problem is formulated to obtain the optimal operating speed for a given accuracy of robotic operation. The errors obtained for different operating speeds can be used in designing and planning robotic operations.

The literature reviewed in this section as well as the literature pertaining to error modeling and analysis in the robot calibration area which was presented in the previous section stresses the importance of this rich and varied research field and how the performance of systems can be significantly improved by performing such error analyses.

2.3 Sensitivity Analysis and Optimization Techniques

Sensitivity analysis is an important tool for the understanding of the effect of error parameters on the goal. Cleghorn et al. (1993) present a technique for optimum tolerancing of planar mechanisms based on error sensitivity analysis. In this case, the goal is the output motion. Here the values of the partial derivatives that form elements of the Jacobian matrix are calculated for a four-bar mechanism. The relative values of these partials are the sensitivity indices, since they can be used as a measure of the contribution to output errors by errors of the input parameters. Examples are presented dealing with typical planar mechanisms. The algorithm is used to obtain and distribute tolerance bands reasonably and economically. Kaizerman et al. (1992) have presented an inverse robot calibration technique that is based on the minimization of the joint variable errors. It is generally impossible to obtain a closed-form inverse kinematic solution to the robot calibration model. Therefore, the authors have used two deterministic sensitivity analysis methods to find the matrix of partial derivatives of the joint variables with respect to the robot link parameters. An example case is presented with simulation of errors. Wu and Lankarani (1992) defined a new parameter called the Transmission Merit Parameter (TMP) which comprehensively reflects the transmission quality and output sensitivity of a mechanism to dimensional disturbance. The TMP is derived from direct differentiation of the independent relationships among the coordinates in the form of the determinant of the Jacobian matrix. This is useful when the mechanism is complex or there is more than one transmission angle. It can also be used in mechanism synthesis as an objective

function that maximizes the transmission quality. The TMP also reflects the output error sensitivity. Zak et al. (1992 and 1994) have presented an approach to optimizing the robot calibration process by including a cost minimization objective along with the residual end-effector pose error objective. This is a multiple-objective non-linear optimization problem. The authors approximate the residual error using a polynomial function known as a response surface. The coefficients of the response surface function are estimated by evaluating the robot's residual error for a number of carefully selected combinations of optimization variables. This can be done either experimentally or by computer simulation. This residual error data is used to estimate the response surface function. This technique was tested by a computer simulation.

2.4 Mathematics and Statistics

Press et al. (1992) have provided a useful reference on mathematics and have also provided programs in C. The chapters on random numbers, minimization, statistical description of data, and modeling of data were especially useful in this work.

Ott (1993) provides a good text in statistics and data analysis. Mathcad is a personal computer based software developed by MathSoft Inc. that is useful in performing mathematical simulations. Mathematica is a numerical and symbolic manipulator described by Wolfram (1991). Quattro Pro is a spreadsheet software developed by Borland. These different software packages were used during different stages of this research work.

2.5 Hardware

Unimation (1987) manufactured the PUMA 562 used in the experiments described in Chapter 5. Science Accessories Corp. (1993) manufactured the acoustic digitizer that is described in Chapter 5. B&W Nuclear Technologies (BWNT) manufactured URSULA, a mobile, underwater robot used for nuclear reactor vessel inspections. BWNT also developed URSULA's base positioning system (BPS).

3. Error Modeling, Identification and Analysis

The literature review revealed that past works suffer from shortcomings in several areas. One significant shortcoming is the lack of a comprehensive methodology that can be applied to new robot system design as well as characterization of existing robot systems. This chapter and Chapter 4 describe an approach that overcomes this difficulty. This chapter treats the subjects of robot system and error modeling, error source identification, and error sensitivity analysis.

3.1 System Modeling

The first step in a successful methodology is to have an effective model. The model should include complete kinematic information about the manipulator as well as a description of the robot base pose in the world coordinate frame and the tool pose in the last link frame. Few researchers have included a complete description of the robot system

geometry in previous studies. The model should also have embedded in it all the parameters that are sources of pose error in the overall system. Also, for mobile robots, it is necessary to model the geometry of the environment in which the mobile robot operates. What follows in the next three subsections is a description of the various parts of the system model.

3.1.1 Robot Link-Joint Modeling

In this subsection the issues of manipulator link-joint modeling as they pertain to end-effector pose errors are presented. Based on this discussion, the model that is most suitable is described.

Five fundamental questions arise from literature review and from studying previous models. These questions are posed in italics in the paragraphs below. Each question is followed by a brief discussion describing the approach used in this dissertation.

- *Should both geometric and non-geometric parameters be included in the error model?*

  No, except in special cases. Renders et al. (1991) have cited various sources of positioning error of the end-effector of an industrial robot due to non-geometric effects like gear backlash, joint and link compliance, gear transmission errors, and temperature effects. They estimate that these errors contribute about 10% of the total error. Geometric parameters like link lengths, link twists, link offsets, initial joint offsets, robot base pose, and tool pose contribute to the remaining 90% of the end-effector pose error. In this dissertation, only geometric parameters are considered in the error model. This accounts for most of the error while keeping

the model as computationally simple as possible. This is important because the inverse kinematics must often be solved in real time while the manipulator is in operation. Also, if force or velocity control is required, then the Jacobian matrix of partial derivatives must be computed. A complex kinematic model makes this more difficult, especially if the model contains discontinuous functions which represent gear backlash or when parameters become functions of joint variables rather than constants. There are examples of special-purpose robots like BWNT's Cobra that have significant link compliance. In such cases it may be necessary to add a scheme to help compensate for deflections.

- *Should the model have a separate error transformation to identify parameter errors or should the correct parameter values be identified and updated in the original transformation matrix?*

  The answer is no. In order to use the model with nominal values plus error transformations, the variations between the ideal and actual link and joint parameters are assumed to be sufficiently small so that they can be approximated as first-order differentials. Higher order terms can be ignored when concatenating the individual link transforms. This assumption means that the nominal parameter values must be accurate. If they are not sufficiently accurate, then the linearization assumption may introduce significant errors in the error identification process. This problem is avoided in this dissertation by attempting to find the proper values of the link kinematic model parameters so that the total manipulator transform yields the best predictions of global positions over the workspace.

- *What number of geometric parameters should be used to represent a link-joint in the robot model?*

  It is well known that six independent parameters are required to describe the relative pose of two coordinate frames in three dimensional space, but it is

possible to represent a link in a robot with less than six parameters because of the geometry and constrained motion of the joints. For example, the Denavit-Hartenberg (DH) model uses just four parameters to represent a link-joint combination. Using the minimum number of parameters is advantageous because the computational problem is simplified and parameter redundancies are reduced or eliminated. The answer is four except is special cases where parameter redundancies exist.

- *Should the same model be used consistently for every link or should different models be used for different links based on link geometry and model suitability?*
  It is believed that each link or transform should employ the model that is most suitable. Therefore, the complete robot system may be modeled using more than one technique. This practice may result in some simplification of the overall kinematic model.

- *Should the robot base pose and the tool pose in the last link frame be modeled?*
  The answer to this question is a definite yes. Not knowing the position and orientation of the robot base can contribute significant errors to the end-effector as they propagate and magnify through the robot manipulator. Many previous researchers have neglected this aspect in their models, as discussed in the literature review.

After considering the afore-mentioned questions, it was decided that the best model to employ for the link-joint modeling was the Denavit-Hartenberg (DH) model. This model is well-established and widely used. Figure 3.1 shows a schematic of the DH model for one robot link. This kinematic representation was originally developed by Denavit and Hartenberg (1955) as a means to model links in lower-pair mechanisms. There are many

variations of the Denavit-Hartenberg convention. They differ in such details as frame numbering. The convention adopted in this dissertation is taken from Craig (1989) in Section 3.4.

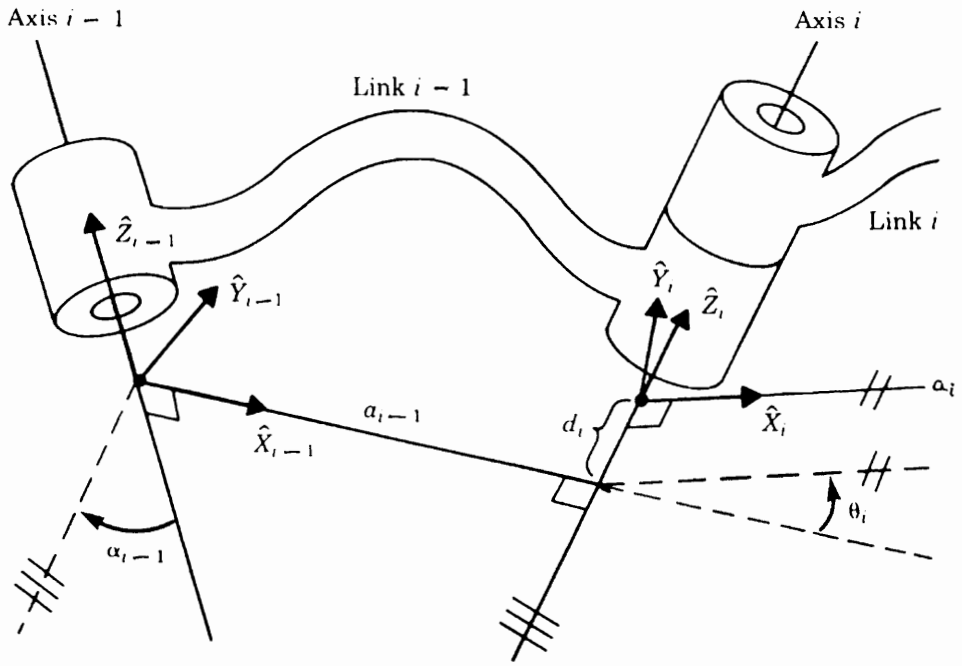

Figure 3.1: Schematic of Denavit-Hartenberg Model

The DH model uses only four parameters to describe a robot link. This is possible because of the way the frames are assigned. The origin of the frame is defined to be at the intersection of the axis of rotation with the common normal between consecutive axes. The X-axis must lie along the common normal. This specification causes the loss of two degrees of freedom in locating the frame, namely a translational displacement along the axis of rotation and a rotational displacement about it. This specification also means that all the parameters that describe a link can be specified only if the location of the previous link axis is known. A brief description of the DH model and the four

parameters is given. During this description, the reader is referred to Figure 3.1. Craig (1989) serves as the source for most of this material.

A manipulator consists of a set of links connected in a chain by joints. A lower pair joint between two bodies means the relative motion is the sliding of two surfaces over one another. Robot manipulators are generally constructed from joints which have just one degree of freedom. The two most common one-degree-of-freedom joints are revolute and prismatic. Revolute joints have a relative rotational motion between the adjoining links. Prismatic joints have a relative translational motion between the links. The base of the robot is considered to be link 0. The first moving link is numbered as link 1 and so on out to the last moving link which is numbered as link n. Usually the end-effector of the serial robot is the last link in the manipulator. Kinematically, a link is a rigid body which defines the relationship between two neighboring joint axes of a manipulator. Joint axes are defined by lines in space. Joint axis i is defined by a line in space, or a vector direction, about which link i rotates or translates with respect to link i-1. In the DH model, a link is kinematically specified by two parameters which define the relative location of the two joint axes in space. For a link i-1, the **link length**, a_{i-1}, is the distance along the common normal between the two joint axes. The second parameter needed to define the relative location of the two axes is the **link twist**. This link twist is measured on an imaginary plane that is perpendicular to the common normal between the two axes; this plane is located such that it contains joint axis i-1. The angle between the projection of axis i on the plane and axis i-1 is the link twist. This angle is measured from axis i-1

to axis i in the right-hand sense about a_{i-1}. This link twist for link i-1 is represented with α_{i-1}.

Two more parameters are required to describe the connection (joint) between two links. A common revolute or prismatic joint axis exists between neighboring links in a robot arm. One parameter that describes the joint connection is the distance along this common axis. This parameter is called the **link offset,** d_i. The link offset d_i is the distance measured along the axis of joint i from the point where a_{i-1} intersects the axis to where a_i intersects the axis. The link offset is variable if the joint is prismatic. A second parameter describes the relative rotation about this common axis between one link and its neighbor. This is the **joint angle**, θ_i. The joint angle θ_i is the angle between a_{i-1} and a_i measured about the axis of joint i. This is variable for a revolute joint.

A frame is attached to each link to describe the location of each link relative to its neighbors. The link frames are numbered according to the link to which they are attached. Frame $\{i\}$ is rigidly attached to link i. The convention used to locate frames on the links is as follows: The Z-axis of frame $\{i\}$, called Z_i, is coincident with the joint axis i. The origin of frame $\{i\}$ is located where a_i intersects joint axis i. X_i points along a_i in the direction from joint i to joint i+1. In the case of $a_i = 0$, X_i is normal to the plane of Z_i and Z_{i+1}. α_i is defined as being measured in the right-hand sense about X_i. Y_i is formed by the right-hand rule to complete the ith frame. Figure 3.1 shows the locations of frames $\{i\text{-}1\}$ and $\{i\}$ for a general manipulator. Frame $\{0\}$ is attached to the robot base, or link

0. This is a fixed frame and is considered to be the reference frame for the robot kinematics. Z_0 is chosen along axis 1 and is coincident with Z_1. Frame {0} is located so that it coincides with frame {1} when the joint parameter (θ_1 for a revolute joint, d_i for a prismatic joint) is zero.

The transformation of frame $\{i\}$ with respect to frame $\{i\text{-}1\}$ is given by equation 3.1:

$$ {}^{i-1}_{i}\boldsymbol{T} = \begin{bmatrix} c\theta_i & -s\theta_i & 0 & a_{i-1} \\ s\theta_i c\alpha_{i-1} & c\theta_i c\alpha_{i-1} & -s\alpha_{i-1} & -s\alpha_{i-1} d_i \\ s\theta_i s\alpha_{i-1} & c\theta_i s\alpha_{i-1} & c\alpha_{i-1} & c\alpha_{i-1} d_i \\ 0 & 0 & 0 & 1 \end{bmatrix} \tag{3.1} $$

where,

${}^{i-1}_{i}\boldsymbol{T}$ is the transformation matrix from frame $\{i\}$ to frame $\{i\text{-}1\}$,
c and s are cosine and sine functions,
a_{i-1} is the distance from Z_{i-1} to Z_i measured along X_{i-1},
α_{i-1} is the angle between Z_{i-1} and Z_i measured about X_{i-1},
d_i is the distance from X_{i-1} to X_i measured along Z_i, and
θ_i is the angle between X_{i-1} and X_i measured about Z_i.

Once the link frames have been defined for the robot manipulator, the kinematic equations are developed. The individual link transformation matrices are computed and multiplied together to find the single transformation that relates frame $\{N\}$ to frame {0}:

$$ {}^{0}_{N}\boldsymbol{T} = {}^{0}_{1}\boldsymbol{T}\ {}^{1}_{2}\boldsymbol{T}\ {}^{2}_{3}\boldsymbol{T} \ldots {}^{N-1}_{N}\boldsymbol{T}. \tag{3.2} $$

This transform, ${}^{0}_{N}\boldsymbol{T}$, will be a function of all n joint variables. The DH model described in this section will be used to describe robot manipulator kinematics in the remainder of this dissertation.

3.1.2 Representation of Position and Orientation

To completely define the position and orientation of a robot base in the world frame, it is necessary to use a six-parameter model. A six-parameter model is also required to represent the tool frame relative to the last link frame of the robot. There are several common methods for representing orientations, including X-Y-Z fixed angles, Z-Y-X Euler angles, and equivalent angle-axis. Section 2.8 in Craig (1989) gives a detailed description of these representations. Position is represented in all the cases by a 3x1 vector. A homogeneous transformation matrix from frame $\{B\}$ to frame $\{A\}$ including rotations using the X-Y-Z fixed angle convention and a translation of x along the X_A axis, y along the Y_A, and z along the Z_A axis is represented as (Craig, 1989):

$$ {}^{A}_{B}\boldsymbol{T} = \begin{bmatrix} c\alpha c\beta & c\alpha s\beta s\gamma - s\alpha c\gamma & c\alpha s\beta c\gamma + s\alpha s\gamma & x \\ s\alpha c\beta & s\alpha s\beta s\gamma + c\alpha c\gamma & s\alpha s\beta c\gamma - c\alpha s\gamma & y \\ -s\beta & c\beta s\gamma & c\beta c\gamma & z \\ 0 & 0 & 0 & 1 \end{bmatrix} \tag{3.3} $$

From equation 3.3 it can be seen that a homogeneous transform contains a 3x3 rotation matrix and a 3x1 position vector. The last row makes this matrix a homogeneous 4x4 transform operator. This X-Y-Z fixed angle convention has been used in this dissertation

to represent the robot base in the world frame and also to represent the tool in the last robot link frame.

3.1.3 Environment Modeling

In the case of a fixed or portable robot system, it is sufficient to model the geometry of links and joints, the robot base pose, and the tool pose. It is generally not required to model the workspace and robot environment in these situations. On the other hand, a mobile robot system will require modeling of its work environment. This is necessary because the robot base pose needs to be calculated every time the robot moves. Therefore, there is a necessity for a base positioning system (BPS). For the BPS to be developed, the work environment of the mobile robot will be modeled. Since this is a situation that is specific to and differs with different mobile robots, there is no general modeling scheme. Chapter 6 contains a description of URSULA's BPS. The nuclear reactor vessel is the work environment of URSULA, and it has been modeled in Chapter 6 as part of the BPS development.

3.2 Identification of Error Sources

Once the robot system has been kinematically modeled, it is necessary to identify the parameters that contribute to end-effector pose errors. These errors are classified as geometric, non-geometric, and dynamic errors. These different classes of errors are

described in the following sub-sections. Again it should be noted that only geometric errors are addressed in this dissertation in the robot system characterization methodology.

3.2.1 Geometric Errors

Geometric or kinematic errors are due to manufacturing errors like machining and assembly. The machined parts deviate from the nominal dimensions due to the tolerances specified. When a significant number of these machined parts are assembled together to form the robot, the tolerance stack-up causes the kinematic errors in the system. Other kinematic errors are also present which are due to location or placement of the robot base in the workcell and placement of the tool relative to the last link frame. A list of these geometric error parameters follows:

1. *Position and orientation of the robot base in the world coordinate system.* There are a total of six geometric error parameters due to the imprecisely known location of the robot base. Three are the robot base position parameters and three are the robot base orientation parameters. The robot base location is represented by the transform given in equation 3.3. To start with, the nominal values of these parameters are known and used in the transform. When the robot system has been characterized, then the actual values of these parameters are calculated and updated into the transform.
2. *Link and joint geometry.* When the DH representation is used, these parameters include the kinematic link length a_i, link offset d_i, and link twist α_i for a revolute jointed manipulator. For each link these three parameters are geometric error parameters. For a six-revolute-joint robot arm, there are a total of 18 link and joint geometric parameters. This is also the case if any prismatic joints are present.

3. *Initial joint angles.* Due to the joint encoder mounting and the drive from the motor to the joint, the initial kinematic joint angle will not be an exact match with the joint encoder zero. For every joint, these initial joint angle values need to be found so that they can be added to the encoder values. In case of prismatic joints the initial joint linear displacements need to be found.

4. *Tool position and orientation.* The description of the tool location relative to the last link frame of the robot system is accomplished by three position and orientation parameters. Errors in these six parameters also contribute to geometric error. Equation 3.3 is used to represent the tool pose in the end-effector frame.

5. *Workpiece pose and knowledge of robot work environment.* In certain robot operations, the end-effector tool performs operations on a workpiece. The pose of this workpiece must generally be known beforehand. Inaccurate workpiece pose will also contribute to errors in the robot operation. An extension of this concept is the knowledge of the robot workspace. The accuracy to which the workspace is known effects how well the robot will perform.

6. *Mobile robot base positioning system (BPS) calibration.* This situation is specific to mobile robots. Since mobile robots require a BPS, the accuracy to which the base pose can be found depends directly on how well the BPS has been calibrated. The calibration of the BPS involves determining its intrinsic geometric parameters. An example of such a calibration is described in Chapter 6 for the case of the BPS of URSULA.

The geometric parameters described above are directly embedded in the kinematic model of the robot system. After identifying the error parameters it is helpful to determine limiting values for these errors. A tolerance for each of these errors is defined based on the knowledge of the system and its component specifications. Mechanical drawings and

component specification sheets are helpful in finding this information. These error ranges are important for use during the sensitivity analysis phase.

The relative positioning errors of actuators are not modeled during the characterization process because this information is used as the basis for the characterization. During the simulation of new robot system design, the joint actuator errors are considered.

3.2.2 Non-Geometric Errors

Errors in the end-effector pose that are not due to the kinematic model description are partly due to non-geometric effects. Some of these are due to thermal expansion/contraction of the links, gear transmission errors, and compliance. The gear transmission errors are an accumulation of gear eccentricity, backlash or binding, and drive assembly errors. Compliance effects may be due to deformations in robot base, links, joints, mechanical connections, and end-effector tools caused by bending, shear, axial, and torsional loads.

As discussed in section 3.1.1, errors due to non-geometric effects are not modeled in this dissertation. Some researchers have addressed these errors partly in their work as described in the literature review of section 2.1.

3.2.3 Dynamic Errors

Some errors are introduced by the control system which are dynamic in nature. These dynamic errors include overshoot, settling time, and steady-state errors during joint actuation. Addressing these errors is beyond the scope of this dissertation.

Noise in measurement observations can be incorporated into the model by using estimation theory (Nahi, 1969; Melsa and Cohn, 1978; Jaech, 1985). Estimation is the process of extracting information concerning a parameter from noise-corrupted observations (experimental data). Estimation is a statistical process that involves modeling the randomness and uncertainties in the experimental data.

3.3 Error Sensitivity Analysis

The geometric parameters have a greater effect on the pose errors than others. It is useful to identify the most critical parameters based on their contribution to the end-effector pose errors. This can be accomplished using the sensitivity analysis technique described later in this dissertation. The objective of sensitivity analysis is to determine the effect of individual parameters on overall system output. Sensitivity analysis methods can be used to complement the physical model for three main purposes: (i) determine the sensitivity of the solution to the input parameters, (ii) identify critical parameters, and (iii) assess confidence levels of the result and uncertainties in parameter estimations.

Kalman filters can also be used to perform sensitivity analysis (Norton, 1986; Catlin, 1989). A Kalman filter is a linear minimum-variance estimator. The Kalman filter is the best linear filter for any distribution and it is the best filter of all possible linear and nonlinear estimators if the measurement noises as well as the initial state are gaussian. Sensitivity analysis is performed by the Kalman filter by weighting through the covariance matrix. It is believed that a better understanding of parameter error distributions is required before estimation theory can be applied to this work. Although Kalman filters are not used in this dissertation, it is recommended to use them in future extensions of this work.

3.3.1 Sensitivity Analysis Techniques

Common sensitivity analysis techniques include systematic perturbation methods, random perturbation methods, and analytical methods.

One method for performing systematic perturbation is the Brute Force Method (BFM). In BFM, the system of equations representing the physical problem is solved repeatedly by varying one input parameter at a time while keeping all others unchanged. This approach, with minor variations has been applied in Chapters 5 and 6. The variations include the way in which the individual parameters are perturbed. Another variation is to keep the individual parameters unchanged while perturbing everything else to their extreme values. Although the BFM requires more computation time than other methods, it is easily implemented and reliable.

3.3.2 *Sensitivity Analysis Results*

The results of the BFM sensitivity analysis are used to find the most critical parameters in the order of their effect on the system goals. The tolerance of these critical parameters is known beforehand. At this point, the strategy may differ depending on whether a new robot system is being designed or an existing system is being calibrated.

3.3.3 *System Design Strategy*

The critical parameters that are identified through the sensitivity analysis are studied. Each parameter perturbation value and its effect on the output is evaluated. If the results are reasonable, then the design is left as it is for that particular parameter dimension and tolerance. If the effect is deemed undesirable, then a decision is made whether to keep the design and calibrate the parameter after building it or to change the design. If a decision is made to change the design, then a tighter tolerance may be specified or the design may be completely revamped. A detailed case study that helps to highlight some of these points is presented in Chapter 6 for the design of URSULA's BPS.

3.3.4 *Existing System Characterization Strategy*

For an existing robot system, the list of critical parameters is analyzed and, based on their individual effects, parameters to be calibrated are identified. This decision depends on the allowable end-effector pose error specification. By studying the individual effects of the parameters and the magnitude of pose error they contribute, the parameters to be

calibrated are isolated. Once the parameter characterization process is completed, the actual parameter values are updated and the overall system is tested for end-effector pose error. If the error is out of the specified bounds, then a few more parameter are added to the list of parameters to be calibrated. Thus, this is an iterative process.

In this chapter, the first three steps of the characterization process have been described. Namely, the system modeling, error source identification and error value tolerancing, and the error sensitivity analysis. Chapter 4 contains a description of the remaining steps in this process.

4. Error Minimization and System Update

The preliminary steps in the robot system characterization methodology were discussed in Chapter 3. The remaining steps will be discussed in this chapter. For the case where an existing system is to be calibrated, the next step is to gather accurate experimental data on robot position. Following this, an error minimization is performed on the critical error parameters using the experimentally gathered position data. This minimization finds the values of the critical system parameters that best fit the gathered position data. Once the critical system parameter values are found, they are implemented into the robot control scheme. All of these steps are described in this chapter. Also, for the case of new robot system design, a strategy for system simulation is presented such that the system design goals are satisfied as far as end-effector pose accuracy is concerned.

4.1 End-Effector Position Measurement Techniques

To characterize a robot it is necessary to find the actual values of the parameters used in the kinematic model by the control system for off-line programming. If the nominal (design) values of these parameters are used instead of the actual measured or computed ones, a significant amount of error may accumulate in the desired pose of the end-effector. In order to find these actual system parameter values through optimal calibration, position measurements of the robot end-effector must be taken and the joint angles that produced these end-effector poses recorded. Once this data is recorded, the best values of the system parameters that fit this data can be found by solving the kinematic equations and using the recorded position data. The natural questions that arise now are where to take the data, how much data to take, and what method should be used to take the data.

System identification is a subset of estimation theory (Norton, 1986). Identification is the process of constructing a mathematical model of a dynamical system from observations and prior knowledge. As mentioned in section 2.1 researchers like Borm and Menq (1991) have addressed the problem of where to take data in the robot workspace by defining an observability measure using system identification principles. This is an efficient way to collect data as just the minimum amount of data is probably sufficient. On the other hand, if data is taken such that the robot arm configurations span the entire workspace, then it should be satisfactory. This would take into consideration the arm

characteristics over the entire workspace. The minimum amount of required data depends on the number of parameters that are being identified. If end-effector point position data is being taken, then each data point corresponds to three scalar kinematic equations. This implies that the minimum number of points required is one-third the number of parameters. Although this leads to a unique solution, it will probably not be the best solution. In reality, it is better to take as many point measurements as possible and cover as much of the workspace as is feasible in order to optimally define the robot geometry. In this way, a solution can be found that best fits the acquired data in a variety of robot configurations. The approach followed in the examples of this dissertation is to take as much position data as possible. Since this calibration process is performed with the robot off line, computation time and efficiency are lesser issues. In case a more time efficient and autonomous method is desired in future, then methods proposed by Bay (1993) or Borm and Menq (1991) can be adopted. If the robot operates in a subset of the workspace, then measurements should be taken in the local workspace of operation. This will give the best definition of the robot geometry for the specific local workspace.

The remaining question to be answered is how to take the measurements. The following sub-sections will briefly describe some techniques for measuring the robot end-effector position.

4.1.1 Laser-Based Techniques

Several common position measurement methods employ a laser. These include laser interferometry, intersecting laser planes of light, and a custom designed method in which a laser is mounted at the end of a robot arm. A brief description of these laser-based position measurement techniques follows.

Laser interferometry offers accurate, precision measurement in working volumes as large as 28.3 m^3 (1000 ft^3). Brown et al. (1986 and 1988) give a detailed description of one such system which consists of a laser tracker, one or more retro-reflectors on a moving object, a laser position sensor coupled to servo motors on the tracker, and an interferometer. A six axis pose measuring system employs multiple trackers to measure the position of three retro-reflectors. Each tracker is encoded to accurately measure the laser's azimuth and elevation pointing angles, while interferometry is used to measure the distance along the beam's length. Positions can reportedly be measured to within 8 microns (0.0003 in.) in 3.05 m (10 ft.).

Another laser-based position measurement system consists of a mobile detector and two or more scanning heads (Spatial Positioning Systems, 1995). Each head produces two moving planes of light that scan a large workspace. The detector's position defines the intersection of the planes of light, which then gives the detectors position in the workspace. This position is calculated from two sets of azimuth and elevation angles from the two heads.

A third measurement system includes a laser which is physically mounted on the robot arm at a certain known location. Three or four accurately located targets are placed in the workcell such that the laser beam can be pointed at these targets. The targets may consist of light sensors. The target locations in the world frame are known. Now the laser is aimed and pointed at the targets and the joint angles are then recorded. This process is repeated for many configurations of the robot arm; the same target can be shot with different arm configurations. With enough data, the required geometric parameters of the robot can be calculated. This approach was implemented by the Robotics and Mechanisms group at Virginia Tech as a possible solution for BWNT's URSULA BPS problem. The first two laser-based systems described offer high performance, but they involve many complex components and are expensive. The laser-on-arm method is not expensive, but it involves careful design and assembly of the laser fixture, and it depends on accurate knowledge of the targets if the base position of the robot is desired, which is true in most of the cases.

4.1.2 Acoustic Systems

Acoustic systems use the time of flight of acoustic signals to determine the distance between acoustic source/receiver pairs. Expensive tracking hardware is not required for most acoustic systems because sound can propagate in all directions. Tidwell et al. (1993) describe such a system for measuring the pose of an underwater mobile robot (URSULA) in a nuclear reactor vessel. Accuracies of 20 mm (0.8 in.) are possible when

operating at ranges up to 100 m (328 ft.) in homogeneous underwater environments. Another acoustic system, used in air, consists of a hand-held pointing device and a fixed digitizing frame that contains three or more sound receivers (Science Accessories Corporation, 1995). Two sound emitters, precisely mounted on the pointing device, help the tip of the pointer to be located within the digitizer's workspace. The pointing device can be attached to the robot end-effector for the purpose of taking position measurements. This system has been employed as the measurement system for the application described in Chapter 5. Accuracies of 0.5 mm (0.020 in.) are reported in volumes of 2.4 m^3 (85 ft^3) as a result of testing done by the author. Acoustic systems are less expensive than those based on laser interferometry, but they are not nearly as accurate and are sensitive to acoustic noise interference and variations in the propagation medium.

4.1.3 Calibration Template

Another approach for measuring end-effector position involves physically touching known points on a calibration template. A pointer-like touch probe is attached to the end-effector. The calibration template is a precise grid of known points rigidly located in the workspace of the robot. The template's location is also known in the world frame which is needed if the robot base pose is to be calculated. Care must be taken to locate the pointer exactly at the grid point with minimal applied force. This can be simple to implement over a small portion of the robot's workspace, but it may be impractical to build a template such that the whole robot workspace is covered. As a result of this, the

parameters that are identified will be reflecting the arm characteristics only in that small region of the workspace.

4.1.4 Computer Vision

Computer vision offers many approaches to sense the pose of objects, including stereo, multi-view monocular, and single-view monocular imaging. Stereo vision utilizes corresponding points in images obtained from two cameras with a known relative pose. The advantage of this method is that specific prior knowledge about the object geometry is not required. The disadvantages are that two cameras must be used and establishing a correspondence in the two images can be difficult. Multi-view monocular imaging is similar to stereo, but uses a single camera that undergoes known relative motion to create multiple images of the same object. Single-view monocular imaging requires only a single view from one camera and can be used if prior knowledge of the object geometry is available. The camera can be mounted on the end-effector with a known geometric object located in the workspace or vice versa. In some applications, computer vision can provide pose accuracies that are substantially better than acoustic systems, and at significantly lower costs than laser systems. The disadvantage to this approach is the long development effort that is often required. The time involved in developing the vision algorithms and in calibrating the camera can be extensive. Fallon et al. (1994a) describe a method to compute the static pose of a workpiece relative to a robot end-effector. Fallon (1995) also presents a technique to improve the positioning performance

of robots by using computer vision. Both the work described in this dissertation and Fallon's work have the goal of improving the positioning capability of robots. The two approaches proposed to achieve the common goal, however, are vastly different. These approaches are not mutually exclusive though, they can be combined to achieve the best of both control methods. Using a built-in vision measurement system to optimize the system calibration parameters as described earlier would be such a common approach. This optimization can be easily performed whenever required, especially after the robot is serviced or re-configured. In addition, the vision system could provide pose information for small control corrections and quality assurance verification.

4.1.5 Theodolite

A theodolite is an instrument that is commonly used in surveying (Cooper, 1982). It gives the azimuth angle of the target relative to the instrument and elevation angle of the target relative to the horizontal. A ranging theodolite also gives the horizontal distance from the theodolite to the target. Either a theodolite or a ranging theodolite can be used as the end-effector position measurement system. If a theodolite is used, it is necessary to use at least two which are placed at fixed known locations in the world frame. A target is placed on the end-effector tool. This target is tracked manually by the two theodolites and two sets of azimuth and elevation angles are obtained. Using triangulation the end-effector position can be measured. If a ranging theodolite is used instead, only one is

needed. It gives the azimuth and elevation angles as well as the range distance information.

4.1.6 Precision Linear Axes

There are precision instruments available with one two, or three linear axes. One such instrument is a Coordinate Measuring Machine (CMM). These linear axes may have sub-micron resolution. One possibility is to use the CMM as the end-effector position measurement system. The end-effector has to be moved to the desired location and then the CMM tool is moved appropriately such that the desired position is measured. Another very precise set of axes is the Anorad axes. They have a resolution of 0.2 microns. Other companies, such as Adept, have linear axes that are modular and can be used to build a custom set of axes (either one, two, or three). For a linear travel of 1000 mm, the positional accuracy of the Adept axes is 50 microns.

The techniques for measuring a robot's end-effector position that were presented here are not intended to be comprehensive. Other techniques like photogrammetry, techniques involving using Linear Variable Differential Transformer (LVDT), and other custom-made methods are also available.

4.2 Error Minimization Techniques

Reinholtz (1983) gives a concise introduction to the theory of optimization. He has applied optimization theory to the synthesis of spatial mechanisms. The purpose of optimization is to find the best result for a given set of circumstances. The best result is usually a minimization or a maximization of some scalar objective function. A maximization problem can usually be represented without any loss of generality as a negative minimization problem. The optimization problem is formulated such that the objective function is expressed as a function of a set of design parameters or variables over which the user has control. Allowable values of the design variables may be limited by constraints which are also expressed as functions of the design variables.

An optimization problem can be stated in the following general form (Rao, 1984):

Find $$\boldsymbol{X} = \begin{Bmatrix} x_1 \\ x_2 \\ \cdot \\ \cdot \\ \cdot \\ x_n \end{Bmatrix} \tag{4.1}$$

which minimizes $f(\boldsymbol{X},\Theta)$ subject to inequality constraints

$$g_j(\boldsymbol{X},\Theta) \leq 0, \qquad j = 1,2,\ldots,m \tag{4.2}$$

and equality constraints

$$l_j(\boldsymbol{X},\Theta) = 0, \qquad j = m+1, m+2, \ldots, p \tag{4.3}$$

Here Θ is an independent set of input variables having a predetermined range, $\boldsymbol{X}$ is called the design vector, and $f(\boldsymbol{X}, \Theta)$ is called the objective function. The design vector $\boldsymbol{X}$ contains the design variables $x_1, x_2, \ldots, x_n$. The end-effector of a 6 degree-of-freedom robot can be described in the world frame by:

$$ {}^{W}_{T}\boldsymbol{T} = {}^{W}_{0}\boldsymbol{T}\ {}^{0}_{1}\boldsymbol{T}\ {}^{1}_{2}\boldsymbol{T}\ {}^{2}_{3}\boldsymbol{T}\ {}^{3}_{4}\boldsymbol{T}\ {}^{4}_{5}\boldsymbol{T}\ {}^{5}_{6}\boldsymbol{T}\ {}^{6}_{T}\boldsymbol{T} \tag{4.4}$$

where,

W denotes the world frame,
T denotes the tool frame,
0 *denotes the robot base frame,*
1, 2, ..., 6 *denote the robot link frames,*
${}^{W}_{0}\boldsymbol{T}$ *and* ${}^{6}_{T}\boldsymbol{T}$ *are represented using the fixed angle convention as shown in equation 3.4,*
and the remaining link description frames are represented using the DH convention as shown in equation 3.1.

The position of a point in the tool frame can be described in the world frame using the result from equation 4.4 as:

$$ {}^{W}_{T}\boldsymbol{T}\ {}^{T}\boldsymbol{P} = {}^{W}\boldsymbol{P} \tag{4.5}$$

where,

${}^{T}\boldsymbol{P}$ *is the position vector defining the point in the tool frame, and*
${}^{W}\boldsymbol{P}$ *is the position vector defining the same point in the world frame.*

Equation 4.5 is a homogeneous vector equation. It contains three scalar equations that represent the x, y, and z coordinates of the point. In the robot system characterization

problem, the design variables are embedded in ${}^{W}_{T}\boldsymbol{T}$. The objective of the optimization problem is to minimize the error between the measured positions of the tool and the nominal values of the tool position. A logical, popular, and tried-and-tested approach to such problems has been to minimize the sum of the squares of the position vector errors for all the data points. This approach is called the least squares minimization. The objective function (O.F.) for the robot system characterization problem is:

$$\sum_{i=1}^{n} \left\| {}^{W}\boldsymbol{P}_{i}^{Measured} - {}^{W}\boldsymbol{P}_{i}^{Nominal} \right\|^{2} \tag{4.6}$$

where,

n is the total number measured data points.

This minimization problem can be solved using an unconstrained nonlinear optimization technique. Most of the available nonlinear optimization techniques have been developed for solving unconstrained problems. This is not a serious limitation because most of these methods can be extended to handle constrained problems, either by directly considering the constraints or by transformation to an unconstrained problem by using penalty functions. Unconstrained nonlinear minimization techniques are divided into two groups: direct search methods and descent (or gradient) methods. The gradient methods require either an analytical or a numerical derivative of the objective function with respect to the design variables, whereas the direct search methods do not. The direct search methods include random search, grid search, pattern search (Powell's method and Hooke and Jeeves' method), method of rotating coordinates (Rosenbrock's method), and

simplex method. The descent methods include steepest descent method, conjugate gradient method (Fletcher-Reeves), Newton's method, and variable metric method (Davidson-Fletcher-Powell).

Eason and Fenton (1974) have given a comparison of the many optimization methods commonly used to solve mechanical design problems. None of the codes tested by them fulfilled their requirement that ideal computer code for design optimization should solve any problem conveniently and at moderate cost. One method did stand out above the others though, namely, the pattern search method of Hooke and Jeeves.

More rigorous identification can be accomplished by using estimation theory to model observation noise (Deutsch, 1965).

4.2.1 Hooke and Jeeves Method

Based on the findings of Eason and Fenton's (1974) regarding the Hooke and Jeeves method and examples of successful application to kinematics problems such as Reinholtz (1983), it was decided to use the Hooke and Jeeves method to solve the optimization problems in this dissertation.

This method is a direct, sequential stepping technique consisting of alternating exploratory and pattern moves. The exploratory move seeks to determine the local behavior of the objective function, and the pattern move uses this information in an attempt to jump to an improved position. Reinholtz (1983) gives a detailed description of

this method for a two-dimensional problem. Calkins (1995) developed the implementation of the Hooke and Jeeves algorithm that was used in this work. It also incorporates range penalty functions in case the design variables are constrained to lie in a particular range. The kinematic equations and the objective function must be supplied by the user. This method was found to be extremely robust and powerful, though it may not be as efficient as other methods. It should be cautioned that none of the nonlinear optimization methods can discriminate between a local and global minimum.

4.2.2 Other Methods

Another method was tested for this application which involved utilizing the direction of steepest descent in conjunction with line-searching techniques. This method was quicker in converging to minimum than the Hooke and Jeeves method, but it was less robust. The reader is referred to Rao (1984) for details on other nonlinear optimization techniques.

4.3 Control-Strategy Implementation Techniques

Once the critical robot system parameters are determined through optimization, their values need to be used in the kinematic model of the control system. This section describes the some ways in which this can be accomplished.

4.3.1 *Calibration Process Goals*

Before implementation can be attempted, it is important to check the characterization results. The optimized values of the parameters are used in the robot system model and a few new data points are used as the test set. The joint angles required for the newly measured configurations are stored. Now the end-effector position is calculated using the updated system model and compared with the measured positions. If the results are within the specified accuracy, the process can be stopped here. If the results are not satisfactory, additional manipulator parameters can be included in the optimization process. This procedure is repeated until the required accuracy is reached or until the parameter set is exhausted and no further improvement can be obtained.

4.3.2 *Denavit-Hartenberg Parameter Update*

One method for the implementation of the optimized system parameter values in the control system is to directly update the DH table and the base and tool transforms. This effectively redefines the geometry of the robot system to better match the measured results. This may at first appear simple from an implementation point of view. However, it is cautioned that this will significantly complicate the inverse kinematics of many robot systems. This is because almost all industrial robots take advantage of special geometry to simplify the inverse kinematics. Inverse kinematics solutions for a general six-revolute-joint robot are presented by Lee et al. (1991). They present a closed-form method for deriving the 16th degree polynomial defining the inverse kinematics.

Numerical techniques are then used to solve this polynomial. Once the sixteen solutions are presented, it is necessary to isolate the correct and required solution. This may be a non-trivial task. Almost all commercially available robots have a simplified geometry that leads to a governing equation of degree four or less. Changing even one parameter value by a small amount may lead to the general sixteen degree polynomial solution.

Another approach to the inverse kinematic computation is to iterate on the forward kinematics. This is the approach employed by the robot simulation software developed by New River Kinematics (1995) called Rhobot Pro. This software has been used in this dissertation as a tool for checking results and as a visualization aid. Rhobot Pro is also used to control the PUMA 562 robot that is discussed in Chapter 5. It is capable of accepting updated values of the robot parameters.

4.3.3 Goal Mapping

Another approach to implementation of optimization results is called goal mapping. This involves developing an algorithm and implementing it in the control system. Essentially this algorithm converts the target goal position of the end-effector into a fictitious goal such that the end-effector actually moves to the desired goal. This is because the control system still has the nominal values for the robot system parameters, but the goal mapping algorithm uses the optimized values to give a fictitious goal. The advantage of this approach is that the nominal values in the control system are untouched and hence the

inverse kinematics is not complicated. The disadvantage of this approach is that the goal mapping algorithm itself may be difficult to develop and implement.

4.4 Simulation in the Design of New Robot Systems

If a robot system design exists only on paper, it will not be possible to take measurements of the end-effector position. Therefore, it is necessary to simulate the robot system with some error introduced in the system parameters to check for their effect on the end-effector positional error. This simulation is intended as a design tool to help in arriving at the optimum design for both cost and accuracy performance. The steps in this simulation process are similar to those in the existing system characterization process. The first step is to model the robot system using the techniques presented in Chapter 3. Then, all the error sources are identified and their ranges are defined based on the components selected and the manufacturing tolerances. The system model, the error parameters, and their ranges are used to perform a sensitivity analysis on the end-effector positional error. Critical parameters are isolated and ranked in the order of their effect on the output error. The next step is to simulate errors and get end-effector position information in lieu of taking measurements. This is described in the following sub-sections.

4.4.1 Define Real World and Ideal World

Simulation of the errors in a robot system involves defining the real world and the ideal world. The real world is the as-built robot and the actual environment, i.e., it contains

errors. The ideal world is the nominal robot and its nominal environment, i.e., all values are exact. To simulate the real world, the critical error parameter values are randomly generated within their respective ranges. These randomly generated values are added to nominal parameter values to define a possible as-built case. At this point, we have a computer simulated as-built robot and its environment. This simulated robot is moved through a pre-determined sequence of joint motions and the end-effector position is recorded along with the joint angles for a series of points in the workspace. Some error can also be added to the end-effector position to simulate the measurement system error. Now, we have simulated measurement data. To get the nominal end-effector position, the ideal world simulation, which contains the nominal kinematic model for the robot system, is used.

4.4.2 Calibration of Critical Parameters

The simulated measured position information is used along with the nominal position information to go through an error minimization process similar to the one described in section 4.2. The optimization results are used to update the critical parameter values in the control system. Then, the newly designed robot system is tested using the modeled results at new points to see if the positional accuracy is acceptable. If the accuracy is acceptable, then the design is deemed acceptable and further development is undertaken. If the accuracy is still unacceptable, then either more accurate components (e.g. more accurate joint encoders) are selected or tolerances on the machined parts are made tighter.

Another option is to decide to add more critical parameters to the list that needs calibration and repeat the simulation. After this second simulation if the robot system meets the accuracy criteria, then the next step is to perform a rigorous overall simulation which is described in the next sub-section. If the desired accuracy is still not met, then the process is repeated until the robot performance is satisfactory.

4.4.3 Testing of Simulation

This overall simulation is performed to test the robustness of the design before the robot is actually built. The simulation involves performing a random generation of error values and going through the previously described calibration/design evaluation simulation over and over many times. The end-effector positional error is the ultimate evaluation criterion. This error is calculated at the end of each simulation iteration. Using a random generation of error parameter values in each iteration and a significant number of iterations, the design's robustness is tested. All the positional error information can be graphed and analyzed to see if it is within acceptable range and confidence interval. If this overall simulation gives acceptable results, the design can be further developed and built. If the results are not satisfactory, then more precise components must be selected or the overall system must be redesigned.

This chapter dealt with end-effector position measurement techniques and critical parameter optimization techniques for existing robot system characterization. It also contains a general strategy for simulation of a robot system design for end-effector

positional accuracy evaluation and parameter calibration. This simulation technique has been applied to the BPS design of URSULA in Chapter 6.

5. Application to an Industrial Robot

This chapter describes the application of the robot system characterization methodology to a PUMA 562 existing industrial robot. A brief description of the PUMA robot is presented first. Then the PUMA system model is developed, followed by the identification of sources of pose errors in the robot system. Next the sensitivity of the PUMA system parameters is discussed. The results of the sensitivity analysis are used to isolate the critical error parameters that require optimization. The experimental position measurement system (an acoustic digitizer) is then described followed by a description of the measurement process. The acoustic digitizer performance is first tested and statistically characterized before it is used to take robot end-effector position measurements. The critical parameters are then optimized using the data gathered in the experimental position measurement process and the results are discussed. Finally, these

optimized parameter values are implemented into the robot control system. The desired end-effector positioning accuracy for the PUMA system is ± 2 mm.

5.1 Description of the PUMA 562 Robot

The UNIMATE PUMA 562 robot is a computer controlled serial robot system manufactured by Unimation Incorporated, which was a Westinghouse company in 1987, the year in which this particular robot was manufactured. The PUMA 562 has six rotational degrees of freedom. A model of the PUMA 562 robot base and serial arm is shown in Figure 5.1. All the coordinate systems are also shown. The coordinate frames were assigned using the Denavit-Hartenberg convention described previously.

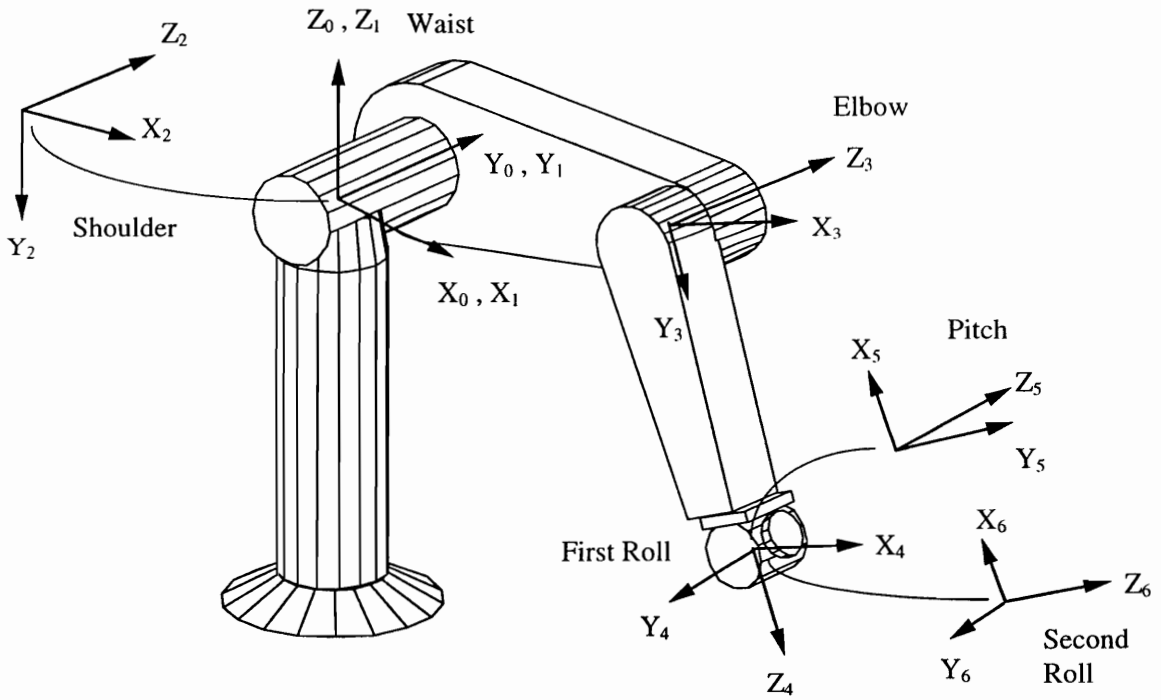

Figure 5.1: Model of PUMA 562

The coordinate frame with subscript 0 is the PUMA fixed frame. This frame is also referred to as the base frame. Frame {1} is attached to the waist joint. The base frame is coincident with the waist joint frame when θ_1 (waist joint angle) is zero. Frame {2} is attached to the shoulder joint. Frame {3} is attached to the elbow joint. The shoulder joint axis and the elbow joint axis are parallel. The axes of joints 4, 5, and 6 have a common intersection point at their origins. The joint axes 4, 5, and 6 are all mutually orthogonal. In many industrial robots, these three joints are referred to as the wrist joints. The wrist joints are in a roll-pitch-roll configuration. Joint 4 is the first wrist roll axis, joint 5 is the wrist pitch axis, and joint 6 is the second wrist roll axis.

Along with the robot arm, the PUMA 562 system consists of the controller, teach pendant, software (VAL II), and peripherals. The controller houses the components that control and power the robot arm. The peripherals include the Video Display Terminal and a disk drive unit. The teach pendant is used to manipulate the PUMA end-effector to desired locations. These locations can be recorded by the teach pendant to enable future robot moves to the same position. Robot programming can be done through the teach pendant or the video display terminal keyboard. In any of the programming methods, all taught points are stored as precision points (position information stored in the form of joint angles), transformations (point locations referenced to the robot base fixed coordinate system), or compound transformations (point locations referenced to previous locations as a measurement from a Cartesian coordinate system fixed to the robot tool

mounting flange). Real-time computations are performed during the actual running of the robot programs to convert stored data to position information.

The controller transmits instructions from its computer memory to the robot arm. Position data, obtained from incremental encoders and potentiometers in the robot arm, is transmitted back to the controller to provide closed loop control of arm motion. The robot interacts with its environment by using external input, output, and control signals.

The robot controller can run VAL II software. This is a high-level language that is a complete robot control system apart from being a programming language. The software is stored on a floppy disk. The disk drive is used to load the software to computer memory.

The robot arm weighs 63 kg (140 lb) and has a reach of 0.92 m (36.2 in.). It can carry a static payload of 4 kg (8.8 lb). The published repeatability of the PUMA 562 robot arm is ± 0.1 mm (± 0.004 in.). For a more detailed description of the PUMA system including mechanical details of the robot arm, the reader is referred to the PUMA equipment manual (Unimation Inc.).

5.2 System Model

Since the PUMA has six revolute joints the Denavit-Hartenberg parameter table consists of six rows. The last column of the DH table contains the joint angles. These joint angles are shown as a sum of the initial angles (zero offset) and the joint displacements.

The zero offsets are parameters that may need to be calibrated through optimization. Table 5.1 shows the DH parameters for the PUMA. Nominal values for the link lengths are given in millimeters in the PUMA equipment manual. Unimation does not adopt the DH convention in their kinematic model. As a result, the zero location of the elbow joint is different from the DH assignment, such that $\theta_3^* = \theta_3 - 180^\circ$ where θ_3^* is the elbow joint angle using Unimation's convention. This angle mapping has been implemented in the code when the joint angles are read in from the data file for the purposes of the work pertaining to this dissertation.

Table 5.1: Nominal Denavit-Hartenberg Parameter Table for PUMA
(angles in degrees, lengths in millimeters)

i	α_{i-1}	a_{i-1}	d_i	θ_i	**Joint Ranges** (in degrees)
1	0	0	0	$\theta_1 = \theta_{o1} + \theta^1$	-160 to +160
2	-90	0	0	$\theta_2 = \theta_{o2} + \theta^2$	-225 to +45
3	0	432	149.5	$\theta_3 = \theta_{o3} + \theta^3$	-225 to +45
4	-90	20.3	433	$\theta_4 = \theta_{o4} + \theta^4$	-110 to +170
5	90	0	0	$\theta_5 = \theta_{o5} + \theta^5$	-100 to +100
6	-90	0	0	$\theta_6 = \theta_{o6} + \theta^6$	-180 to +180

where,

θ_{oi} are initial joint angles and θ^i are relative joint displacements for i = 1, 2, ... , 6. The joint ranges are the physical limits of the joint motion set in the software.

Equation 5.1 describes the position of a point on the tool in the world frame:

$$ {}^{W}_{0}\boldsymbol{T}\ {}^{0}_{1}\boldsymbol{T}\ {}^{1}_{2}\boldsymbol{T}\ {}^{2}_{3}\boldsymbol{T}\ {}^{3}_{4}\boldsymbol{T}\ {}^{4}_{5}\boldsymbol{T}\ {}^{5}_{6}\boldsymbol{T}\ {}^{6}_{T}\boldsymbol{T}\ {}^{T}\boldsymbol{P} = {}^{W}\boldsymbol{P} \tag{5.1} $$

where,

${}^{W}_{0}\boldsymbol{T}$ *is the transformation matrix from fixed PUMA base frame to world frame,*
${}^{0}_{1}\boldsymbol{T}$ *is the transformation matrix from waist frame to fixed PUMA base frame,*
${}^{1}_{2}\boldsymbol{T}$ *is the transformation matrix from shoulder frame to waist frame,*
${}^{2}_{3}\boldsymbol{T}$ *is the transformation matrix from elbow frame to shoulder frame,*
${}^{3}_{4}\boldsymbol{T}$ *is the transformation matrix from first wrist roll frame to elbow frame,*
${}^{4}_{5}\boldsymbol{T}$ *is the transformation matrix from wrist pitch frame to first wrist roll frame,*
${}^{5}_{6}\boldsymbol{T}$ *is the transformation matrix from second wrist roll frame to wrist pitch frame,*
${}^{6}_{T}\boldsymbol{T}$ *is the transformation matrix from tool frame to second wrist roll frame,*
${}^{T}\boldsymbol{P}$ *is the position vector of the desired point in the tool frame, and*
${}^{W}\boldsymbol{P}$ *is the position vector of the desired point in the world frame.*

The transformation matrices and the position vectors in equation 5.1 are described below in equation form:

$$ {}^{W}_{0}\boldsymbol{T} = \begin{bmatrix} c\alpha c\beta & c\alpha s\beta s\gamma - s\alpha c\gamma & c\alpha s\beta c\gamma + s\alpha s\gamma & x \\ s\alpha c\beta & s\alpha s\beta s\gamma + c\alpha c\gamma & s\alpha s\beta c\gamma - c\alpha s\gamma & y \\ -s\beta & c\beta s\gamma & c\beta c\gamma & z \\ 0 & 0 & 0 & 1 \end{bmatrix} \tag{5.2} $$

where,

x, y, and z describe the position of the fixed PUMA base frame in the world frame,
α, β, and γ describe the fixed-angle orientation of the fixed PUMA base frame in the world frame.

$$ {}^{0}_{1}\boldsymbol{T} = \begin{bmatrix} \left(c\theta_{o1}c\theta^{1} - s\theta_{o1}s\theta^{1}\right) & -\left(s\theta_{o1}c\theta^{1} + c\theta_{o1}s\theta^{1}\right) & 0 & a_0 \\ \left(s\theta_{o1}c\theta^{1} + c\theta_{o1}s\theta^{1}\right)c\alpha_0 & \left(c\theta_{o1}c\theta^{1} - s\theta_{o1}s\theta^{1}\right)c\alpha_0 & -s\alpha_0 & -s\alpha_0 d_1 \\ \left(s\theta_{o1}c\theta^{1} + c\theta_{o1}s\theta^{1}\right)s\alpha_0 & \left(c\theta_{o1}c\theta^{1} - s\theta_{o1}s\theta^{1}\right)s\alpha_0 & c\alpha_0 & c\alpha_0 d_1 \\ 0 & 0 & 0 & 1 \end{bmatrix} \tag{5.3} $$

where, the link parameters (for i = 1) are shown and described in Table 5.1.

$$ {}^{1}_{2}\boldsymbol{T} = \begin{bmatrix} \left(c\theta_{o2}c\theta^2 - s\theta_{o2}s\theta^2\right) & -\left(s\theta_{o2}c\theta^2 + c\theta_{o2}s\theta^2\right) & 0 & a_1 \\ \left(s\theta_{o2}c\theta^2 + c\theta_{o2}s\theta^2\right)c\alpha_1 & \left(c\theta_{o2}c\theta^2 - s\theta_{o2}s\theta^2\right)c\alpha_1 & -s\alpha_1 & -s\alpha_1 d_2 \\ \left(s\theta_{o2}c\theta^2 + c\theta_{o2}s\theta^2\right)s\alpha_1 & \left(c\theta_{o2}c\theta^2 - s\theta_{o2}s\theta^2\right)s\alpha_1 & c\alpha_1 & c\alpha_1 d_2 \\ 0 & 0 & 0 & 1 \end{bmatrix} \tag{5.4} $$

where, the link parameters (for i = 2) are shown and described in Table 5.1.

Similarly, transformation matrices ${}^{2}_{3}\boldsymbol{T}$ to ${}^{5}_{6}\boldsymbol{T}$ can be described using the same DH convention and using the link parameters shown in Table 5.1, and

$$ {}^{6}_{T}\boldsymbol{T} = \begin{bmatrix} c\alpha_T c\beta_T & c\alpha_T s\beta_T s\gamma_T - s\alpha_T c\gamma_T & c\alpha_T s\beta_T c\gamma_T + s\alpha_T s\gamma_T & x_T \\ s\alpha_T c\beta_T & s\alpha_T s\beta_T s\gamma_T + c\alpha_T c\gamma_T & s\alpha_T s\beta_T c\gamma_T - c\alpha_T s\gamma_T & y_T \\ -s\beta_T & c\beta_T s\gamma_T & c\beta_T c\gamma_T & z_T \\ 0 & 0 & 0 & 1 \end{bmatrix} \tag{5.5} $$

where,

x_T, y_T, and z_T describe the position of the tool frame in the last link frame, i.e., the second wrist roll joint frame,

α_T, β_T, and γ_T describe the fixed-angle orientation of the tool frame in the last link frame.

$$ {}^{T}\boldsymbol{P} = \begin{Bmatrix} 0 \\ 0 \\ 0 \\ 1 \end{Bmatrix} \tag{5.6} $$

where,

the desired point on the tool is defined such that it is always at the origin of the tool frame.

Equations 5.2 to 5.6 describe the individual transformation matrices that are part of equation 5.1, which maps the position of a desired point on the tool into the world frame. To get an accurate position of a point in the world frame, it is necessary to have accurate values of the parameters in equation 5.1. Since only nominal values of these parameters are known, a characterization process must be undertaken to find the as-built values of the parameters in equation 5.1 that best describes the geometry of the physical robot system. Once this characterization process has been completed, equation 5.1 can be used to position the tool of the robot at a desired point location. The following sections describe the characterization process for the PUMA robot system.

5.3 Sources of Pose Error

The system model of the PUMA is analyzed to identify the system parameters. The system parameters that are potential sources of error are then listed. These parameters can be obtained from equation 5.1. The sources of robot end-effector pose error are listed below:

1. The description of the pose of the robot base in the world frame (${}^{W}_{0}\boldsymbol{T}$) contains six parameters. These parameters are x, y, z, α, β, and γ. These parameters depend on robot installation in the work area and are prone to error. These need to be characterized every time the robot is installed in a new work environment for tasks that involve accurate positioning. (Total 6 parameters).
2. For all the six robot arm links the DH parameters are sources of pose error. These DH parameters are link lengths ($\mathbf{a_{i-1}}$), link twist angles (α_{i-1}), and link offsets ($\mathbf{d_i}$).

Also, the initial joint angles (joint offsets) for all six joints are sources of error. In the DH table these are represented by θ_{oi}. Therefore there are four parameters per link. (Total 24 parameters).

3. The tool frame is represented in the second wrist roll frame by the fixed-angle convention. There are three position parameters (x_T, y_T, and z_T) and three orientation parameters (α_T, β_T, and γ_T) in this transformation matrix (${}^{6}_{T}\boldsymbol{T}$). These six parameters are also sources of pose error. But in our case, only the three position parameters are considered as sources of error since we are only interested in the position of a point on the tool. In cases where orientation is important the three orientation parameters are also included as sources of pose error. (Total 3 parameters).

These are the 33 error parameters. These parameters need to be bounded based on the knowledge of PUMA, its joints, encoders, and the tool. The error range values are presented below.

1. The position of the robot base in the world frame can be measured approximately to within 10-15 mm. Assuming it can be approximated to within ± 15 mm, this number is used as the error range for x, y, and z. The orientation of the robot base can be measured approximately to within ± 2 deg. This number will be used as the error range for α, β, and γ.

2. Even though there may be geometric tolerances on the links and joints for manufacture and assembly, it is possible that the as-built values of the system parameters vary significantly more than these tolerances. This is because the DH convention represents the kinematic description of the robot, which does not correspond physically to the robot links. Therefore, for the purposes of sensitivity analysis, broad error values were used. For all six link lengths ($\mathbf{a_{i-1}}$) the error range value of ±2.5 mm was used. For the link twist angles (α_{i-1}), the error range used is ±1

deg. For the link offset ($\mathbf{d_i}$) the range used is ±5 mm. A large value is used for this because it is a parameter that can vary a large amount with just a small skew in the joint axis. For the initial joint offset angles (θ_{oi}) the error range used is ±10 deg. The joint offset angle is prone to a large error because the encoders are mounted on the joint servomotor end of the joint drive system. After the encoder there is a gearing system through which motion is transmitted before the joint. Because of this situation the joint physical zero does not correspond to the encoder zero. Large errors are possible. Even though the PUMA robot comes with a diskette which contains potentiometer calibration values, a change in the components or disassembly will change these values. Also, if this calibration information is unavailable then characterization is even more important. Furthermore, all the desired parameters can be characterized at the same time instead of performing different calibration procedures for each different type of parameter.

3. The tool frame origin position can be approximated to within ± 2 mm. This error range will therefore be used for x_T, y_T, and z_T. These parameters are part of ${}^{6}_{T}\boldsymbol{T}$.

The sources of geometric error in the PUMA robot system have been described in this section. These error parameters have been assigned an error range for the purpose of sensitivity analysis based on possible error values for the parameters.

5.4 Sensitivity Analysis

The effect of the 33 error parameters on the end-effector position error is analyzed in this section. This sensitivity analysis algorithm was coded in C. The steps in the sensitivity analysis code are outlined below.

1. Read in nominal values of the parameters, the joint angle limits, and the error ranges for all the parameters from a data file.

2. Include loops such that many robot configurations can be used to test sensitivity. For each joint angle, four positions were used in its joint angle range. Include all six joint angles in this nested loop module. These are the joint angle values at which the position of the end-effector is evaluated.

3. Next, for all the 33 error parameters, we calculate the tool pose with the nominal values. Then we perturb one parameter at a time to its extreme error range and re-evaluate tool pose. This tool pose is compared with the nominal tool pose. The difference of the two gives the error position vector and also the biggest error rotation angle. These two values are printed in an output file. This process of finding the position error vector and largest rotation error angle for the 33 parameters is repeated for all the joint angle configurations generated in step 2.

4. The perturbation of the individual parameters is performed in four different ways. First, all parameters are kept at the nominal value and each one is individually perturbed to the positive extreme value in its error range. Second, all parameters are kept at the nominal value and each parameter is individually perturbed to the negative extreme value in its error range. The third way is to keep all the parameters at the positive extreme value in the error range and to individually perturb each parameter value to the negative extreme. Finally, all the parameters are kept at the negative extreme and each parameter value is individually perturbed to the positive extreme. There are convexity assumptions here.

This sensitivity analysis was performed using the nominal parameter values shown in section 5.2 and the error range values shown in section 5.3.

The results of the sensitivity analysis show that translation parameters have a one-to-one effect on the position of the tool frame. If the error value is 2 mm, then we will see a 2 mm error in the output due to this parameter. This effect is uniform throughout the robot. When there is interaction between more than one translational error parameter, it becomes hard to visualize the effect on the output. Translational error parameters individually do not have any effect on the orientation of the tool frame. Another observation made from the sensitivity analysis results is that errors in the initial joint angles caused the most error in the position of the tool frame. This is because angular errors are amplified out at the end of the arm. Therefore, the closer an angular error parameter to the base or waist joint (away from the tool frame) the greater its effect on the tool frame error. Of course the particular joint angle configuration dictates which error parameters are most critical. In other words, it is possible, in some configurations, for the elbow joint error to have a greater effect than the waist or shoulder joints on the tool frame error. From these results we can conclude that all the angle parameters require characterization, since their effect is magnified. They also contribute to tool frame orientation errors. For the translational parameters a decision can be made based on what tool frame positioning accuracy is desired. Since in our case it was assumed that the robot base position error could be as great as 15 mm, it was decided to add these parameters into the optimization. In fact, all the 33 parameters were added to the optimization since none of them are known to within $\pm$ 2 mm, which is the desired positioning accuracy for the tool. It was still important to perform sensitivity analysis because the effect of the angular parameters could be

quantified and also insights about the system design were gained. A sample of the parameters and their effects are shown in Table 5.2 below. A complete set of 33 parameters for one joint configuration and one perturbation style are given in Appendix 1.

Table 5.2: Sensitivity Results for Nominal Set, Positive Individual
(Joint angle configuration: $\theta_1 = -160$, $\theta_2 = -225$, $\theta_3 = -225$, $\theta_4 = -110$, $\theta_5 = -100$, $\theta_6 = -180$)
(Lengths in millimeters, angles in degrees)

	Error Range	Position Error (mm)	Max. Rotation Error (deg)
Base x (x)	15	15	0
Base Rz (α)	2	12.9	-2 about z
Alpha 2 (α_2)	1	6.9	-0.69 about x
Theta 3 (θ_{o3})	10	75.3	0.18 about z
d 4 (d_4)	5	5	0
a 5(a_5)	2.5	2.5	0
Yt(y_T)	2	2	0
Theta 1 (θ_{o1})	10	64.5	-10 about z
Theta 4 (θ_{o4})	10	44.3	-2.07 about y
Theta 6 (θ_{o6})	10	36.3	0.51 about x

The conclusion from the sensitivity analysis is to optimize all the 33 parameters. The following sections will describe the PUMA tool position data measurement and the optimization process.

5.5 Position Data Measurement

The next step after sensitivity analysis is to take position measurements of the robot arm end-effector while recording the joint angle values. The measurement system that was

used is an acoustic digitizer manufactured by Science Accessories Corporation (SAC, 1993).

5.5.1 Acoustic Digitizer Description

The acoustic digitizer is a Science Accessories Corp. model GP-12XL. It has a 2.4 m x 2.4 m x 2.4 m working volume. Figure 5.3 shows a photograph of the acoustic digitizer microphone array. The digitizer comes with the microphone array, hand-held probe with emitters, a pilot calibration assembly, software, and cables. There are four microphones arranged in a diamond-shaped array at known distances from each other (90 cm).

Acoustic digitizers are based on sound propagation between two points (a sound emitter and a sound receiver) at a speed which is known or can be calibrated. If a sound wave travels from a single emitter to three or more receivers that are positioned relative to each other in a known geometry, and the speed of sound and times of flight are known, it is possible to calculate the location of that emitter in three dimensional space.

One practical limitation of acoustic digitizers is that every emitter/receiver combination being used requires a direct line of sight. The probe emitters should face the microphone array. The higher the degree to which the speed of sound is calibrated, the higher the level of digitized accuracy. The SAC acoustic digitizer supports two types of real time speed-of-sound compensation, namely, probe compensation and pilot compensation.

These methods measure the speed of the sound in the digitizing environment at the time of digitizing.

Probe compensation works well in 1 m x 1m x 1m volumes. Probe compensation relies on knowing the distance between the two probe emitters and iteratively adjusting the speed-of-sound compensation factor until the digitized distance between the emitters is correct. A photograph of the probe is shown in Figure 5.2. The probe consists of two emitters and a probe tip which can be seen in the photograph. The distance of the probe tip from the two emitters is a calibrated distance that is supplied by the manufacturer along with the digitizer equipment. The digitized point is the probe tip. Pilot compensation is more accurate, particularly in larger volumes, than probe compensation. Pilot compensation requires additional hardware called the pilot bar which is assembled to the microphone array and is shown in Figure 5.3. Pilot compensation uses an emitter fixed at a calibrated distance from one or more receivers. Each time the offset probe is digitized, the pilot distance is also digitized, allowing calculation of the current speed of sound.

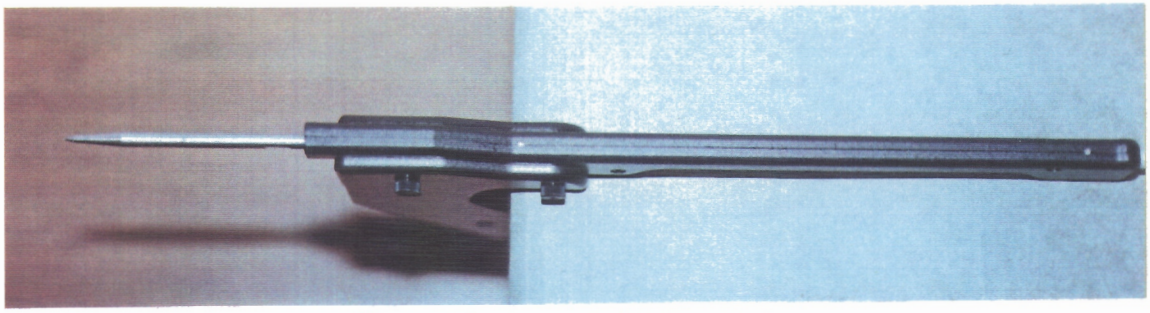

Figure 5.2: Acoustic Digitizer Probe

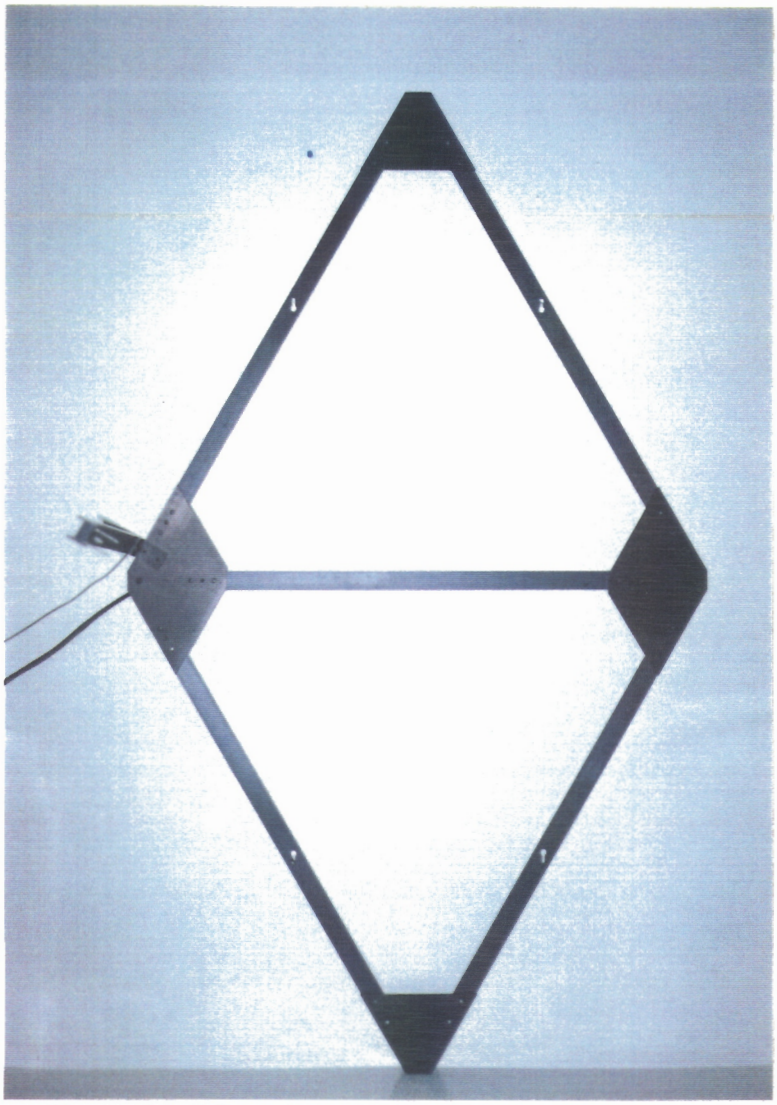

Figure 5.3: Microphone Array of the Acoustic Digitizer

The GP-12XL control box is attached to a computer through a serial line. The digitizer software runs in DOS. The software allows the user to store the digitized data in a text file as x, y, and z position information. The probe emitters are digitized by either pressing a trigger on the hand-held offset probe or by pressing the F8 key on the computer keyboard. The software also allows the user to take 1-5 samples each time the trigger or

the key is pressed. For more details on the software the reader is referred to SAC's manual (SAC, 1993).

5.5.2 Digitizer Relative Accuracy Characterization

Before attempting to use the acoustic digitizer to take position measurements, an effort was made to characterize its relative position measurement accuracy. This information was not available from the manufacturer. The manufacturer does advertise the resolution to be 0.002 in. This number is a result of using the counter frequency to determine the number of counts it takes for a signal to travel from the emitter to the microphone for a known distance. The resolution is different from the repeatability, relative accuracy, or the absolute accuracy. Therefore it was decided to perform measurement tests against a milling machine which is advertised as having a relative positioning accuracy of 0.0005 in.

The microphone array was rigidly attached to the milling machine bed and the offset probe was rigidly connected to the milling machine chuck. Relative movements of the milling machine were recorded. At the same time, a large number of digitizer data points (approximately 100 x 5 samples/digitized keystroke) were recorded for the same milling machine positions. The relative distances were compared. The results showed that the average relative accuracy of the digitizer was ±0.017 in. (0.43 mm). Assuming the milling machine was not as accurate as advertised since it had not been calibrated for over

5 years it was decided to use ±0.020 in. (0.5 mm) as the relative accuracy of the acoustic digitizer. Tests were also performed to check the effect of noise and temperature variance on the digitizer performance. A heat gun was used to raise the temperature of the air near to microphones. This did not have a significant effect. Ambient acoustic noise interfered with the acoustic signals from the emitters and had a significant effect. It was concluded that the environment in which the digitizer is to be used needs to be as quiet as possible. An effort was made to maintain such an environment during the position measurement experiments with the PUMA. The tests also revealed that the acoustic digitizer needs about one hour of warm-up time. Digitizer data was consistent only after about an hour.

The number of samples required for every data point can be determined by examining the statistical distribution of random errors. If enough samples are taken for a data point, then the acoustic digitizer errors can be compensated by averaging if these errors are assumed to be random. The standard deviation of 5000 (1000 x 5) samples was calculated to be 0.005 in (0.127 mm). Then for a 99% confidence interval of width 0.001 in. (0.025 mm) the sample size is calculated from Ott (1993, page 208):

$$n = \frac{\left(z_{\alpha/2}\right)^2 \sigma^2}{E^2} \tag{5.7}$$

where,

n is the sample size,
$z_{\alpha/2}$ is the z-value for the confidence intervals which can be found in Table 5.1 on page 203 of Ott's book,
σ is the standard deviation, and
2E is the width of the confidence interval.

From equation 5.7 the sample size was calculated to be 665.64. A number of 670 was used. Since each keystroke actually takes 5 samples of digitized data, 670 samples were used which corresponds to 134 keystrokes. This was the number of samples taken for each data point.

5.5.3 Experimental Setup

Before any measurements were attempted, an effort was made to take as much of the backlash or bindings out of the joints as possible as per the instructions given in the PUMA equipment manual. There was still some backlash left in joints 4 and 6. The PUMA and acoustic digitizer are shown in the photograph in Figure 5.4. The digitizer microphone array was rigidly attached to the PUMA frame with C-clamps such that there could be no relative motion between the robot and the digitizer. The offset probe was rigidly attached to the end-effector flange at the end of the PUMA arm by means of a fixture. The acoustic digitizer coordinate system was assigned as the world coordinate frame for the PUMA since all the digitizer data was referenced to that frame. The approximate location of PUMA's fixed base frame in the world frame was measured as x = 560 mm, y = 265 mm, z = 350 mm, α = -32 deg, β = 0 deg, and γ = 0 deg. The approximate position of the probe tip in the second wrist roll frame was measured to be x_T = -8 mm, y_T = -208 mm, z_T = 150 mm. Since the probe tip is a point, there is no orientation associated with it. So the three rotation parameters α_T, β_T, and γ_T are set to zero.

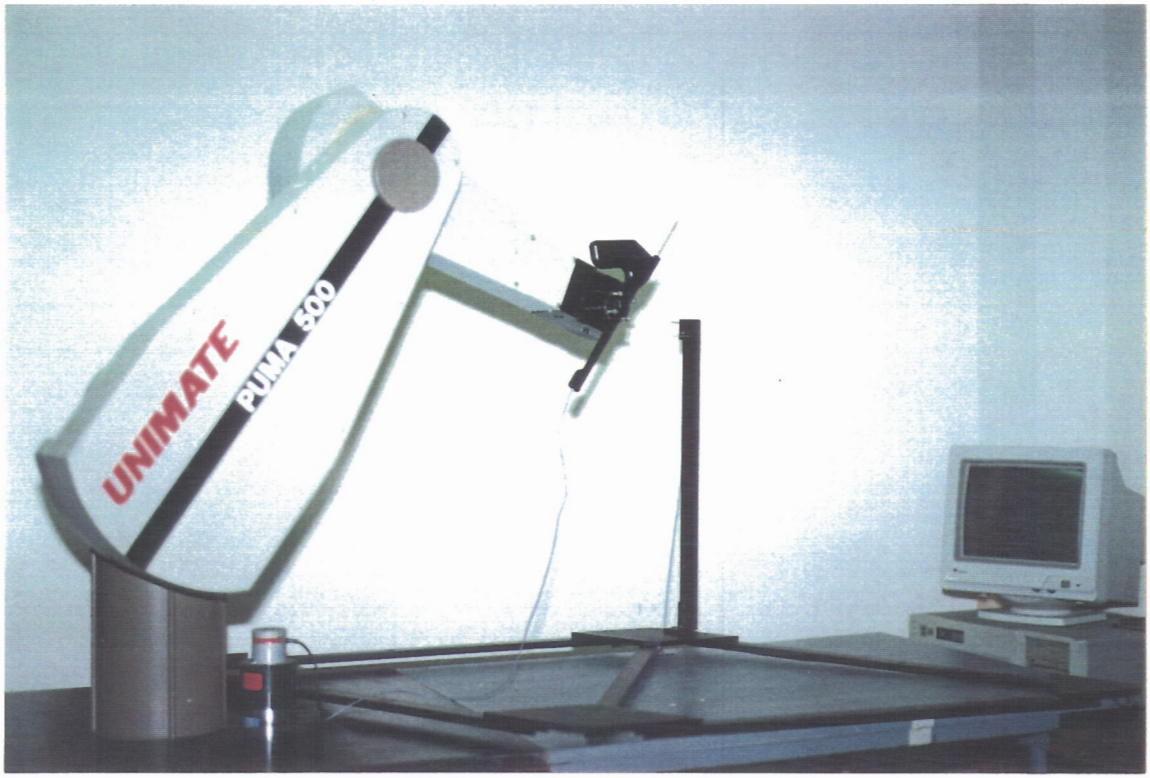

Figure 5.4: PUMA and Acoustic Digitizer Setup

A total of 100 data points were recorded. The teach pendant was used to move the robot joints such that the probe tip reached a desired location in the microphone array workspace while the emitters faced the microphones with no physical obstructions. The PUMA joint angles were also recorded for these data points. The next section describes the optimization of the parameters and the calibration results.

5.6 Parameter Optimization

The PUMA forward kinematics were coded in C-language and implemented as a module in the optimization engine developed by Joe Calkins. The input to the program is a data

file with a sequence of data for each point. The data for each point is entered such that the six joint angles are listed first, followed by all the samples for the data point. This is followed by a character to tell the program that the data for that particular point has ended. All the points are entered in this file sequentially. The samples for each point is averaged by the program and the average values are used as the measured tool position. The nominal values were used as the starting points for the optimization. The objective function is the square of the position error of the tool as explained in Chapter 4. The results of the parameter optimization are shown in Table 5.4. Evaluation of the residuals show that the minimum absolute residual error is 0.1 mm, the average absolute residual error is 0.6 mm, the maximum absolute residual error is 2.0 mm, and the objective function value is 49.867753.

The joint angle zero offsets were coarsely determined by visual means and recorded. These visually determined values of the joint angle offsets are used to check the optimization results. The comparison between the coarse estimates and the optimized values of the joint angle offsets are shown in Table 5.3.

Table 5.3: Joint Angle Zero Offsets (in degrees)

	θ_{o1}	θ_{o2}	θ_{o3}	θ_{o4}	θ_{o5}	θ_{o6}
Estimated	0.0	0.0	-2.9	0.0	3.3	-8.5
Optimized	0.89	0.26	-2.84	0.50	2.90	-8.21

Table 5.4: Parameter Optimization Results
(Angles in degrees, lengths in mm)

Parameters	Nominal Values	Optimized Values
Base X	560	557.199565
Base Y	265	265.623301
Base Z	340	334.106140
Base Rx	0	-0.972294
Base Ry	0	-0.217839
Base Rz	-32	-32.831484
Link 1 Alpha	0	0.524038
Link 1 a	0	-4.071697
Link 1 d	0	6.631116
Link 1 Theta Offset	0	0.886573
Link 2 Alpha	-90	-90.074567
Link 2 a	0	0.478741
Link 2 d	0	6.046096
Link 2 Theta Offset	0	0.259030
Link 3 Alpha	0	0.004621
Link 3 a	432	432.096463
Link 3 d	149.5	146.2205
Link 3 Theta Offset	0	-2.842551
Link 4 Alpha	-90	-90.30491
Link 4 a	20.3	20.22573
Link 4 d	433	432.636019
Link 4 Theta Offset	0	0.498658
Link 5 Alpha	90	90.016683
Link 5 a	0	0.23534
Link 5 d	0	-0.039068
Link 5 Theta Offset	0	2.900205
Link 6 Alpha	-90	-90.042208
Link 6 a	0	-0.195161
Link 6 d	0	-1.098543
Link 6 Theta Offset	0	-8.213363
Tool X	-8	-10.845857
Tool Y	-208	-208.039784
Tool Z	150	150.000

The results obtained were checked in Rhobot Pro, a robot simulation software package. They were also compared with results obtained using the nominal values. Results for six of the tested points are shown in Table 5.5. It can be seen that the characterization process was a success when compared to results using just the nominal values. It is, of course, possible to take more care in measuring the base position and the tool position, which may reduce some of the error for the nominal case. Also, using the approximate joint offset values could improve the results substantially. Another point to be noted is that the factory calibrated values could not be obtained despite a diligent effort to obtain them. Comparison with the factory calibration would have been a good gauge of the success of the characterization process.

Table 5.5: Comparison of Optimized and Nominal Positions (in millimeters)

Measured Point	Absolute Error of Optimized Point	Absolute Error of Nominal Point
659.855, -138.419, 55.659	1.0	12.1
746.921, -268.636, 607.413	0.7	19.7
994.685, -564.696, 206.759	0.6	26.0
1029.899, -416.493, 366.705	0.6	26.4
1167.555, 110.261, 292.941	1.3	18.9
1123.082, 177.366, 213.054	0.7	13.5

5.7 Control System Update

The optimized parameters were implemented and checked in a simulation that was developed in Rhobot Pro. Rhobot Pro based control of PUMA is done by using iterative forward kinematics to perform inverse kinematics.

In summary, this chapter presented the application of the robot system characterization methodology to the PUMA 562 industrial robot. The results obtained are good from a simulation standpoint and when compared to using just nominal values.

6. Application to the Design of a Mobile-Robot Base Positioning System (BPS)

This chapter describes the application of the robot system characterization methodology to the design of a base positioning system (BPS) for a mobile, underwater, nuclear-reactor-vessel-inspection robot called URSULA. First, a brief background of URSULA's BPS problem is presented. Next, the URSULA BPS system model is described and the sources of pose error in the BPS and the reactor vessel are identified. Then, a sensitivity analysis discussion is presented. The results of the sensitivity analysis are used to decide upon the critical parameters that require calibration and to help select suitable subcomponents for the design. An exhaustive simulation of the design and its positioning performance is then presented. The chapter concludes with a discussion of actual system performance.

6.1 Background

URSULA, a mobile, underwater inspection robot developed by BWNT was introduced in Chapter 1. Figure 6.1 shows two URSULA mobile robots cooperating to inspect welds inside a nuclear reactor vessel. Figure 6.2 is a photograph showing URSULA scanning a weld in a nuclear reactor vessel mock up.

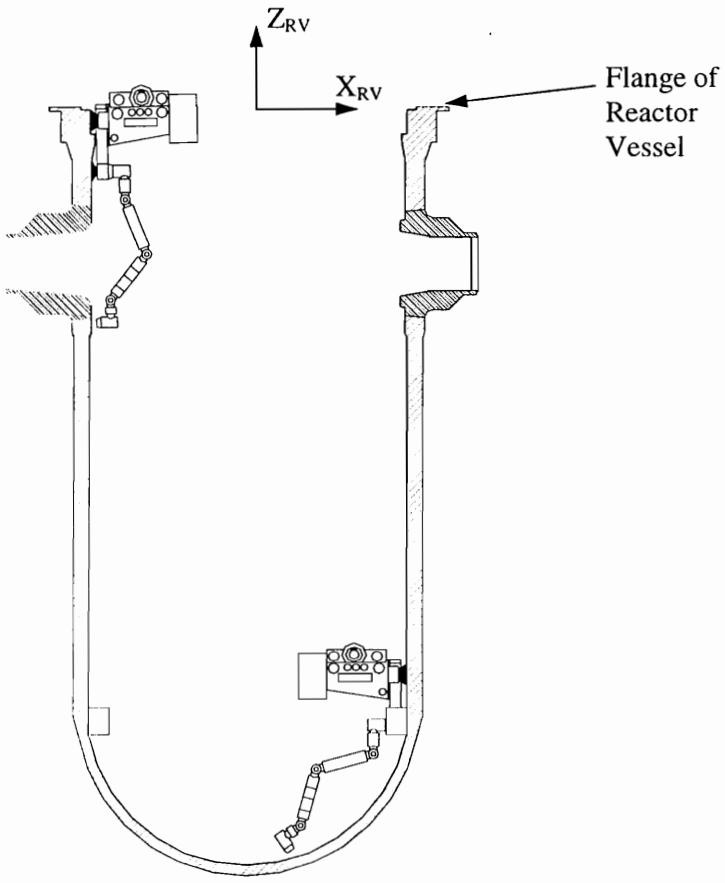

Figure 6.1: Two URSULA Robots Inside a Nuclear Reactor Vessel

Mobile robot positioning accuracy involves a suitable robot base positioning system (BPS), and arm positioning system (APS), as well as efficient calibration procedures for

both these systems. Since these robot systems are used in nuclear environments human involvement should be minimized during equipment setup, calibration, operation, and maintenance. Some traditional calibration schemes would be difficult or impractical for such contaminated equipment.

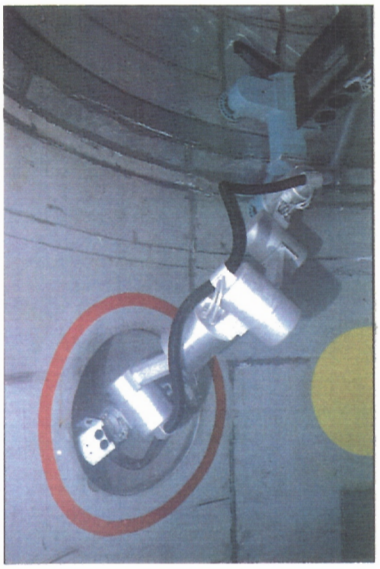

Figure 6.2: URSULA Scanning a Weld in a Reactor Vessel Mock Up

Determining the position and orientation (pose) of a robotic end-effector involves two basic coordinate transformations. The first transformation describes the end-effector pose with respect to the base of the manipulator, while the second transformation describes the pose of the base with respect to the world coordinate system. In typical fixed base applications, the pose of the robot base in the world coordinate system is usually known and fixed, while the pose of the end-effector in the base coordinate system is determined from a kinematic model and joint feedback. In mobile robot systems, the base pose is not fixed and must be determined as the robot moves with respect to the world coordinate

system. Since URSULA is a mobile underwater robot, a positioning system for determining the base pose in the world coordinate system is required. In this application the reactor vessel coordinate system is considered the world coordinate system. As with traditional approaches, determining the global pose of URSULA may be considered in two parts. First, the pose of the end-effector relative to the robot's tripod base coordinate system is determined using a kinematic model and joint feedback. The second part is to compute the pose of the tripod base with respect to the reactor vessel (world) coordinate system.

The initial design concept for the URSULA system called for an acoustic-transceiver-based BPS. Tidwell et al. (1993) presented the details of the development and testing of this system. This system finds the position of a mobile robot by measuring the time-of-flight of acoustic signals that are emitted and received by transceivers. Typically, one transceiver is placed on an underwater robot or remotely operated vehicle (ROV) and three transceivers are mounted at known locations in the world coordinate system. Standard triangulation techniques are then used with the time-of-flight (TOF) measurements and the known speed of sound in water to determine the position information. Because the speed of sound is a function of water temperature, unacceptable error is introduced into the system by the temperature variations found in the cooling reactor water. To improve the accuracy in the presence of temperature gradients, special algorithms were developed to decrease the temperature dependence of the system. This system was investigated for possible implementation for reactor vessel inspection by

placing three fixed transceivers at known locations in the reactor vessel flange stud holes. Three transceivers and two inclinometers are placed on URSULA. This hardware configuration combined with velocity compensation software enables the modified system measure both position and orientation of the robot's tripod base in the reactor vessel. This method was abandoned due to unreliable hardware and poor performance problems due to noise in the reactor environment.

Another BPS approach that was considered involved using a laser rigidly mounted on the serial arm near the end-effector of URSULA. The robot arm itself can be used to aim and shoot the laser at known targets in the vessel frame. Then, using the geometry and kinematic models of the arm, vessel, laser position on the arm, and the data obtained from shooting the targets, the best fit to the solution of URSULA's pose is calculated using non-linear optimization techniques. This method proved to be cumbersome in initial testing and did not meet base positioning accuracy requirements.

Since the first two attempts at solving the BPS problem for URSULA were unsuccessful, a new approach was needed. At this stage in the project, the time and cost-of-development constraints were more stringent, so accurate performance predictions and system modeling were essential. A few brainstorming sessions were held between the members of the BWNT group and the Robotics and Mechanisms Group from Virginia Tech. It was decided to break up the problem and to use different sensors to obtain the required information. A depth gauge (differential pressure transducer) would be used to

find the depth (z) of URSULA in the reactor vessel. Two inclinometers were already present on URSULA that can give two orientation parameters. Assuming URSULA to be in complete contact with the reactor vessel wall, the radius, r, is known. The only parameter that remained to be found was the circumferential location of URSULA in the vessel (θ). Therefore ideas that were aimed at finding θ were generated. The most promising ideas that met the time and estimated-cost constraints were reviewed and screened. Included among the ideas were approaches that involved computer vision, an approach involving acoustic technology, and several ideas based on laser pointing. The laser-based ideas included both laser beams and intersecting laser planes of light. All these ideas were modeled in Mathcad 5.0 (MathSoft, Inc.). The base positioning error was simulated in these models based on the reactor vessel geometry and the implementation details of each concept. The requirement of BWNT was to find the position of URSULA within 0.5 in. in the three Cartesian coordinates (i.e., its base location was required to be known within one-half inch cube). Only one of the modeled ideas met this requirement. This particular idea involves finding the circumferential position (θ) using a laser with two encoded revolute axes mounted at the center of a beam across the flange of the reactor vessel. This unit will hereafter be referred to as the laser-pan-tilt BPS. This unit is essentially a two degree-of-freedom robot. The pose of the laser is found in the reactor vessel (world) coordinate system using a calibration technique that was developed for this purpose. This calibration scheme is performed in the reactor vessel, and can be undertaken even with contaminated equipment as there is

no direct human involvement. Another calibration procedure is also performed for the intrinsic parameters of the laser-pan-tilt unit itself. This procedure is also performed in the reactor vessel, thereby avoiding the human handling necessary in traditional calibration schemes. Once calibration is complete, the circumferential location of URSULA at any position in the reactor vessel can be determined. This is accomplished by pointing the laser beam at a photosensor target mounted on the tripod base at a known location. Once URSULA is moved to a new location in the vessel, the laser beam is directed to hit the target on URSULA. When the laser beam is targeted on URSULA, the two encoded-axis readings representing the kinematics of the laser-pan-tilt unit, and the target to tripod base transform determined from the other sensor inputs are used to calculate the circumferential position (θ) of the tripod base.

In summary, the positioning method for URSULA described above and currently being used by BWNT is a combination of different techniques to obtain different pose parameters. The tripod base pose parameters are r, θ, z, α, β, γ. The position parameters in cylindrical coordinates are r, θ, z. The fixed-angle orientation parameters with respect to the world coordinate system in Cartesian coordinates are α, β, γ. Cylindrical coordinates are used for the position because the reactor vessel is cylindrical in shape. A depth gauge (differential pressure transducer) is used to give the depth (z) of the tripod base in the reactor vessel. Two inclinometers are mounted on the tripod base to give the two inertial orientation angles (β, γ). The radial position (r) of the tripod base and α are

determined from the circumferential position (θ) of the tripod base assuming URSULA is attached to the wall of an ideal vessel of known radius.

The Robotics and Mechanisms Group at Virginia Tech assisted in the BPS development by selecting the laser, the depth gauge, the optical glass, and the active sensors used as the laser targets. Since discussing these topics will digress from the characterization methodology description, it was decided to restrict the discussion to only those parts of this design project that are relevant to this dissertation.

The remainder of this chapter is focused on the use of the characterization methodology to design and develop the laser-pan-tilt BPS.

6.2 System Model

Figure 6.3 shows an isometric view of the laser-pan-tilt BPS. It has two revolute joints providing two rotational degrees of freedom, i.e., the pan axis and the tilt axis. The pan axis is coincident with the z-axis of the world frame (reactor vessel frame). The tilt axis is perpendicular to and intersects the pan axis. With these two rotations it is possible to aim the laser at any point in the reactor vessel.

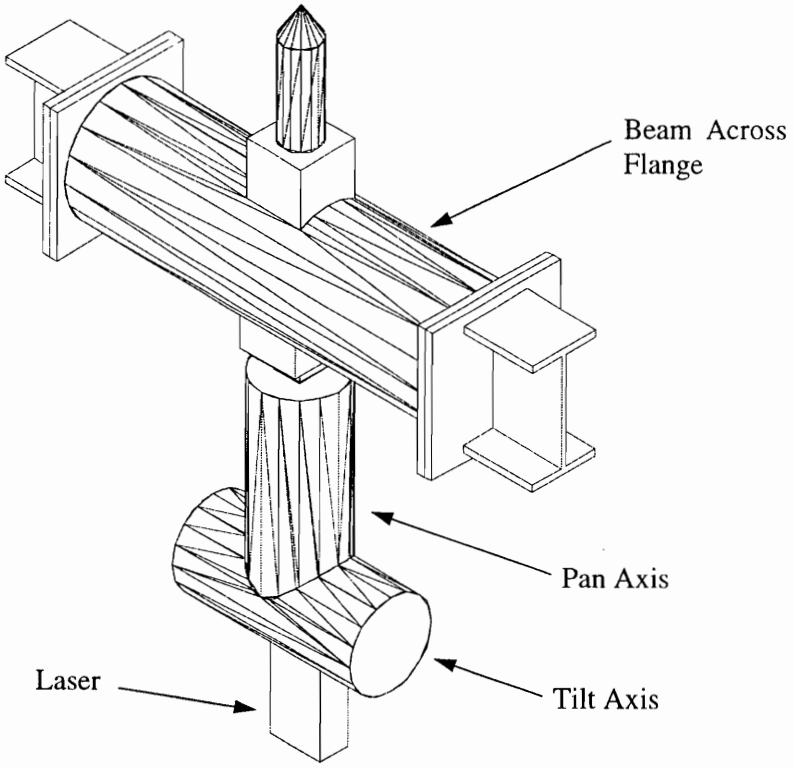

Figure 6.3: Laser-Pan-Tilt BPS

The pan and tilt axis encoders give the two angle readings which are called θ and ϕ respectively. Part of the beam that is assembled on the flange in the middle of the reactor vessel is also shown in Figure 6.3. The beam is mounted to accurately machined stud holes in the flange. The laser-pan-tilt BPS is mounted on this beam. The laser is attached to the tilt axis of the BPS.

The coordinate frames of the laser-pan-tilt BPS and the reactor vessel are shown in Figure 6.4. By design, the pan and tilt axes are mutually perpendicular intersecting axes. There is a fixed coordinate frame for the BPS that is represented by the subscript 0. The pan

axis coordinate frame is subscripted with 1 and it is coincident with the BPS fixed coordinate frame. The pan axis frame moves with the pan axis, i.e., it has a rotation about the Z_1 axis. The tilt axis frame (represented by subscript 2) origin is coincident with the origin of the pan axis frame and the BPS fixed frame, but it is perpendicular to the pan axis as can be seen in Figure 6.4. This tilt axis frame has a rotation about the Z_2 axis. The laser frame is attached to the tilt axis frame and is coincident with it. It also rotates with the tilt axis frame. The laser frame is represented by the subscript L. The Z_2 and Z_L frames are perpendicular to the plane of the paper and they point into the paper.

Based on this coordinate system convention, a Denavit-Hartenberg table (Table 6.1) has been constructed for the BPS. Since the BPS is essentially a two degree-of-freedom robot, the DH table contains two rows. The last column of the DH table for the BPS contains the pan and tilt joint angles. The joints angles are shown as a sum of the initial angles (zero offsets) and the joint displacements. The zero offsets are considered as potential parameters for optimization. By definition, four of the parameters are zero and they cannot have any error.

Table 6.1: Denavit-Hartenberg Parameter Table for BPS
(angles in degrees, lengths in inches)

i	α_{i-1}	a_{i-1}	d_i	θ_i
1	0	0	0	$\theta_1 = \theta_o + \theta$
2	-90	0	0	$\theta_2 = \phi_o + \phi$

where,

θ_o and ϕ_o are initial pan and tilt joint angles respectively,
$\alpha_0 = 0$, $a_0 = 0$, $d_1 = 0$, and $d_1 = 0$ by definition,
$\alpha_1 = -90$ and $a_1 = 0$ are the axes perpendicularity and the link offset respectively, therefore they are parameters that can have errors.

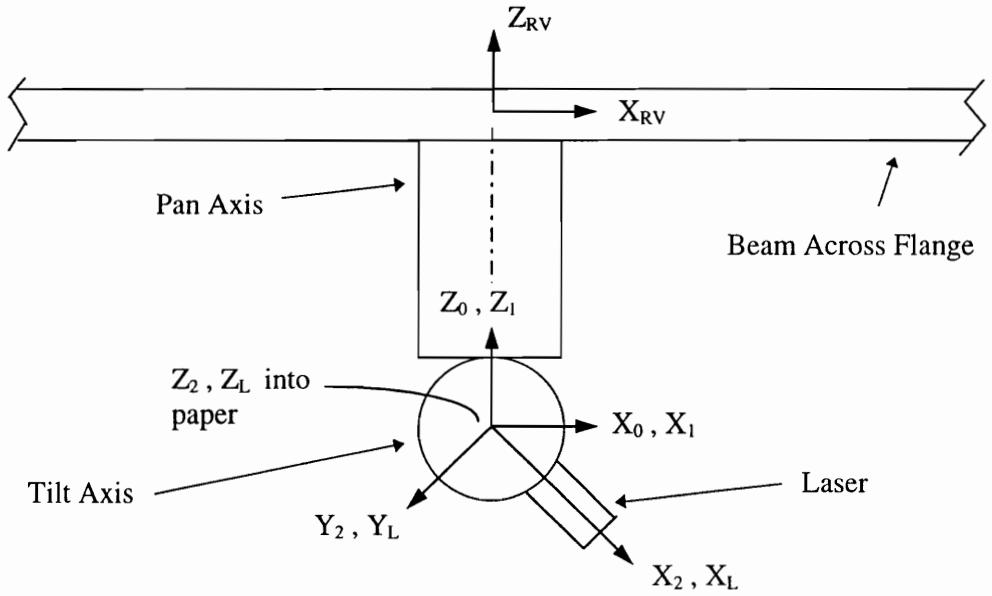

Figure 6.4: Reactor Vessel and BPS Coordinate Systems

When the laser is targeted on a point, the location of that point in the world frame is given by equation 6.1:

$$ {}^{RV}_{0}\boldsymbol{T}\ {}^{0}_{1}\boldsymbol{T}\ {}^{1}_{2}\boldsymbol{T}\ {}^{2}_{L}\boldsymbol{T}\ {}^{L}\boldsymbol{P} = {}^{RV}\boldsymbol{P} \qquad (6.1) $$

where,

${}^{RV}_{0}\boldsymbol{T}$ is the transformation matrix from fixed BPS frame to reactor vessel frame,
${}^{0}_{1}\boldsymbol{T}$ is the transformation matrix from pan-axis frame to fixed BPS frame,
${}^{1}_{2}\boldsymbol{T}$ is the transformation matrix from tilt-axis frame to pan-axis frame,
${}^{2}_{L}\boldsymbol{T}$ is the transformation matrix from laser frame to tilt-axis frame,
${}^{L}\boldsymbol{P}$ is the position vector of the desired target point in the laser frame, and

${}^{RV}\boldsymbol{P}$ *is the position vector of the desired target point in the reactor vessel frame*

The transformation matrices and the position vectors in equation 6.1 are described below in equation form:

$$ {}^{RV}_{0}\boldsymbol{T} = \begin{bmatrix} c\alpha c\beta & c\alpha s\beta s\gamma - s\alpha c\gamma & c\alpha s\beta c\gamma + s\alpha s\gamma & x \\ s\alpha c\beta & s\alpha s\beta s\gamma + c\alpha c\gamma & s\alpha s\beta c\gamma - c\alpha s\gamma & y \\ -s\beta & c\beta s\gamma & c\beta c\gamma & z \\ 0 & 0 & 0 & 1 \end{bmatrix} \tag{6.2} $$

where,

x, y, and z describe the position of the fixed BPS frame in the reactor vessel frame,
α, β, and γ describe the fixed-angle orientation of the fixed BPS frame in the reactor vessel frame.

$$ {}^{0}_{1}\boldsymbol{T} = \begin{bmatrix} (c\theta_o c\theta - s\theta_o s\theta) & -(s\theta_o c\theta + c\theta_o s\theta) & 0 & a_0 \\ (s\theta_o c\theta + c\theta_o s\theta)c\alpha_0 & (c\theta_o c\theta - s\theta_o s\theta)c\alpha_0 & -s\alpha_0 & -s\alpha_0 d_1 \\ (s\theta_o c\theta + c\theta_o s\theta)s\alpha_0 & (c\theta_o c\theta - s\theta_o s\theta)s\alpha_0 & c\alpha_0 & c\alpha_0 d_1 \\ 0 & 0 & 0 & 1 \end{bmatrix} \tag{6.3} $$

where,

the Denavit-Hartenberg convention is used to describe the pan-axis frame in the fixed BPS frame, and all the Denavit-Hartenberg link parameters (for i = 1) are described in Table 6.1.

$$ {}^{1}_{2}\boldsymbol{T} = \begin{bmatrix} (c\phi_o c\phi - s\phi_o s\phi) & -(s\phi_o c\phi + c\phi_o s\phi) & 0 & a_1 \\ (s\phi_o c\phi + c\phi_o s\phi)c\alpha_1 & (c\phi_o c\phi - s\phi_o s\phi)c\alpha_1 & -s\alpha_1 & -s\alpha_1 d_2 \\ (s\phi_o c\phi + c\phi_o s\phi)s\alpha_1 & (c\phi_o c\phi - s\phi_o s\phi)s\alpha_1 & c\alpha_1 & c\alpha_1 d_2 \\ 0 & 0 & 0 & 1 \end{bmatrix} \tag{6.4} $$

where,

again the Denavit-Hartenberg convention is used to describe the tilt-axis frame in the pan-axis frame, and all the Denavit-Hartenberg link parameters (for i = 2) are described in Table 6.1.

$$ {}^{2}_{L}\boldsymbol{T} = \begin{bmatrix} c\alpha_L c\beta_L & c\alpha_L s\beta_L s\gamma_L - s\alpha_L c\gamma_L & c\alpha_L s\beta_L c\gamma_L + s\alpha_L s\gamma_L & x_L \\ s\alpha_L c\beta_L & s\alpha_L s\beta_L s\gamma_L + c\alpha_L c\gamma_L & s\alpha_L s\beta_L c\gamma_L - c\alpha_L s\gamma_L & y_L \\ -s\beta_L & c\beta_L s\gamma_L & c\beta_L c\gamma_L & z_L \\ 0 & 0 & 0 & 1 \end{bmatrix} \tag{6.5} $$

where,

x_L, y_L, and z_L describe the position of the laser frame in the tilt-axis frame,
α_L, β_L, and γ_L describe the fixed-angle orientation of the laser frame in the tilt-axis frame.

$$ {}^{L}\boldsymbol{P} = \begin{Bmatrix} xl \\ 0 \\ 0 \\ 1 \end{Bmatrix} \tag{6.6} $$

where,

xl is the length of the laser beam from the laser frame origin to the target point. The beam will be along the X_L axis according to the coordinate frame assignment convention. This laser length (xl) is an unknown quantity in equation 6.1.

Equations 6.2 to 6.6 describe the individual transformation matrices that are part of equation 6.1. The position of a target point in the reactor vessel (world) frame is given by equation 6.1. This target point can be a point on URSULA, in which case the position of a point on URSULA can be found.

It can be clearly deduced that if the BPS is to be used to find the circumferential position (θ) of URSULA in the reactor vessel, then every parameter value must be known in

equation 6.1 except, of course, *xl* which is always unknown. Since only nominal values of all the parameters are known, there is a characterization that must be attempted to find the as-built values of the parameters in equation 6.1. Once this characterization process has been completed, equation 6.1 can be used to find the position of URSULA repeatedly as required.

The following sections describe the characterization process for the BPS design and then describe how the BPS is used to calculate the circumferential position (θ) of URSULA.

6.3 Sources of Pose Error

The system model of the laser-pan-tilt BPS is analyzed to identify all the system parameters. First all the system parameters that are sources of pose error in the BPS are listed. These parameters can be obtained from equation 6.1. The list follows:

1. x, y, z, α, β, and γ are from ${}^{RV}_{0}\boldsymbol{T}$; they are sources of error. They describe the pose of the laser-pan-tilt BPS in the reactor vessel frame. These errors depend on the beam manufacture and assembly. These are important parameters, especially the orientation parameters, because, if they are wrong, the error in the position of URSULA can be significant due to magnification. (Total 6 parameters).

2. θ_o is a source of error from ${}^{0}_{1}\boldsymbol{T}$. This is the initial angle (joint offset) for the pan axis. This also can be significant. (Total 1 parameter).

3. α_1, a_1, and ϕ_o are sources of error from ${}^{1}_{2}\boldsymbol{T}$. ϕ_o is the initial joint angle for the tilt axis. α_1 and a_1 are the DH parameters of the second link in the BPS. These depend on how the BPS has been manufactured and assembled. (Total 3 parameters).

4. x_L, y_L, z_L, α_L, β_L, and γ_L are from ${}^{2}_{L}\boldsymbol{T}$ and they are sources of error. They describe the pose of the laser in the tilt-axis frame. (Total 6 parameters).

5. In order to characterize the BPS, it is necessary to take measurements of its laser positioning. One method of doing this is to place laser targets at known locations in the reactor vessel. The number of parameters needing characterization dictates the number of targets required. Every target point shot with the laser is represented by three scalar equations. But for every point shot with the laser there is one unknown that is added, i.e., the length of the laser beam (xl). Every point therefore represents two pieces of information. If 16 parameters (the total number from items 1-4) need to be characterized, then 8 targets would be needed. Also this characterization process needs to be performed in the reactor vessel after the BPS is installed. Since 8 targets in the reactor vessel was deemed to be unacceptable, it was decided to narrow down the list of parameters to the most critical only. This process is described in the next sub-section. In any case, each target represents three position parameters that are possible sources of error. (Total 3 parameters per target).

6. The joint angle readings of the pan and tilt axes are sources of error (θ and ϕ). These readings depend on the positioning accuracy of the joints and the accuracy and resolution of the encoders that measure the angles. There are a set of two readings for every target point shot. Therefore, the number of parameters will be twice the number of targets for characterization plus the target on URSULA. (Total is 2 times the number of targets plus two).

7. The error parameters due to the target position knowledge of URSULA. These consist of knowledge of radius of vessel, targeting error in circumferential direction, and the depth information from the depth gauge. (Total 3 parameters).

8. The two inclinometers on URSULA are sources of error in reading the orientation angles. Each inclinometer is responsible for two sources of error. One is the error due to its mounting inaccuracy on URSULA and the other due to the accuracy of the inclinometer itself. (Total 4 parameters).

These are all the sources of error. After the sensitivity analysis of the BPS parameters is performed, the number of targets needed in the reactor vessel for characterization will be known. Once the number of targets is determined, the exact number of error parameters will be known. Next, the possible range of error for these error parameters is presented.

1. The BPS position parameters, x, y, and z, depend on the beam assembly tolerances. They are $\pm$ 0.25 in. The BPS orientation parameters are also dependent on the beam mounting. They are $\pm$ 1 degree. These numbers are from the beam assembly tolerances. The pose parameters of the BPS were loosely toleranced because it was decided that they were going to be characterized.

2. It was decided to mount the targets directly on the reactor vessel flange, which is a relatively accurate machined surface with known tolerances. Based on this, the error ranges for the targets on the flange were isolated as follows. In the x and y directions, the guide-lug tolerances were identical, i.e., $\pm$ 0.044 in. Added to this are the target assembly errors of $\pm$ 0.01 in. and a laser sighting error of $\pm$ 0.1 in. Therefore, the total error range in the x and y directions for the targets is $\pm$ 0.154 in. In the z direction, the tolerance on the guide lug location is tighter, $\pm$ 0.005 in. The target assembly error is the same, i.e., $\pm$ 0.01 in. and the laser sighting error remains $\pm$ 0.1 in. Therefore the

total error range in the z direction for the target is $\pm$ 0.115 in. This defines the error range for the targets on the flange that are required for BPS characterization.

3. The error range of the pan and tilt joint angles is a sum of the synchro resolution and the joint step resolution. A synchro with an absolute accuracy of 3 arc minutes was used for both the pan and tilt axes. But there is a 5 to 1 gear reduction employed on the joint such that the synchro resolution reduces to 0.6 arc minutes, which is 0.01 deg. The joint controller uses a 12 bit word, therefore it can divide a complete circle into 4096 step sizes. But since the 5 to 1 gear reduction is employed the number of step sizes actually become 5x4096 = 20480. Therefore, a single joint step is 360/20480 = 0.0175 deg. Therefore the total error range for the joint angle readings are $\pm$ (0.01 + 0.0175) = $\pm$ 0.0275 deg.

4. The initial joint angles can be off by as much as $\pm$ 0.5 deg for the pan and tilt axes because the synchro is mounted on the motor end before the gear reduction.

5. The laser assembly on the tilt axis has the following machine and assembly tolerances. For x_L, y_L, and z_L, it is $\pm$ 0.02 in. For α_L, β_L, and γ_L, the tolerance is $\pm$ 0.25 deg. These are manufacturing specifications of BWNT.

6. The link offset between the pan and tilt links of the BPS (a_1) has a possible error range of 0.02 in. from the design drawings. The tolerance on the pan and tilt axis perpendicularity (α_1) is 1 arc minute which is 0.0167 deg. These numbers are also from the manufacturing and assembly tolerances of BWNT.

7. For the target on URSULA the following parameters effect the overall system performance. The radius of the reactor vessel is known to $\pm$ 0.5 in over the circumference. Add to this the target mounting error of 0.05 in. and laser sighting error of 0.1 in. Therefore the total error in the radial direction is $\pm$ 0.65 in. In the z direction, the error range includes the depth gauge accuracy of $\pm$ 0.2 in., the assembly

error of ± 0.05 in., and the targeting error of ± 0.1 in. The total error range in the z direction is ± 0.35 in. In the circumferential direction (θ), a target mounting error of ± 0.1 in. and laser sighting error of ± 0.1 in., can be added to the final value calculated by using the BPS. The reactor vessel also has a cladding error of ± 0.125 in. which can effect the local height of URSULA's tripod feet.

8. The two inclinometers have an accuracy of ± 0.05 deg. Since they are relative devices there is no mounting error.

The magnitudes of the error sources discussed above have been obtained from manufacturers literature, component and assembly drawings and through subcomponent testing and measurement. These parameters are critical to accurate prediction of system performance and the resulting system design.

6.4 Sensitivity Analysis

The first step in the sensitivity analysis was to decide which BPS parameters require calibration so that the number of targets required on the reactor vessel flange can be selected. The pose of the fixed BPS frame in the reactor vessel frame contains six parameters which definitely need characterization because every time the BPS is installed in a reactor vessel, these parameters will have new values. Also, for every target added we are adding one unknown for the laser length. A Mathcad model of the robot system was developed. This model had a real world simulation module and an ideal world simulation module. This output of this model was the circumferential position error of

URSULA. Nominal values of the parameters were used as a starting point in the analysis. This case gave an output error of zero, which helped to confirm that the model was working correctly. Following this, each parameter was individually perturbed to its maximum error and the output error on URSULA's circumferential (hereafter referred to as theta) position error was recorded. This Mathcad analysis was performed for a set of arbitrary locations of URSULA in the reactor vessel. The results showed that the most sensitive parameter was β_L, which is the orientation of the laser frame about the Y_2 axis (Tilt axis frame). This parameter definitely needed calibration, since an error of 0.2 deg produced an error of 1.131 in. for the theta position of URSULA. Unfortunately, this parameter could not be calibrated using the target-on-flange procedure described above. In this configuration, the laser is pointing horizontally at the target, which implies that the Y_2 axis coincides with Z_0 axis. The rotation angle β_L is redundant with α in this configuration. This led to a different procedure for β_L calibration, which is described in a later sub-section.

The second most sensitive parameter was α_1 which is the perpendicularity of the pan and tilt axes of the BPS. An error of 0.01 deg in α_1 produced a theta position error of 1.217 in. Once again, this parameter cannot be calibrated using the flange-target procedure because α_1 errors have no effect on system accuracy when the beam is pointed at the flange. The system is also sensitive to the initial angle θ_0 of the pan axis, which unfortunately is also redundant with α. Another calibration procedure for these two

parameters will be described later. System performance was found to be insensitive to the remaining parameters, and calibration was not required. The results of this preliminary sensitivity analysis show that the sensitive parameters that need calibration are those that cannot be calibrated using the flange-target approach. Therefore, only the pose parameters x, y, z, α, β, and γ need to be characterized using the flange-target approach. This implies for six parameters from our previous discussion we need a minimum of three targets. Three targets will ensure 9 equations in 9 unknowns (6 pose unknowns and 3 laser length unknowns). Four targets were selected to give additional information to use in the optimization process. Using four targets implies 12 equations in 10 unknowns. Now that the number of targets are known, the total number of error source parameters are 45.

At this point, an exhaustive sensitivity analysis was performed that checked the sensitivity of all the 45 error parameters. This sensitivity analysis code was written in C and C++ and also includes parts of code written by James Gayle and Joe Calkins. The purpose of this analysis was to identify the most sensitive parameters that contribute to the theta positioning error of URSULA. Once these parameters were identified, a decision was made as to which parameters needed calibration. Calibration procedures for these parameters also were developed. The input data file for the sensitivity analysis program is given in Appendix 2. The strategy employed for the sensitivity analysis is as follows. In the first run, all 45 parameter values are kept at the nominal values and then each one is perturbed one at a time to the positive extreme of its error range. The position

of URSULA is calculated along with the error associated with the perturbed parameter value. This analysis was performed for eight different locations of URSULA in the reactor vessel. These locations are at two heights, i.e., at flange height (z = 0 in.) and at the bottom-most position of URSULA in the vessel (z = -280 in.). At each of these two heights, there are four circumferential locations of URSULA, i.e., θ = 0, 90, 180, and 270 deg. The results from these eight positions are considered to be a good representation of the complete reactor vessel. Also, other runs were performed that used different combinations of nominal, positive extreme, and negative extreme error parameter values. Values were then individually perturbed to positive extreme, nominal, and/or negative extreme of range.

The results of the sensitivity analysis helped in isolating the individual effects of the various parameters on the positioning accuracy of URSULA and also helped to identify the critical parameters which need calibration. This analysis confirmed the results of the Mathcad analysis. The two most sensitive parameters were β_L and α_1 in that order. At this point it was decided to develop a calibration procedure for β_L and then re-run the simulation.

The full results of one sample run of the sensitivity analysis are shown in the Appendix. A small subset of this output is shown in Table 6.2. As can be seen from the table, β_L is by far the most sensitive parameter and α_1 ranks a distant second. The next sub-section discusses the calibration procedure for β_L. It should be noted that this sensitivity analysis

program includes the fixed BPS pose characterization performed using the four flange-targets. This explains why the error in these six parameters is zero in the sensitivity analysis output. The depth gauge has an error of 0.35 in. in the z direction, which shows up directly in the sensitivity analysis because we are not solving for z and we do not use the depth gauge information to calculate the theta position of URSULA. It is within the required 0.5 in. specification for the z depth.

Table 6.2: Sample of Sensitivity Analysis Output for Nominal Set, Positive Individual Perturbation
(Refer to Appendix 2 for complete code output)

	Depth at 0.0 inches				**Depth at -280.0 inches**			
Theta -	**0.0^0**	**90.0^0**	**180.0^0**	**270.0^0**	**0.0^0**	**90.0^0**	**180.0^0**	**270.0^0**
Radius r	0.0000	0.0000	0.0000	0.0000	0.0000	0.0000	0.0000	0.0000
Target y_0	0.0018	0.0005	0.0007	0.0006	0.0018	0.0005	0.0007	0.0006
Target z_2	0.0000	0.0001	0.0000	0.0001	0.0000	0.0043	0.0000	0.0043
z_L	0.0108	0.0108	0.0108	0.0108	0.0108	0.0108	0.0108	0.0108
β_L	0.0023	0.0023	0.0023	0.0023	2.6999	2.6999	2.6999	2.6999
α_1	0.0016	0.0016	0.0016	0.0016	0.0698	0.0698	0.0698	0.0698

6.5 Calibration Parameters

It can be seen from the sensitivity analysis results that the system is most sensitive to errors in β_L. This is the laser orientation parameter that describes the laser frame rotation about the Y_2 axis, i.e., the tilt axis frame. As explained previously, this parameter cannot be calibrated using the flange-target procedure. The procedure devised for calibrating β_L

involves shooting a point on the reactor vessel wall with the tilt axis at a joint angle of zero, making a note of this point, and rotating the pan axis 180 deg and then the tilt axis 180 deg. The new point is also noted, and the circumferential angle difference between these two points is measured. Half of this angle difference is used as the calibrated value of β_L. A calibration procedure written in C has been implemented in the control system and the simulation software. This calibration procedure calibrated β_L to within 0.05 deg consistently in simulation studies. Sensitivity analysis showed this to be an acceptable result.

With β_L calibrated, an exhaustive simulation with the fixed BPS characterization was carried out. The purpose of this simulation was to analyze possible theta positional errors for URSULA to check for acceptability of the design. Another aspect of the design was to check the acceptability of the 3 arc minute synchro resolution. Although this appeared to be acceptable from the sensitivity analysis, with all other errors built into the model, the simulation would give a final result on this issue.

The initial values of the joint angles need calibration for the sake of implementing into the controller. The initial angle for the pan axis θ_o is a redundant parameter with the α parameter. As a result it gets characterized in the fixed BPS frame calibration procedure and zero is entered in the controller for this value. The procedure for the tilt axis initial joint angle ϕ_o is similar to the procedure for β_L. The procedure is the same as described

before, but this time the vertical angle difference is measured and halved. This value will be the initial angle for ϕ_o.

6.6 Simulation

This simulation is intended to mimic the performance of the BPS in the real world prior to hardware fabrication. The purpose of the simulation is to evaluate the theta positional error of URSULA using the laser-pan-tilt BPS. By performing a large number of simulation runs and studying the resulting theta positional error of URSULA the design will be evaluated. A decision can be made if better components or additional calibration is required for other parameters. The simulation code was written in C and C++ and partly incorporates code written by James Gayle and Joe Calkins.

The simulation involves performing the following steps:

1. Read in the nominal values as the error perturbation ranges from the parameter data file. A sample file is shown in Appendix 2.
2. Simulate real world by randomly generating parameter error values within the respective ranges for every parameter. Generate pan and tilt joint angle values required to read the four targets on the flange which have errors built into them.
3. Generate pose of URSULA given a theta position, depth value, 2 inclinometer values, and radial position of the feet of URSULA. Use this pose information to calculate the position of the target on URSULA. This is performed with simulated error.
4. Generate pan and tilt angle values required to sight the laser on the URSULA target given the position of the target in the world frame.

5. Calibrate β_L given the simulated error values in the system using the procedure outlined previously. Use this value of β_L in future steps in the simulation instead of the ideal value of zero.
6. Add pan and tilt angle errors that are randomly generated to the values calculated in step 2 for the four targets. Given these values, the fixed BPS pose parameters are characterized. The nominal values of the other parameters are used at this juncture because this should simulate the ideal world, i.e., no errors. The calibrated value of β_L is used. At this stage we have effectively simulated the fixed BPS characterization procedure using the four targets on the reactor vessel flange.
7. Using the fixed BPS pose, the nominal values for the other parameters and the calibrated β_L value, the pose of URSULA is optimized by using the depth gauge value, theta position, radial feet position, and inclinometer values.
8. Compare the values of URSULA position from step 3 and step 7. Calculate the difference between these two values to give positional error of URSULA.
9. Compare the values of URSULA orientation from step 3 and step 7. Calculate the differences between these values and print the maximum error value and label between the three rotation parameters.

This exhaustive simulation was carried out for a total of 109,060 iterations of URSULA theta positional error evaluation. The results from this simulation are presented in the next sub-section.

6.7 System Performance

The exhaustive simulation of 109,060 runs produced the following results.

1. Maximum theta positional error magnitude of URSULA = 0.800394 in.
2. Maximum overall URSULA positional error magnitude = 0.900928 in.

3. Maximum rotational error = 1.066729 deg.
4. Maximum value that β_L is calibrated within = 0.0512 deg.
5. The random value for β_L corresponding to situation in step 4 = -0.192564 deg.
6. The calibrated value of β_L corresponding to situation in step 4 = -0.141364 deg.
7. Number of times theta error was more than 0.1 in. = 48,273
8. Number of times theta error was more than 0.2 in. = 16,724
9. Number of times theta error was more than 0.25 in. = 9,510
10. Number of times theta error was more than 0.3 in. = 5,274
11. Number of times theta error was more than 0.4 in. = 1,477
12. Number of times theta error was more than 0.5 in. = 323
13. Number of times theta error was more than 0.6 in. = 51
14. Number of times theta error was more than 0.7 in. = 4
15. Number of times theta error was more than 0.8 in. = 1

From the above results it can be seen that in 99.7% of the cases URSULA's base theta position was within the required ± 0.5 in. range. URSULA is moved around only 60 times in an inspection outage. Since the simulation randomly placed URSULA in the vessel 109,060 times, the simulation of the design and characterization is considered a success. These results are with β_L calibration incorporated and α_1 not calibrated. Also, these results are for a synchro that has an accuracy of 3 arc minutes. The simulation shows that a more accurate synchro is not required and α_1 does not require calibration. The design will meet the performance specifications with the fixed BPS pose characterization and β_L calibration. Also, before operation it is necessary to find the tilt axis initial joint angle as described earlier.

In summary, this chapter described the successful application of the robot system characterization methodology to the design of URSULA's BPS. The system was modeled along with the reactor vessel environment. The sensitivity analysis was performed first to decide on the BPS parameter characterization and the number of targets required on the reactor vessel flange. Then the analysis was conducted to find the sensitivity of all the 45 error parameters to the URSULA positioning error. This identified parameters that needed calibration. Suitable calibration procedures were developed and implemented. Then an exhaustive simulation was performed to analyze the BPS design performance. The design was successful and the BPS was developed and tested in a reactor vessel mockup and was found to consistently find the theta position of URSULA within ± 0.5 in. The BPS was also taken to site along with URSULA to perform weld inspections in a reactor vessel. Although there are no quantitative results for comparison, the performance was found to be successful qualitatively.

7. Conclusions

This chapter reviews and highlights the accomplishments described in this dissertation. It also contains some conclusions about the newly-developed robot system characterization methodology and its potential for broad application.

7.1 Summary

The development and successful application of a robot system characterization methodology that improves the performance of robot systems has been described in this dissertation. This methodology involves modeling, identification, analysis, and minimization of errors in robot geometric parameters. The goal of this methodology is to find the set of parameters that best fits the measurement or simulation data for the robot end-effector position.

The motivation for this work was presented first. Brief descriptions and definitions of robot systems, pose errors, and sources of pose errors were included followed by a short discussion of the robot system characterization methodology. Previous experiences with robot system development and calibration were also presented. The literature review in the areas of robot design and calibration, error modeling, sensitivity analysis and optimization techniques, mathematics, software , and hardware was presented next. The robot system characterization methodology was described in detail which included the description of the robot system modeling techniques, identification of error sources, and sensitivity analysis. Kinematic link description techniques are first used to model the robot system in relation to the environment reference. Next, knowledge of the robot system, its environment and detailed component specifications were used to identify the sources of error that results in a list of error parameters and their error ranges. Sensitivity analysis was performed on these error parameters to determine which have the greatest effect on system accuracy. The description of the methodology continued with a presentation of various techniques of experimental data measurement, followed by description of optimization techniques and implementation of the optimized parameter values of an existing robot into the control system. A simulation strategy for new robot system design was also described. This characterization process is iterative. The application of this methodology to a Unimation PUMA 562 industrial robot was discussed. The results show that the performance of the robot improved significantly after the characterization was performed. The application of the characterization

methodology to the design of a base positioning system for an underwater, mobile, nuclear-reactor-vessel-inspection-robot was presented last. This base positioning system performed well both in computer simulations and in the field.

This methodology has broad application to the robot calibration field. If this characterization process was adopted, then there could be significant cost savings in the robot design and manufacture process. Expensive precision components could be replaced with less precise ones and manufacturing and assembly tolerances could be relaxed There are also possible savings in design time.

It is believed that this work has made significant contributions in several important areas. These are briefly reviewed in the following list:

1. More than any previous work this research is comprehensive from the development of the robot system characterization methodology through the application of this process.
2. It has been shown that this general robot system characterization methodology is applicable not only to existing robot systems, but also to new robot system design, as presented in Chapter 6. No previous research has been found that applies such a methodology to the design of new robot systems.
3. This methodology is performance-goal-oriented and therefore practical. No other work has been found that is clearly directed at satisfying actual performance goals.
4. In new system design, decisions about cost-performance tradeoffs can be made using this methodology.

These contributions improve upon previous research in the area of robot design and calibration. There has been a significant amount of recent work in the area of robot calibration, which shows the need for a good robot system characterization methodology.

The results of the PUMA system characterization were good. Significant improvements were made in tool positioning accuracy. Using nominal values for the PUMA system parameters yielded absolute position errors of up to 20 mm and an average error of 12 mm. After the characterization process, the maximum absolute error was 2.0 mm and the average absolute error dropped to 0.6 mm. Comparison with the factory calibrated values was not possible due to unavailability of the information. A significant advantage of this methodology is that all geometric parameters can be calibrated at one time using one process.

A very significant aspect of this methodology is that it was successfully applied to the design of URSULA's BPS as described in Chapter 6. The limitations imposed by the design constraints were strict and a rigorous conceptual design phase was warranted. But ultimately, the goal of developing and using a BPS that could find URSULA's position to $\pm$ 0.5 in. in each of the coordinates was accomplished. The simulations based on the characterization methodology presented in this dissertation showed that URSULA's positioning was within the performance goal of $\pm$ 0.5 in. 99.7% of the time. Subsequent to that the BPS was manufactured, assembled and used in the field successfully.

7.2 Recommendations for Future Work

Now that the methodology has been proven to work, more computationally efficient algorithms and techniques can be implemented to perform the same functions. For example, sensitivity analysis techniques like the Direct Sensitivity Approach (DSA) and the Adjoint Sensitivity Method (ASM) can be tested and the best one can be implemented. Similarly, other optimization techniques that may be more efficient and robust than Hooke and Jeeves' pattern search method can be explored and the best one used along with a suitable objective function formulation. Current efforts are being undertaken by another researcher toward this end and preliminary results show the gradient-based methods to be slightly better than Hooke-Jeeves method. Non-geometric parameters like backlash, and link and joint compliance can be added to the methodology. Similarly control system errors like offshoot and settling can be modeled. While taking measurements, a process using Kalman filters can be implemented that automates the data acquisition similar to that described in Bay (1993). This process can also be used to decide on where and how much data to take. Statistical modeling of uncertainties in the system can also be incorporated into the model using estimation theory. A general, six degree-of-freedom robot inverse kinematics algorithm can be implemented such that the controller can perform the inverse kinematics even after updating of system parameter values (Lee and Reinholtz, accepted for publication in 1994). The current data measurement techniques rely on joint angle information from the robot system. This means that the technique is dependent on the joint relative positioning accuracy. An

improved technique can be devised such that this dependence is eliminated. The hardware can be designed such that it is attached to the required joints and relative angle measurements can be taken from these added sensors. The advantage is that this system can be designed to the required accuracy and the complete characterization system is independent of the robot. In other words, the complete system can be made portable.

References

1. Adept Technology, Inc., San Jose, CA.

2. Anorad Corporation, Hauppauge, NY.

3. B&W Nuclear Technologies (BWNT), Lynchburg, VA.

4. Bay, J. S., 1993, "Autonomous Parameter Identification by Optimal Learning Control," *IEEE Control Systems Magazine*, Vol. 13, No. 3, June, pp. 56-61.

5. Berg, J. O., 1991, "Robot Calibration for Off-Line Programming," *Industrial Robot*, Vol. 18, No. 2, pp. 29-31.

6. Bhatti, P. K., and Rao, S. S., 1988, "Reliability Analysis of Robot Manipulators," *Journal of Mechanisms, Transmissions, and Automation in Design*, Vol. 110, pp. 175-181.

7. Borland International, Inc., "Quattro Pro for Windows", Scotts Valley, CA.

8. Borm, J. H., and Menq, C. H., 1991, "Determination of Optimal Measurement Configurations for Robot Calibration Based on Observability Measure," *The International Journal of Robotics Research*, Vol. 10, No. 1, pp. 51-63.

9. Broderick, P. L., and Cipra, R. J., 1988, "A Method for Determining and Correcting Robot Position and Orientation Errors Due to Manufacturing," *Journal of Mechanisms, Transmissions, and Automation in Design*, Vol. 110, No. 1, 3-10.

10. Brown, L. B., Merry, J. B., and Wells, D. N., 1986, "Coordinate Measurement With a Tracking Laser Interferometer," *Lasers & Applications*, October.

11. Brown, L. B., and Merry, J. B., 1988, "Interferometric Accuracy in Three-Dimensional Measurements: A Precision Laser Tracking System," *SME Proceedings, Precision Metrology with Coordinate Measurement Systems.*

12. Calkins, J. M., 1994, "Real-Time Compensation of Static Deflections in Robotic Manipulators," Masters Thesis, Department of Mechanical Engineering, Virginia Polytechnic and State University, Blacksburg, VA.

13. Catlin, D. E., 1989, *Estimation, Control, and the Discrete Kalman Filter*, Springer-Verlag, New York City, NY.

14. Chen, J., and Chao, L. M., 1987, "Positioning Error Analysis for Robot Manipulators with All Rotary Joints," *IEEE Journal of Robotics and Automation*, Vol. RA-3, No. 6, pp. 539-545.

15. Chiu, H., Ozaki, H., Sato, E., Suzuki, T., Oho, A., and Aruira, Y., 1993, "An Analysis Using Offset Curves for Profiles, Manufacturing and Errors of Plane Cams," *JSME International Journal*, Series C, Vol. 36, No. 1, pp. 110-118.

16. Cleghorn, W. L., Fenton, R. G., and Fu, J. F., 1993, "Optimum Tolerancing of Planar Mechanisms Based on an Error Sensitivity Analysis," *Journal of Mechanical Design*, Vol. 115, No. 2, pp. 306-313.

17. Cooper, M. A. R., 1982, *Modern Theodolites and Levels*, Second Edition, Granada, New York, NY.

18. Craig, J. J., 1989, *Introduction to Robotics: Mechanics and Control*, Second Edition, Addison-Wesley Publishing Company, Reading, MA.

19. Denavit, J., and Hartenberg, R. S., 1955, "A Kinematic Notation for Lower-Pair Mechanisms Based on Matrices," *Journal of Applied Mechanics*, Vol. 22, pp. 215-221.

20. Deutsch, R., 1965, *Estimation Theory*, Prentice-Hall, Inc., Englewood Cliffs, NJ.

21. Dhande, S. G., and Chakraborty, J., 1973, "Analysis and Synthesis of Mechanical Error in Linkages - A Stochastic Approach," *Journal of Engineering for Industry*, Series B, Vol. 95, No. 3, pp. 672-676.

22. Dhande, S. G., and Chakraborty, J., 1975, "Mechanical Error Analysis of Cam-Follower Systems - A Stochastic Approach," *Proceedings of the Fourth World Congress on the Theory of Machines and Mechanisms*, University of New Castle upon Tyne, England, September 8-12, Vol. 4, pp. 957-962.

23. Dhande, S. G., and Chakraborty, J., 1978, "Mechanical Error Analysis of Spatial Linkages," *Journal of Mechanical Design*, Vol. 100, No. 4, pp. 732-738.

24. Eason, E. D., and Fenton, R. G., 1974, "A Comparison of Numerical Optimization Methods for Engineering Design," *Transactions of the ASME: Journal of Engineering for Industry*, February, pp. 196-200.

25. Everett, L. J., Driels, M., and Mooring, B. W., 1987, "Kinematic Modelling for Robot Calibration," *Proceedings of the IEEE International Conference on Robotics and Automation*, Vol. 1, pp. 183-189.

26. Fallon, J. B., 1995, "Improving the Kinematic Control of Robots with Computer Vision," PhD Dissertation, Department of Mechanical Engineering, Virginia Polytechnic and State University, Blacksburg, VA.

27. Fallon, J. B., Reinholtz, C. F., Vallance, R. R., Voruganti, R.S., and Abbott, A. L., 1994a, "Improving Robot System Performance Using Computer Vision," *Proceedings of the 1994 ASME Mechanisms Conference*, Minneapolis, MN.

28. Fallon, J. B., Shooter, S. B., Reinholtz, C. F., and Glass, S. W., 1994b, "URSULA: Design of an Underwater Robot for Nuclear Reactor Vessel Inspection," *Proceedings of the ASCE Specialty Conference on Robotics for Challenging Environments, Co-located with Space 94*, Albuquerque, New Mexico, Feb. 26 - Mar. 3, pp. 311-319.

29. Ferreira, P. M., and Liu, C. R., 1986a, "A Contribution to the Analysis and Compensation of the Geometric Error of a Machining Center," *Annals of the CIRP/CIRP Annals - Manufacturing Technology*, Vol. 35/1/1986, pp. 259-262.

30. Ferreira, P. M., and Liu, C. R., 1986b, "An Analytical Quadratic Model for the Geometric Error of a Machine Tool," *Journal of Manufacturing Systems*, Vol. 5, No. 1, pp. 51-63.

31. Ferreira, P. M., and Liu, C. R., 1993, "A Method for Estimating and Compensating Quasistatic Errors of Machine Tools," *Journal of Engineering for Industry*, Vol. 115, pp. 149-159.

32. Goswami, A., Quaid, A., and Peshkin, M., 1993, "Complete Parameter Identification of a Robot from Partial Pose Information," *Proceedings of the IEEE International Conference on Robotics and Automation*, Vol. 1, pp. 168-173.

33. Green, P. A., and Philpott, M. L., 1994, "Error Modeling of Reverse Engineered Free Form Surfaces," *Transactions of NAMRI/SME*, Vol. XXII, pp. 259-266.

34. Groover, M. P., Weiss, M., Nagel, R., and Odrey, N. G., 1986, *Industrial Robotics: Technology, Programming, and Applications*, McGraw-Hill Book Company, New York, NY.

35. Hayati, S. A., 1983, "Robot Arm Geometric Link Parameter Estimation," *Proceedings of the 22nd IEEE Conference on Decision and Control*, Vol. 3, pp. 1477-1483.

36. Hayati, S., and Mirmirani, M., 1985, "Improving the Absolute Positioning Accuracy of Robot Manipulators," *Journal of Robotic Systems*, Vol. 2, No. 4, pp. 397-413.

37. Hayati, S., Tso, K., and Roston, G., 1988, "Robot Geometry Calibration," *Proceedings of the IEEE International Conference on Robotics and Automation*, Vol. 2, pp. 947-951.

38. Hollerbach, J. M., and Bennet, D. J., 1988, "Automatic Kinematic Calibration Using a Motion Tracking System," *Robotics Research, The Fourth International Symposium*, MIT Press, Cambridge, MA, pp. 191-198.

39. Hollerbach, J. M., 1989, "A Survey of Kinematic Calibration," *The Robotics Review 1*, ed. Khatib, O., Craig, J. J., and Lozano-Perez, T., The MIT Press, Cambridge, MA, pp. 207-242.

40. Huang, M. Z., and Masory, O., 1991, "Robot Accuracy Enhancement Using a Simple Measurement Method for Automatic Identification of Kinematic Parameters," *Proceedings of the 2nd National Applied Mechanisms & Robotics Conference*, November 3-6, Cincinnati, Ohio, pp. IIC.3-1-5.

41. Ishii, M., 1991, "Kinematic Model and Calibration of a Robot Manipulator," *Advanced Robotics*, Vol. 5, No. 3, pp. 337-347.

42. Jaech, J. L., 1985, *Statistical Analysis of Measurement Errors*, John Wiley and Sons, New York, NY.

43. Kaizerman, S., Benhabib, B., Fenton, R. G., and Zak, G., 1992, "A Sensitivity Analysis Based Method for Robot Calibration," *Proceedings of the 1992 ASME Design Technical Conferences - 22nd Biennial Mechanisms Conference*, Scottsdale, Arizona, September 13-16, DE-Vol. 45, pp. 119-127.

44. Khalil, W., Gautier, M., and Enguehard, Ch., 1991, "Identifiable Parameters and Optimum Configurations for Robots Calibration," *Robotica*, Vol. 9, pp. 63-70.

45. Kim, K., and Kim, M. K., 1991, "Volumetric Accuracy Analysis Based on Generalized Geometric Error Model in Multi-Axis Machine Tools," *Mechanisms and Machine Theory*, Vol. 26, No. 2, pp. 207-219.

46. Kiridena, V. S. B., and Ferreira, P. M., 1994a, "Kinematic Modeling of Quasistatic Errors of Three-Axis Machining Centers," *International Journal of Machine Tools and Manufacture*, Vol. 34, No. 1, pp. 85-100.

47. Kiridena, V. S. B., and Ferreira, P. M., 1994b, "Parameter Estimation and Model Verification of First Order Quasistatic Error Model for Three-Axis Machining Centers," *International Journal of Machine Tools and Manufacture*, Vol. 34, No. 1, pp. 101-125.

48. Kiridena, V. S. B., and Ferreira, P. M., 1994c, "Computational Approaches to Compensating Quasistatic Errors of Three-Axis Machining Centers," *International Journal of Machine Tools and Manufacture*, Vol. 34, No. 1, pp. 127-145.

49. Lee, H. Y., and Reinholtz, C. F., "Inverse Kinematics of Serial-Chain Manipulators", Accepted in 1994 for Publication in *The ASME Journal of Mechanical Design*.

50. Lee, H. Y., Fallon, J. B., Cordle, W. H., and Reinholtz, C. F., 1993, "Inverse Kinematic Analysis of a Mobile Underwater Inspection Robot," *Proceedings of the 3rd National Applied Mechanisms & Robotics Conference*, November 7-10, Cincinnati, Ohio, pp. AMR-93-085-01-06.

51. Lee, H. Y., Woernle, C., and Hiller, M., 1991, "A Complete Solution for the Inverse Kinematics Problem of the General 6R Robot Manipulator," *ASME Journal of Mechanical Design*, Vol. 113, No. 4, pp. 481-486.

52. Lin, P. D., and Ehmann, K. F., 1993, "Direct Volumetric Error Evaluation for Multi-Axis Machines," *International Journal of Machine Tools and Manufacture*, Vol. 33, No. 5, pp. 675-693.

53. Lo, C. H., Yuan, J., and Ni, J., 1994, "Error Link Metrology and Flexible Error Synthesis Model for Correcting Quasi-Static Machine Errors," *Transactions of NAMRI/SME*, Vol. XXII, pp. 267-273.

54. Mallik, A. K., and Dhande, S. G., 1987, "Analysis and Synthesis of Mechanical Error in Path-Generating Linkages Using a Stochastic Approach," *Mechanisms and Machine Theory*, Vol. 22, No. 2, pp. 115-123.

55. MathSoft Inc., "Mathcad for Windows", Cambridge, MA.

56. McKerrow, P. J., 1991, *Introduction to Robotics*, Addison-Wesley Publishing Company, Reading, MA.

57. Melsa, J. L., and Cohn, D. L., 1978, *Decision and Estimation Theory*, McGraw-Hill Book Company, New York, NY.

58. Menq, C. H., and Borm, J. H., 1988, "Statistical Measure and Characterization of Robot Errors," *Proceedings of the IEEE International Conference on Robotics and Automation*, Vol. 2, pp. 926-931.

59. Menq, C. H., Borm, J. H., and Lai, J. Z., 1988, "Estimation and Observability Measure of Parameter Errors in a Robot Kinematic Model," *Proceedings of the*

USA-Japan Symposium on Flexible Automation, Minneapolis, MN, Vol. 1, pp. 73-79.

60. Menq, C. H., Borm, J. H., and Lai, J. Z., 1989, "Identification and Observability Measure of a Basis Set of Error Parameters in Robot Calibration," *Journal of Mechanisms, Transmissions, and Automation in Design*, Vol. 111, No. 4, pp. 513-518.

61. Moon, K. S., Azadivar, F., and Kim, K., 1992, "A Stochastic Optimization of the Production Speed of Robots Based on Measured Geometric and Nongeometric Errors," *International Journal of Production Research*, Vol. 30, No. 1, pp. 49-62.

62. Mooring, B. W., 1983, "The Effect of Joint Axis Misalignment on Robot Positioning Accuracy," *Proceedings of the 1983 ASME Computers in Engineering Conference and Exhibit*, Vol. 2, pp. 151-155.

63. Mooring, B. W., and Tang, G. R., 1984, "An Improved Method for Identifying the Kinematic Parameters in a Six Axis Robot," *Proceedings of the ASME International Computers in Engineering Conference and Exhibit*, Las Vegas, NV, August 12-16, pp. 79-84.

64. Mou, J., and Liu, C. R., "An Error Correction Method for CNC Machine Tools Using Reference Parts," *Transactions of NAMRI/SME*, Vol. XXII, pp. 275-282.

65. Nahi, N. E., 1969, *Estimation Theory and Applications*, John Wiley and Sons, New York, NY.

66. New River Kinematics, 1995, "Rhobot Pro for Windows", Radford, VA.

67. Norton, J. P., 1986, *An Introduction to Identification*, Academic Press, Orlando, FL.

68. Ott, R. L., 1993, *An Introduction to Statistical Methods and Data Analysis*, Fourth Edition, Duxbury Press, Belmont, California.

69. Prakasa Rao, B. L. S., 1992, *Identifiability in Stochastic Models*, Academic Press, Boston, MA.

70. Prenninger, J. P., Vincze, M., and Gander, H., 1993, "Contactless Position and Orientation Measurement of Robot End-Effectors," *Proceedings of the IEEE International Conference on Robotics and Automation*, Vol. 1, pp. 180-185.

71. Press, W. H., Teukolsky, S. A., Vetterling, W. T., and Flannery, B. P., 1992, *Numerical Recipes in C: The Art of Scientific Computing*, Second Edition, Cambridge University Press.

72. Rao, S. S., 1984, *Optimization: Theory and Applications*, Second Edition, John Wiley & Sons, New York, NY.

73. Reinholtz, C. F., 1983, "Optimization of Spatial Mechanisms," PhD Dissertation, Department of Mechanical Engineering, University of Florida, Gainsville, FL.

74. Renders, J. M., Rossignol, E., Becquet, M., and Hanus, R., 1991, "Kinematic Calibration and Geometrical Parameter Identification for Robots," *IEEE Transactions on Robotics and Automation*, Vol. 7, No. 6, 721-732.

75. Roth, Z. S., Mooring, B. W., and Ravani, B., 1987, "An Overview of Robot Calibration," *IEEE Journal of Robotics and Automation*, Vol. RA-3, No. 5, pp. 377-385.

76. Salerno, R. J., 1993, "Positional Control Strategies for a Modular, Long-Reach Truss-Type Manipulator," PhD Dissertation, Department of Mechanical Engineering, Virginia Polytechnic and State University, Blacksburg, VA.

77. Science Accessories Corp., 1993, *GP - 12: 3D Digitizing System Manual*, Shelton, CT.

78. Shamma, J. S., and Whitney, D. E., 1987, "A Method for Inverse Robot Calibration," *Journal of Dynamic Systems, Measurement, and Control*, Vol. 109, No. 1, pp. 37-43.

79. Shooter, S. B., 1990, "Conceptual Design of Manipulators for Limited Access Workspaces," Masters Thesis, Department of Mechanical Engineering, Virginia Polytechnic and State University, Blacksburg, VA.

80. Shooter, S. B., Reinholtz, C. F., and Dhande, S. G., 1992, "On the Kinematic Design of Manipulators for Limited Access WorkSpaces (LAWS), *Proceedings of the 1992 ASME Design Technical Conferences - 22nd Biennial Mechanisms Conference*, Scottsdale, Arizona, September 13-16, DE-Vol. 45, pp. 485-491.

81. Shooter, S. B., and Reinholtz, C. F., 1992, "Extrinsic Calibration of Portable Manipulators," *Proceedings of the 1992 ASME Design Technical Conferences - 22nd Biennial Mechanisms Conference*, Scottsdale, Arizona, September 13-16, DE-Vol. 45, pp. 501-506.

82. Spatial Positioning Systems, Blacksburg, VA.

83. Stone, H. W., Sanderson, A. C., and Neuman, C. P., 1986, "Arm Signature Identification," *Proceedings of the IEEE International Conference on Robotics and Automation*, Vol. 1, pp. 41-48.

84. Stulce, J. R., 1995, "Conceptual Design and Motion Programming of a Multibody Passive-Legged Crawling Vehicle," PhD Dissertation, Department of Mechanical Engineering, Virginia Polytechnic and State University, Blacksburg, VA.

85. Stone, H. W., and Sanderson, A. C., 1988, "Statistical Performance Evaluation of the S-Model Arm Signature Identification Technique," *Proceedings of the IEEE International Conference on Robotics and Automation*, Vol. 2, pp. 939-946.

86. Tidwell, P. H., Glass, S. W., Hildebrand, J. J., Reinholtz, C. F., and Shooter, S. B., 1994, "COBRA - Design and Development of a Manipulator for Nuclear Steam Generator Maintenance," *Journal of Applied Mechanisms*, Vol. 2, No. 2.

87. Tidwell, P. H., Glass, S. W., Hildebrand, J. J., Reinholtz, C. F., and Shooter, S. B., 1991, "COBRA - Design and Development of a Manipulator for Nuclear Steam Generator Maintenance," *Proceedings of the 2nd National Applied Mechanisms & Robotics Conference*, November 3-6, Cincinnati, Ohio, pp. IVB.1-1-10.

88. Tidwell, P. H., Hendricks, M. W., Fallon, J. B., Stulce, J. R., Beisgen, L. C. V., Maples, A. B., and Reinholtz, C. F., 1993, "Acoustic Pose Determination Applied to an Underwater Mobile Robot," *Proceedings of the 3rd National Applied Mechanisms & Robotics Conference*, November 7-10, Cincinnati, Ohio, pp. AMR-93-084-01-06.

89. Toyama, S., and Hatae, S., 1992, "Identification and Compensation of Mechanical Errors for a SCARA Robot," *Journal of the Japan Society of Precision Engineering (Seimitsu Kogaku Kaishi)*, Vol. 58, No. 6, pp. 999-1004.

90. Unimation Incorporated, 1987, *Unimate PUMA 500 Series Equipment Manual*, Pittsburgh, PA.

91. Veitschegger, W. K., and Wu, C. H., 1986, "Robot Accuracy Analysis Based on Kinematics," *IEEE Journal of Robotics and Automation*, Vol. RA-2, No. 3, pp. 171-179.

92. Veitschegger, W. K., and Wu, C. H., 1987, "A Method for Calibrating and Compensating Robot Kinematic Errors," *Proceedings of the IEEE International Conference on Robotics and Automation*, Vol. 1, pp. 39-44.

93. Wang, S. M., and Ehmann, K. F., 1994a, "Compensation of Geometric and Quasi-Static Deformation Errors of a Multi-Axis Machine," *Transactions of NAMRI/SME*, Vol. XXII, pp. 283-289.

94. Wang, S. M., and Ehmann, K. F., 1994b, "Automated Evaluation of Volumetric Errors of Multi-Axis Machines," *Transactions of NAMRI/SME*, Vol. XXII, pp. 291-296.

95. Whitney, D. E., Lozinski, C. A., and Rourke, J. M., 1984, "Industrial Robot Calibration Method and Results," *Proceedings of the ASME International Computers in Engineering Conference and Exhibit*, Las Vegas, NV, August 12-16, pp. 92-100.

96. Wolfram, S., 1991, *Mathematica: A System for Doing Mathematics by Computer*, Second Edition, Addison-Wesley Publishing Company, Reading, MA.

97. Wu, F., and Lankarani, H. M., 1992, "A New Parameter for Transmission Quality and Output Sensitivity Analysis of Mechanisms," *Proceedings of the 1992 ASME Design Technical Conferences - 22nd Biennial Mechanisms Conference*, Scottsdale, Arizona, September 13-16, DE-Vol. 46, pp. 103-109.

98. Yang, J. H., 1992, "Transmission Error Analysis of a Parallel Symmetric Geared Linkage Mechanism," *Proceedings of the 1992 ASME Design Technical Conferences - 22nd Biennial Mechanisms Conference*, Scottsdale, Arizona, September 13-16, DE-Vol. 46, pp. 89-92.

99. Yang, Z., and Sadler, J. P., 1992, "Finite Element Analysis of Revolute Manipulators with Link and Joint Compliance by Joint-Beam Elements," *Proceedings of the 1992 ASME Design Technical Conferences - 22nd Biennial Mechanisms Conference*, Scottsdale, Arizona, September 13-16, DE-Vol. 45, pp. 619-625.

100. Yang, B. D., and Menq, C. H., 1993, "Compensation for Form Error of End-Milled Sculptured Surfaces Using Discrete Measurement Data," *International Journal of Machine Tools and Manufacture*, Vol. 33, No. 5, pp. 725-740.

101. Yao, Y. L., and Mohd Yusoff, M. R., 1992, "A CAD-Based Error Mapping and Layout Facility for Precision Robotic Operations," *Robotics & Computer-Integrated Manufacturing*, Vol. 9, No. 6, pp. 505-511.

102. Zak, G., Benhabib, B., Fenton, R. G., and Saban, I., 1991, "Improvement of Robot Kinematic Parameter Estimation Through the Weighted Least Squares Solution Method," *Proceedings of the 2nd National Applied Mechanisms & Robotics Conference*, November 3-6, Cincinnati, Ohio, pp. IIC.2-1-5.

103. Zak, G., Fenton, R. G., and Benhabib, B., 1992, "Optimization of the Robot Calibration Process," *Proceedings of the 1992 ASME Design Technical*

Conferences - 22nd Biennial Mechanisms Conference, Scottsdale, Arizona, September 13-16, DE-Vol. 45, pp. 537-544.

104. Zak, G., Fenton, R. G., and Benhabib, B., 1993, "A Simulation Technique for the Improvement of Robot Calibration," *Journal of Mechanical Design*, Vol. 115, No. 3, pp. 674-679.

105. Zak, G., Fenton, R. G., and Benhabib, B., 1994, "Determination of the Optimum Cost-Residual Error Trade-off in Robot Calibration," *Journal of Mechanical Design*, Vol. 116, No. 1, pp. 28-35.

106. Zhuang, H., Roth, Z. S., and Hamano, F., 1990, "Observability Issues in Kinematic Error Parameter Identification of Manipulators," *Proceedings of the American Control Conference*, San Diego, CA, Vol. 3, pp. 2287-2293.

107. Zhuang, H., and Roth, Z. S., 1991, "A Closed Form Solution to the Kinematic Parameter Identification of Robot Manipulators," *Proceedings of the IEEE International Conference on Robotics and Automation*, Vol. 3, pp. 2682-2688.

108. Zhuang, H., Roth, Z. S., and Hamano, F., 1992a, "A Complete and Parametrically Continuous Kinematic Model for Robot Manipulators," *IEEE Transactions on Robotics and Automation*, Vol. 8, No. 4, pp. 451-463.

109. Zhuang, H., Roth, Z. S., and Hamano, F., 1992b, "Observability Issues in Kinematic Identification of Manipulators," *Journal of Dynamic Systems, Measurement, and Control*, Vol. 114, No. 2, pp. 319-322.

110. Zhuang, H., Wang, L. K., and Roth, Z. S., 1993, "Error-Model-Based Robot Calibration Using a Modified CPC Model," *Robotics & Computer-Integrated Manufacturing*, Vol. 10, No. 4, pp. 287-299.

111. Ziegert, J., and Datseris, P., 1988, "Basic Considerations for Robot Calibration," *Proceedings of the IEEE International Conference on Robotics and Automation*, Vol. 1, pp. 932-938.

Appendix 1

This is the input data to the PUMA sensitivity analysis code.

```
6 links   PUMA 562 System D&H Kinematic Parameters
(i)  (alpha i-1) (a i-1) (d i) (joint limits)   dh table (For joint 6 actual limit 532 deg)
 1       0       0     0     320
 2      -90      0     0     270
 3       0      432   149.5   270
 4      -90     20.3   433    280
 5       90      0     0     200
 6      -90      0     0     360
560 265 350   0 0 -32   Base transform
-8 -208 150   0 0   0   Tool tip transform to link 6 (Or you could define a link 7)
1  2.5  5  10     link 1 alpha err, a err, d err, theta err
1  2.5  5  10     link 2 errors   (error in dh table)
1  2.5  5  10     link 3 etc
1  2.5  5  10
1  2.5  5  10
1  2.5  5  10     link 6
15 15 15   2 2 2   Base transform error
 2  2  2   0 0 0   Tool tip transform to link 6 error
```

This is sample sensitivity analysis results for all 33 parameters with one joint angle configuration and a parameter perturbation style of positive individual with the remaining parameters at nominal values.

Absolute Distance Error (mm), Style 1: Nominal set, Positive Individual

1	-160.00 -225.00 -225.00 -110.00 -100.00 -180.00	Xb 15.000 -0.000 Rx
1	-160.00 -225.00 -225.00 -110.00 -100.00 -180.00	Yb 15.000 -0.000 Rx
1	-160.00 -225.00 -225.00 -110.00 -100.00 -180.00	Zb 15.000 -0.000 Rx
1	-160.00 -225.00 -225.00 -110.00 -100.00 -180.00	RXb 13.759 -1.696 Rx
1	-160.00 -225.00 -225.00 -110.00 -100.00 -180.00	RYb 5.025 -1.696 Ry
1	-160.00 -225.00 -225.00 -110.00 -100.00 -180.00	RZb 12.921 -2.000 Rz
1	-160.00 -225.00 -225.00 -110.00 -100.00 -180.00	Alpha0 6.880 -0.848 Rx
1	-160.00 -225.00 -225.00 -110.00 -100.00 -180.00	a0 2.500 -0.000 Rx
1	-160.00 -225.00 -225.00 -110.00 -100.00 -180.00	d1 5.000 -0.000 Rx
1	-160.00 -225.00 -225.00 -110.00 -100.00 -180.00	Theta1 64.526 -10.000 Rz
1	-160.00 -225.00 -225.00 -110.00 -100.00 -180.00	Alpha1 6.710 -0.208 Ry
1	-160.00 -225.00 -225.00 -110.00 -100.00 -180.00	a1 2.500 -0.000 Rx
1	-160.00 -225.00 -225.00 -110.00 -100.00 -180.00	d2 5.000 -0.000 Rx
1	-160.00 -225.00 -225.00 -110.00 -100.00 -180.00	Theta2 29.321 0.180 Rz
1	-160.00 -225.00 -225.00 -110.00 -100.00 -180.00	Alpha2 6.882 -0.691 Rx
1	-160.00 -225.00 -225.00 -110.00 -100.00 -180.00	a2 2.500 -0.000 Rx
1	-160.00 -225.00 -225.00 -110.00 -100.00 -180.00	d3 5.000 -0.000 Rx
1	-160.00 -225.00 -225.00 -110.00 -100.00 -180.00	Theta3 75.322 0.180 Rz
1	-160.00 -225.00 -225.00 -110.00 -100.00 -180.00	Alpha3 7.860 -1.000 Rz
1	-160.00 -225.00 -225.00 -110.00 -100.00 -180.00	a3 2.500 -0.000 Rx
1	-160.00 -225.00 -225.00 -110.00 -100.00 -180.00	d4 5.000 -0.000 Rx
1	-160.00 -225.00 -225.00 -110.00 -100.00 -180.00	Theta4 44.330 -2.069 Ry
1	-160.00 -225.00 -225.00 -110.00 -100.00 -180.00	Alpha4 3.678 0.198 Rx
1	-160.00 -225.00 -225.00 -110.00 -100.00 -180.00	a4 2.500 -0.000 Rx
1	-160.00 -225.00 -225.00 -110.00 -100.00 -180.00	d5 5.000 -0.000 Rx
1	-160.00 -225.00 -225.00 -110.00 -100.00 -180.00	Theta5 26.184 -3.272 Ry
1	-160.00 -225.00 -225.00 -110.00 -100.00 -180.00	Alpha5 4.476 -0.997 Rx
1	-160.00 -225.00 -225.00 -110.00 -100.00 -180.00	a5 2.500 -0.000 Rx
1	-160.00 -225.00 -225.00 -110.00 -100.00 -180.00	d6 5.000 -0.000 Rx
1	-160.00 -225.00 -225.00 -110.00 -100.00 -180.00	Theta6 36.284 0.507 Rx
1	-160.00 -225.00 -225.00 -110.00 -100.00 -180.00	Xt 2.000 -0.000 Rx
1	-160.00 -225.00 -225.00 -110.00 -100.00 -180.00	Yt 2.000 -0.000 Rx
1	-160.00 -225.00 -225.00 -110.00 -100.00 -180.00	Zt 2.000 -0.000 Rx

Appendix 2

This is the sensitivity analysis input data for URSULA BPS design.

```
-29.06 -7.07  -15.89   Foot 1 rel to Base
-29.06 18.22  -17.431  Foot 2 rel to Base
   0    0  -18.633    Foot 3 rel to Base
-6.875   -2   -8.047      Laser Target rel to Base
1.0                Foot 1 Error
1.0                Foot 2 Error
1.0                Foot 3 Error
1.0                Laser Frame Z error  (side to side in laser frame)
0.0                Laser Frame Y Error (up-down in laser frame)
1.0                Pressure Gage Z Error
1.0                Left Right Inclinometer
0.0                Back Front Inclinometer
4             Number of circumferential locations to put Ursula
0 90 180 270   Theta Circumferential Values
2             Number of depth locations
0 -280         Depth values
***** Nominal Values of the Parameters
80.0            Radius of RV
4                  Number of Targets
 80.0   0.0   0.0
  0.0  80.0   0.0    xyz location of targets
-80.0   0.0   0.0
  0.0 -80.0   0.0
0.0 0.0            Initial Pan and Tilt  (theta_i,phi_i)
0.0 0.0 0.0          Gimbal Pose x, y, z
0.0 0.0 0.0          Gimbal Pose alpha, beta, gamma
0.0 0.0 0.0          Laser Pose x, y, z  (extrinsic)
0.0 0.0 0.0          Laser Pose al,bl,gl
0.0 -90.0          Gimbal D-H parameters a1, alpha1   (d2 = 0)
0.0 0.0           Inclinometer readings (R-L, F-B)
0.0 0.0           Extrinsic Inclinometer Mounting
***  Ranges of Perturbation
0.65 inch          radius deviation              1
0.35 inch          depth range zu                1   2
0.25  inch         x Target                  4
```

0.25 inch	y Target	4	
0.25 inch	z Target	4	14
0.025 deg	theta	4	
0.025 deg	phi	4	22
0.5 deg	Initial theta	1	
0.5 deg	Initial phi	1	24
0.25 inch	x gimbal pose	1	
0.25 inch	y gimbal pose	1	
0.25 inch	z gimbal pose	1	
1 deg	alpha gimbal pose	1	
1 deg	beta gimbal pose	1	
1 deg	gamma gimbal pose	1	30
0.1 inch	x laser pose	1	
0.1 inch	y laser pose	1	
0.1 inch	z laser pose	1	
0.5 deg	alpha laser pose	1	
0.5 deg	beta laser pose	1	
0.5 deg	gamma laser pose	1	36
0.02 inch	a1 of Gimbal D-H	1	
0.016666666666667 deg	alpha1 of Gimbal D-H	1	
0.05 deg	right left inclinometer	1	
0.05 deg	front back inclinometer	1	40
0.0 deg	right left extrinsic inclinometer	1	
0.0 deg	front back extrinsic inclinometer	1	44

This is the sensitivity analysis results for URSULA BPS design for one particular parameter perturbation style (Individual parameter is perturbed to positive extreme while the remaining parameters are kept at nominal values).

Distance Error in Inches, Style 1: Nominal set, Positive Individual

	Depth 0.000000 inches				Depth -280.000000 inches			
Theta-	0.00	90.00	180.00	270.00	0.00	90.00	180.00	270.00
Radius	0.0000	0.0000	0.0000	0.0000	0.0000	0.0000	0.0000	0.0000
Target X0	0.0000	0.0000	0.0000	0.0000	0.0000	0.0000	0.0000	0.0000
Target Y0	0.0018	0.0005	0.0007	0.0006	0.0018	0.0005	0.0007	0.0006
Target Z0	0.0000	0.0001	0.0000	0.0001	0.0000	0.0043	0.0000	0.0043
Target X1	0.0006	0.0018	0.0005	0.0007	0.0006	0.0018	0.0005	0.0007

Target Y1	0.0000	0.0000	0.0000	0.0000	0.0000	0.0000	0.0000	0.0000
Target Z1	0.0001	0.0000	0.0001	0.0000	0.0043	0.0000	0.0043	0.0000
Target X2	0.0000	0.0000	0.0000	0.0000	0.0000	0.0000	0.0000	0.0000
Target Y2	0.0007	0.0006	0.0018	0.0005	0.0007	0.0006	0.0018	0.0005
Target Z2	0.0000	0.0001	0.0000	0.0001	0.0000	0.0043	0.0000	0.0043
Target X3	0.0005	0.0007	0.0006	0.0018	0.0005	0.0007	0.0006	0.0018
Target Y3	0.0000	0.0000	0.0000	0.0000	0.0000	0.0000	0.0000	0.0000
Target Z3	0.0001	0.0000	0.0001	0.0000	0.0043	0.0000	0.0043	0.0000
Theta_i	0.0000	0.0000	0.0000	0.0000	0.0000	0.0000	0.0000	0.0000
Phi_i	0.0000	0.0000	0.0000	0.0000	0.0000	0.0000	0.0000	0.0000
X Gimbal	0.0000	0.0000	0.0000	0.0000	0.0000	0.0000	0.0000	0.0000
Y Gimbal	0.0000	0.0000	0.0000	0.0000	0.0000	0.0000	0.0000	0.0000
Z Gimbal	0.0000	0.0000	0.0000	0.0000	0.0000	0.0000	0.0000	0.0000
a Gimbal	0.0000	0.0000	0.0000	0.0000	0.0000	0.0000	0.0000	0.0000
b Gimbal	0.0000	0.0000	0.0000	0.0000	0.0000	0.0000	0.0000	0.0000
g Gimbal	0.0000	0.0000	0.0000	0.0000	0.0000	0.0000	0.0000	0.0000
X Laser	0.0000	0.0000	0.0000	0.0000	0.0000	0.0000	0.0000	0.0000
Y Laser	0.0000	0.0000	0.0000	0.0000	0.0000	0.0000	0.0000	0.0000
Z Laser	0.0108	0.0108	0.0108	0.0108	0.0108	0.0108	0.0108	0.0108
a Laser	0.0000	0.0000	0.0000	0.0000	0.0000	0.0000	0.0000	0.0000
b Laser	0.0023	0.0023	0.0023	0.0023	2.6999	2.6999	2.6999	2.6999
g Laser	0.0000	0.0000	0.0000	0.0000	0.0000	0.0000	0.0000	0.0000
a1 Gimbal	0.0000	0.0000	0.0000	0.0000	0.0000	0.0000	0.0000	0.0000
alpha1 Gimbal	0.0016	0.0016	0.0016	0.0016	0.0698	0.0698	0.0698	0.0698
L-R Inclinom	0.0078	0.0078	0.0078	0.0078	0.0078	0.0078	0.0078	0.0078
F-B Inclinom	0.0000	0.0000	0.0000	0.0000	0.0000	0.0000	0.0000	0.0000
Extr L-R Incl	0.0000	0.0000	0.0000	0.0000	0.0000	0.0000	0.0000	0.0000
Extr R-B Incl	0.0000	0.0000	0.0000	0.0000	0.0000	0.0000	0.0000	0.0000
Depth	0.3500	0.3500	0.3500	0.3500	0.3500	0.3500	0.3500	0.3500
Theta Target 1	0.0003	0.0001	0.0001	0.0001	0.0003	0.0001	0.0001	0.0001
Phi Target 1	0.0000	0.0000	0.0000	0.0000	0.0000	0.0006	0.0000	0.0006
Theta Target 2	0.0001	0.0003	0.0001	0.0001	0.0001	0.0003	0.0001	0.0001
Phi Target 2	0.0000	0.0000	0.0000	0.0000	0.0006	0.0000	0.0006	0.0000
Theta Target 3	0.0001	0.0001	0.0003	0.0001	0.0001	0.0001	0.0003	0.0001
Phi Target 3	0.0000	0.0000	0.0000	0.0000	0.0000	0.0006	0.0000	0.0006
Theta Target 4	0.0001	0.0001	0.0001	0.0003	0.0001	0.0001	0.0001	0.0003
Phi Target 4	0.0000	0.0000	0.0000	0.0000	0.0006	0.0000	0.0006	0.0000
Foot 1 radius	0.2536	0.2536	0.2536	0.2536	0.2536	0.2536	0.2536	0.2536
Foot 2 radius	0.2475	0.2475	0.2475	0.2475	0.2475	0.2475	0.2475	0.2475
Foot 3 radius	0.6339	0.6339	0.6339	0.6339	0.6339	0.6339	0.6339	0.6339
Theta Ursula	0.0269	0.0269	0.0269	0.0269	0.0269	0.0269	0.0269	0.0269
Phi Ursula	0.0000	0.0000	0.0000	0.0000	0.0000	0.0000	0.0000	0.0000

Vita

Ravinder Srinivas Voruganti was born to Voruganti Pandu Rangaiah and Voruganti Suguna on November 21, 1965, in Devarkonda, A. P., India. After finishing high school in 1983 he joined the M. N. Regional Engineering College in Allahabad, India, where he received his Bachelor's Degree in Mechanical Engineering with First Class. On completion of his undergraduate studies, he joined the R&D department of TVS Electronics, Bangalore, India as a Design Engineer. Sensing the urge to pursue higher education, he joined the Mechanical Engineering Department in Virginia Polytechnic Institute and State University (Virginia Tech) for graduate studies. He received a Master of Science Degree in 1990. He is currently pursuing the Doctor of Philosophy degree in mechanical engineering at Virginia Tech.

Ravi was married to Dr. K. Bala Tripura Sundari on March 11, 1993. Ravi hopes to contribute positively to the engineering profession over a long and productive career.